CHARACTERIZING THE CROSS-REGULATORY COMPLEX, OTUB1:E2

by
Lauren E. Que

A dissertation submitted to Johns Hopkins University in conformity with the requirements for the degree of Doctor of Philosophy

Baltimore, Maryland
May 2019

Abstract

The ubiquitin system regulates several diverse biological processes in eukaryotes. The process of ubiquitination involves a multienzymatic E1-E2-E3 cascade that serves to activate ubiquitin, conjugate the C-terminus of ubiquitin, and finally to ligate the ubiquitin molecule to a substrate protein via the E3 ligase. Deubiquitinating enzymes (DUBs) reverse these ubiquitin modifications. OTUB1 is a highly expressed DUB that specifically cleaves K48 poly-ubiquitin chains. It helps to regulate ubiquitin concentrations in the cell through its catalytic and non-canonical activities. OTUB1 possesses a unique property among DUBs in that it binds to a subset of ubiquitin conjugating enzymes, E2s, independently of its catalytic activity. By interacting with E2s, a cross-regulation occurs in which the E2s stimulate OTUB1's isopeptidase activity and, in turn, OTUB1 inhibits the E2's ability to transfer ubiquitin. Mass spectrometry/proteomics studies revealed that OTUB1 interacts with 7 E2s in cells: UBE2D1, UBE2D2, UBE2D3, UBE2N, UBE2E1, UBE2E2, and UBE2E3. It is unclear whether cross-regulation occurs *in vivo.* To investigate the mechanism involved in the OTUB1:E2 cross-regulatory complex, I utilized a series of biochemical and kinetic assays. First, I looked at stimulation by determining EC_{50}s and Michaelis Menten kinetic parameters using a FRET assay and quantified the degree of stimulated isopeptidase activity with each E2. I found that binding of an E2 lowers the K_M of OTUB1 for K48 diUb, at a broad range of stimulation depending on the E2, with little to no change in the k_{cat}. This result indicates that the E2 increases OTUB1's affinity for K48 diUb. I used ITC to confirm this, my results indicate that the interactions between OTUB1 and the E2 produces an increase in OTUB1's affinity for K48 chains. I next sought to characterize OTUB1's inhibitory effects on E2 ubiquitin conjugation. Similar to previous studies, OTUB1 blocks both UBE2N and UBE2D proteins from free chain poly-ubiquitination. Unlike UBE2D or UBE2N where OTUB1 inhibits their poly-ubiquitination activity, OTUB1 predominantly

serves to stop autoubiquitylation of UBE2E enzymes. Further *in vivo* studies revealed that autoubiquitylation of UBE2E1 targets it from proteasomal degradation. By inhibiting autoubiquitylation, OTUB1 stabilizes UBE2E1; a novel role for OTUB1.

First Reader: Cynthia Wolberger

Second Reader: James Berger

Acknowledgments

I would like to thank first and foremost my husband, Sean Klein, Ph.D. Sean was my sound board, confidante, and best friend during graduate school. When experiments weren't working or when everything was becoming too stressful, Sean was always there (usually with a bottle of whiskey) to help me through it all.

Thank you to Cynthia Wolberger, Ph.D. for her guidance and mentorship. I am most appreciative for the Wolberger lab. We were a cohesive and yet dysfunctional group that got along so well. Thank you to Sara Haile, who broke up the monotony with her impromptu lab yoga sessions and coffee/tea breaks. Thank you to Marie Morrow for her continued advice and guidance on my project. Thank you to Patrick Lombardi whose every so persistent optimism and happiness provide a much needed foil to my pessimism. I would also like to thank Mike Morgan, Nik Hoffmann, Evan Worden, Xiangbin Zhang, and Mel Nune for fostering an enjoyable learning environment.

Table of Contents

List of Tables

List of Figures

Chapter 1: Ubiquitin conjugating and deconjugating enzymes working in concert together

1.1 Ubiquitination, a multienzymatic process

Ubiquitin is a small 76 amino acid protein that is covalently attached to substrate and plays a role in diverse cellular pathways within the eukaryotic cell. Historically, the first function identified for ubiquitin was its role in the proteasomal degradation of a protein substrate. Since then, the field has uncovered ever expanding roles for this small modifier. Not only does ubiquitin participate in other proteolytic pathways such as endolysosomal degradation and autophagy (Clague and Urbé, 2010; Kirkin et al., 2009), but it is also essential for non-degradative processes such as intracellular trafficking, DNA damage repair mechanisms, cell cycle and division, and other regulatory pathways (Chen and Sun, 2009; Schnell and Hicke, 2003; Swatek and Komander, 2016).

The ubiquitin C-terminus is conjugated to lysine residues via a multienzymatic process, the E1-E2-E3 cascade (**Figure 1.1.a)**. First, an E1 ubiquitin activating enzyme activates the C-terminal carboxylate of ubiquitin with ATP to form a highly reactive Ub-AMP adenylate (Pickart, 2001). The active site cysteine on the E1 then attacks the activated ubiquitin to form a thioester linkage with the C-terminus of ubiquitin, E1~Ub. Next, E1~Ub binds to a ubiquitin conjugating enzyme, E2, and transfers the ubiquitin from the E1 to the E2 catalytic cysteine, producing a thioester linked ubiquitin molecule to the E2, E2~Ub **(Figure 1.2.c)** (Ye and Rape, 2009). Finally, an E3 ligase mediates the transfer of ubiquitin from the charged E2 to a substrate by simultaneously interacting with both the E2 and substrate (Zheng and Shabeck, 2017), resulting in formation of

an isopeptide linkage between the ubiquitin C-terminus and the lysine ε-amino in a target substrate.

Ubiquitin itself has lysine residues and can be a substrate of the E1-E2-E3 cascade, resulting in formation of polyubiquitin chains (Komander and Rape, 2012). Ubiquitin contains seven lysines (K6, K11, K22, K29, K33, K48, K63) and an N-terminal amino group (M1) that can be covalently modified with another ubiquitin molecule. Ubiquitin chains are denoted by the isopeptide linkage that connects the acceptor ubiquitin lysine ε-amino to the C-terminus of the donor ubiquitin **(Figure 1.2)**. E2 enzymes are generally responsible for specifying the type of ubiquitin linkage (David et al., 2010). Different chain types signal for very different biological outcomes **(Table 1.1)**. Of the various chain types, K48- and K63-linked polyubiquitin chains are the most abundant types of chains found in cells (Clague et al., 2015). K48 chains target proteins for proteasomal degradation, whereas K63 chains signal for double stranded DNA damage repair mechanisms in addition to signaling for autophagy (Komander and Rape, 2012; Li and Ye, 2008). K11 chains play a role in cell cycle control (Matsumoto et al., 2010). The metazoan anaphase-promoting complex (APC/C) makes K11 chains that signal for proteasomal degradation and mitotic exit. In addition, K29 chains inhibit Wnt signaling (Fei et al., 2013), K33 chains serve as negative regulators for both AMP-activated protein kinases (Al-Hakim et al., 2008) and T-cell antigen receptors (Huang et al., 2010), and linear linkages or M1 chains are key regulators of NF-KB signaling (Gerlach et al., 2011; Iwai and Tokunaga, 2009). The diversity of biological outcomes regulated by these various chain types emphasizes the importance of the ubiquitin system in cells.

Total ubiquitin levels in human cells are estimated to be between 17-85 μM depending on cell type (Clague et al., 2015). Cellular ubiquitin exists in different forms: 'free ubiquitin', 'activated or

charged' to an enzyme, 'conjugated' to a target substrate, or formed in 'chains' **(Figure 1.2.c)**. Over 60% of ubiquitin in humans cells is found in the form of monoubiquitylation, with a large subset of that percentage pertaining to ubiquitin that is conjugated to histones (Clague et al., 2015). Monoubiquitinated H2A (Zhou et al., 2008) and H2B (Chandrasekharan et al., 2009) play a critical role in transcription regulation. 11% of the total ubiquitin in the cell is found conjugated in chains, particularly in either K48- or K63- linkages (Clague et al., 2015).

1.2 E2 Ubiquitin Conjugating Enzymes specify linkage type

In mammals, there are ~40 E2s that conjugate ubiquitin or ubiquitin-like modifiers (Stewart et al., 2016 ; Ye and Rape, 2009). All E2s contain a highly conserved 150-amino acid ubiquitin conjugating (Ubc) domain that adopts an α/β fold composed of four α-helices and four β-sheets connected by several loops **(Figure 1.3.a)** (Stewart et al., 2016). The Ubc domain contains a catalytic cysteine that forms a thioester with the ubiquitin C-terminus. The N-terminal helix α_1 and several loop regions serve as key surfaces that interact with both E1 and E3 enzymes (Eletr et al., 2005; Ye and Rape, 2009). Since the E2 cannot be simultaneously bound to both proteins, the E1 must dissociate from the E2 after generating the E2~Ub thioester intermediate in order to allow an E3 ligase to bind and mediate transfer of the ubiquitin from the E2 to the substrate (Eletr et al., 2005; Stewart et al., 2016). In the absence of an E3 ligase, E2 activity is low and is typically non-specific (Ozkan et al., 2005; Petroski and Deshaies, 2005).

E2 enzymes are subdivided into four classes based on domain architecture **(Figure 1.3.b)** (Stewart et al., 2016). Differences in classes are based on extensions to the Ubc domain (Class I) at either the N- (Class III) or C-terminus (Class II). Additionally, Class IV E2s contain both N- and C-terminal extensions. These extensions are often intrinsically disordered and can impart

additional functionality to the E2 (Schumacher et al., 2013). The UBE2E family of enzymes comprises Class III E2s whose N-terminal extension limits polyubiquitinating activity (Schumacher et al., 2013). The C-terminal extension of UBE2K, a Class II E2, interacts with ubiquitin and is necessary for assembling K48-linked chains in a processive manner (Haldeman et al., 1997). Of the 40 different E2 enzymes, a subset are E2 variants (UEV) that possess a Ubc domain that lacks a catalytic cysteine and is therefore unable to conjugate ubiquitin (Hofmann and Pickart, 1999b; Sancho et al., 1998; VanDemark et al., 2001). As described below, these UEV proteins have a specialized function in assisting UBE2N to synthesize K63 chains (Eddins et al., 2006; Hofmann and Pickart, 1999a).

E2 linkage specificity likely occurs from the E2, charged with a donor ubiquitin, positioning the acceptor ubiquitin in such a way that exposes the acceptor lysine for attack. This is best understood in the case of K63-linked chains, which are synthesized by UBE2N in humans and Ubc13 in yeast (Eddins et al., 2006; Hofmann and Pickart, 1999b; Yin et al., 2009). Biochemical and structural studies have elucidated the mechanism by which Ubc13/Mms2 forms K63 chains (Eddins et al., 2006; Hofmann and Pickart, 1999a). When Ubc13 is charged with the donor ubiquitin, the acceptor ubiquitin is non-covalently bound to Mms2 (Eddins et al., 2006) in an orientation that places K63 of the acceptor ubiquitin in a position to attack the thioester linkage of Ubc13~Ub. This process can occur iteratively, leading to elongation of K63-linked polyubiquitin chains. The human homologues, UBE2N/UEV1A, function in an identical manner (Yin et al., 2009).

Despite sharing a high degree of sequence and structural similarity, there is high variability in the types of chains that an E2 can form (David et al., 2010). Some E2s primarily initiate the conjugation of a polyubiquitin chain by monoubiquitinating the substrate, while others elongate

the chain (David et al., 2010). Some E2 enzymes are promiscuous and can generate several different polyubiquitin linkages. The UBE2D family of E2s function with a wide variety of E3 ligases to form different K48-, K29-, and K11-linked chains, as well as monoubiquitinated substrates (Brzovic and Klevit, 2006; Brzovic et al., 2006; David et al., 2010; Sakata et al., 2010). The UBE2E family of E2s (Banka et al., 2015; Schumacher et al., 2013), UBE2E2 and UBE2E3, have been found predominantly through mass spectrometry studies to form mixtures of K48, K63, and K11 chains (David et al., 2010). Certain E2 enzymes can be quite specific for the type of the linkage type they form. As mentioned above, UBE2N/UEV1a makes only K63-linked polyubiquitin chains. However, UBE2N/UEV1a only elongates ubiquitin chains and cannot initiate formation of a K63-linked chain on a non-ubiquitin substrate. UBE2N/UEV1a therefore cannot to monoubiquitylate a substrate unless that substrate is free ubiquitin (Petroski and al., 2007; Windheim et al., 2008). UBE2S selectively forms K11 chains on the E3, anaphase-promoting complex (APC/C), and, similar to UBE2N/UEV1a, only functions as a chain elongator (Jin et al., 2008; Williamson and al., 2009). UBE2K is a Class II E2 whose C-terminal extension is needed to selectively form K48-linked chains on monoubiquitinated substrates with RING E3s (Buetow and al., 2015; Chen and Pickart, 1990; Middleton and Day, 2015; Plechanovov et al., 2012). In the absence of an E3, UBE2K forms primarily diUbiquitinfrom free ubiquitin (Chen and Pickart, 1990; Middleton and Day, 2015). These chain-elongating E2s rely on monoubiquitinating E2s (UBE2D, UBE2W, UBE2C) to initiate formation of a chain on a substrate protein. Since UBE2D enzymes lack lysine specificity, they can promiscuously conjugate monoubiquitin to substrates in concert with a diverse array of E3 ligases (Brzovic and Klevit, 2006). UBE2W is unique in that it primarily monoubiquitinates substrates by conjugating ubiquitin to the N-terminus of substrate proteins (Fletcher et al., 2015; Scaglione et al., 2013; Tatham et al., 2013). UBE2C monoubiquitinates the E3 ligase, APC/C, allowing UBE2S to further polyubiquitinate with K11 chains which then signals for substrate proteasomal

degradation during mitosis (Matsumoto et al., 2010; Rape et al., 2006). In addition to the UBE2D family of enzymes, there are several E2s that catalyze chain initiation and elongation for specific chain types. UBE2R1 (also known as Cdc34) is an E2 that cooperates with the E3, SCF, to efficiently form K48-linked chains on a cell cycle inhibitor which triggers the degradation of the inhibitor and signals the cells for entry into S phase (Petroski and Deshaies, 2005; Verma et al., 1997).

In addition to being highly specific and processive in chain elongation, UBE2N/UEV1a (K63), UBE2K (K48), UBE2R1 (K48), UBE2D3 (promiscuous, predominantly K48) and UBE2S (K11), rank as the most abundant E2 enzymes found in human cells (Stewart et al., 2016). Regulation of these very abundant and efficient E2s may come from limited availability of monoubiquitinating E2s, free ubiquitin, and interacting E3 ligases.

1.3 E3 Ubiquitin Ligases

The transfer of ubiquitin from the charged E2 to a specific substrate is catalyzed by E3 ligases. There are three types of E3 ligases: HECT, RING, and RBR, which differ in the mechanism by which they facilitate the transfer of ubiquitin (Berndsen and Wolberger, 2014; Zheng and Shabeck, 2017). HECT E3 ligases contain a catalytic cysteine that transfers the ubiquitin from a charged E2 and forms a thioester linkage with the C-terminus of the donor ubiquitin, E3~Ub (Pickart, 2001; Wang and Pickart, 2005). The substrate ε-lysine then attacks the thioester linkage on E3~Ub, which transfers the ubiquitin molecule to the substrate. A majority of E3s belong to the RING family, which contain a RING or U-box domain that coordinates two zinc atoms in order catalyze the transfer of ubiquitin from E2 to substrate without any E3 catalytic activity (Deshaies and Joazeiro, 2009; Metzger et al., 2014). RING E3s do not form a thioester

ubiquitin intermediate like the HECT ligases, but instead act as a mediator to bring the charged E2 and the target substrate in close proximity to one another (Plechanovov et al., 2012). The RING domain contains a conserved cysteine and histidine residue that are structurally arranged in a cross-brace configuration to coordinate zinc atoms (Borden, 2000; Freemont, 2000; Lovering et al., 1993). The RING domain provides a globular platform to mediate protein-protein interactions (Borden, 2000). Finally, RBR E3 ligases contain features of both HECT and RING E3s. RBRs form a E3~Ub through a catalytic cysteine, as do HECT E3 ligases, and recruit the charged E2 by a RING domain (Spratt et al., 2014).

The small ubiquitin-like modifier (SUMO) protein functions similarly to ubiquitin as a post-translational modification (Hay, 2005). RNF4 is a mammalian RING E3 that belongs to the SUMO-Targeted Ubiquitin Ligase (STUbL) family of E3s that ubiquitinate poly-SUMO substrates (Lallemand-Breitenbach et al., 2008; Sun et al., 2007; Tatham et al., 2008; Uzunova et al., 2007). RNF4 contains four N-terminal SUMO interacting motifs (SIMs) that bind to poly-SUMO as well as C-terminal RING domain that contacts both the E2 and donor ubiquitin in E2~Ub (Moilanen et al., 1998; Tatham et al., 2008). In response to arsenic therapy, Promyelocytic Leukemia Protein (PML) is modified by a poly-SUMO chain that recruits RNF4 and is subsequently ubiquitinated and degraded (Lallemand-Breitenbach et al., 2008; Tatham et al., 2008). This reaction shows varying degrees of processivity depending on the interaction between the E2 enzyme and the RNF4 RING domain (DiBello et al., 2016).

1.4 Deubiquitinating Enzymes

Deubiquitinating enzymes (DUBs) are specialized proteases that remove the ubiquitin modification and disassemble polyubiquitin chains. DUBs recognize ubiquitin and cleave the

isopeptide linkage that connects the ubiquitin C-terminus to the lysine ε-amino of either a protein substrate or another ubiquitin molecule. The ubiquitin whose C-terminus directly contacts the active site of the DUB is referred to as the distal ubiquitin, while ubiquitin molecule containing the lysine that connects to C-terminus of the distal ubiquitin is referred to as the proximal ubiquitin. In humans there are ~100 different DUBs that are implicated in diverse biological pathways including ubiquitin processing, cell cycle regulation, neurodegenerative diseases, inflammatory responses, and tumor migration and growth (Clague et al., 2012; Clague et al., 2019; Turcu et al., 2009). DUBs are divided into seven different families, classified based on the type of catalytic domain. Six of the DUB families are cysteine proteases: ubiquitin specific proteases (USP), ovarian tumor proteases (OTU), ubiquitin C-terminal hydrolases (UCH), Josephins (MJD), MINDY, and ZUP1 (Burrows and Johnston, 2012; Clague et al., 2019; Haahr et al., 2018; Komander et al., 2009; Mevissen et al., 2013; Turcu et al., 2009). The remaining DUB family is exemplified by the zinc-dependent Jab/MPN (JAMM) metalloprotease (Shrestha et al., 2014; Turcu et al., 2009). Just as there are many different types of ubiquitin linkages, chain length, and types of modifications, there are equally abounding possibilities for ubiquitin recognition and the specificity of deubiquitinating enzymes.

DUBs must be able to navigate the intricacies of the ubiquitin system—differentiating between mono- and poly-ubiquitinated species and discriminating between cleaving one linkage type over another. Some DUBs, like MINDY, act as exonucleases, as they preferentially process a chain starting from the distal ubiquitin (Abdul Rehman et al., 2016). Others are endonucleases that cleave preferentially within a chain. USPs comprise the largest family of deubiquitinating enzymes, with over 50 known USP DUBs in humans (Clague et al., 2019; Nijman et al., 2005). These DUBs vary significantly in catalytic rate and show modest preference for linkages types, with only USP30 and CYLD showing specificity for cleaving K6 and both M1 and K63 chains,

respectively (Faesen et al., 2011; Ritorto et al., 2014). By contrast, members of the OTU family of DUBs are typically quite specific for different chain types, with different family members exhibiting distinct chain preference **(Table 1.2)**. The OTU DUBs, OTUB1, OTUD4, and A20 are specific for cleaving K48 linked chains, while OTUD1 and phosphorylated OTUD4 cleave K63 chains (Mevissen et al., 2013; Wang et al., 2009). Cezanne cleaves K11 chains, TRABID cleaves K29 and K33 chains, and OTULIN cleaves linear M1 (Bremm et al., 2010; Evans et al., 2003; Mevissen et al., 2013; Tran et al., 2008). Some deubiquitinating enzymes from the other DUB families also show specificity for particular chain types. MINDY cleaves K48-linked chains (Abdul Rehman et al., 2016), MYSM1 (MJD) and BAP1 (UCH) remove monoubiquitin from histones (Panda et al., 2015; Sahtoe et al., 2016), and ZUP1 cleaves K63-linked chains (Haahr et al., 2018). Linkage specificity is either encoded by the catalytic domain or is determined by the interactions between the DUB and a protein interactor.

1.5 Deubiquitinating enzyme activity can be modulated by forming complexes with other proteins

Many DUBs are found in complex with other proteins (Sowa et al., 2010), which in some cases have been shown to modulate DUB activity (Ventii and Wilkinson, 2008). For example, USP1 must complex with a non-catalytic subunit, UAF1, in order to deubiquitinate key regulators, FANCD2 and FANCI, in the DNA damage response (Cohn and D'Andrea, 2008). USP14, UCH37, and Rpn11 all need to associate with the 26S proteasome in order to exhibit any deubiquitinating activity (Ventii and Wilkinson, 2008). In fact, a screen using MALDI-TOF Mass spectrometry of basal isopeptidase activity for 42 DUBs revealed that the majority of these enzymes in their apo form had little to no catalytic activity (Ritorto et al., 2014), raising the possibility that many of them may rely on partner proteins that increase their activity.

Several DUBs have been found to associate with E3 ligases and, less frequently, E2 enzymes (Sowa et al., 2010). A few of these DUB:E3 ligase pairs have a direct role in tumor progression and growth. For example, the DUB:E3 pair, BAP1 (UCH):BRCA1, is implicated in breast and lung cancer growth (Jensen et al., 1998) and USP2a:Mdm2 is directly linked to apoptosis and the development of prostate cancer (Priolo et al., 2006). Other DUB:E3 pairs that serve to regulate the catalytic activities of both enzymes include: USP4:Ro52, USP7:Mdm2, USP20:VHL, USP8:Nrdp1, USP33:VHL, and USP28:FBW7alpha (Li et al., 2004; Li et al., 2002; Li et al., 2005; Popov et al., 2007; Ventii and Wilkinson, 2008; Wada and Kamitani, 2006; Wu et al., 2004). For most of these pairs, it is believed that both DUB and E3 regulate one another's activity. In the absence of their DUB interactors, Ro52 and Mdm2 are autoubiquitylated, which then signals for proteasomal degradation of these E3 ligases (Clegg et al., 2008). However, when bound to their respective DUBs, USP4a and USP7, autoubiquitination is inhibited (Meulmeester et al., 2005; Wada and Kamitani, 2006). Therefore the DUB protects the E3 from degradation. In turn, Ro52 affects the stability of USP4a by ubiquitylating the DUB and targeting it for degradation (Wada and Kamitani, 2006). For some DUB:E3 pairs determined through *in vitro* methods, such as USP7:ICP50 (Holowaty et al., 2003) and USP9:Mind bomb1 (Mib1) (Choe et al., 2007), the biological significance of the DUB-E3 interaction is still not known. There are rarer cases of DUBs partnering with E2 ubiquitin conjugating enzymes. OTUB1 (OTU) is one such DUB. By binding to charged UBE2N, OTUB1 is able to sequester and prevent this E2 from forming K63 chains at double stranded DNA breaks (Nakada et al., 2010; Wiener et al., 2012). In turn, UBE2N has been found to stimulate the deubiquitinating activity of this DUB (Wiener et al., 2013). More details about this unique DUB:E2 interaction are discussed below.

Two essential themes concerning DUBs and their non-substrate protein binders have emerged from extensive studies. First, many DUBs function in complex with another non-substrate protein. Second, unless bound to its partner protein, DUB activity is low. The fact that so many DUBs are complexed with either E3 ligases or E2s demonstrates that the process of ubiquitylation and deubiquitylation is not a simple sequential cycle. Rather, DUBs and ubiquitylating enzymes work in concert with one another, regulating each other's activity in order to modulate and maintain ubiquitination in response to extracellular events.

1.6 OTUB1, a non-canonical deubiquitinase

OTUB1 is a highly expressed OTU DUB that is specific for reversing K48-linked modifications (Wang et al., 2009). OTUB1 is expressed in a wide variety of different human tissue cells, with high expression in the brain (Fagerberg et al., 2014). Knocking out OTUB1 in mice results in embryonic lethality (Pasupala et al., 2018) and knocking down this DUB produces mice with reduced grip strength (Schwanhäusser et al., 2011). The most complete structure of OTUB1 is of a hybrid recombinantly expressed *C. elegans* OTU domain with a human 40 amino acid N-terminal fusion (Wiener et al., 2013; Wiener et al., 2012) **(Figure 1.4b)**. As the N-terminus is predicted to be intrinsically disordered in the apo state, this structure elucidated for the first time the α-helical fold of the N-terminus (Edelmann et al., 2008; Wiener et al., 2012). OTUB1 contains two distinct ubiquitin binding sites, a distal and proximal site **(Figure 1.4c)**, with the N-terminal helix providing additional contacts for the proximal ubiquitin binding site (Wiener et al., 2012). The structure showed the OTUB1 catalytic triad comprised of an aspartate, cysteine and histidine residue are positioned where the K48 linkage would be **(Figure 1.4d)**.

The DUB activity of OTUB1 is implicated in numerous biological roles **(Table 1.3).** By stabilizing the transcription factors FOXM1 (Karunarathna et al., 2016; Wang et al., 2016) and ERα (Stanišić et al., 2009), OTUB1 is a regulator of transcriptional activation and to a more broader extent, is a regulator of ovarian, breast, and endometrial cancers. Additionally, OTUB1 deubiquitinates particular E3 ligases such as: TRAF3 & TRAF6, which are essential in controlling virus triggered interferon induction (Li et al., 2010); c-IAP, which regulates NF-κB and MAPK signaling in addition to modulating apoptosis (Goncharov et al., 2013); and GRAIL, which regulates T-cell anergy (Soares et al., 2004).

In addition to its canonical deubiquitinating activity, OTUB1 non-catalytically binds to and inhibits the ubiquitin conjugating activity of E2 enzymes. In addition to the two different ubiquitin binding sites, OTUB1 also contains an E2 binding site **(Figure 1.4.c, e)**. The N-terminal helix not only provides contacting surfaces for the proximal ubiquitin but also for interacting with an E2. The ability of OTUB1 to inhibit E2 enzymes in a non-canonical manner was first discovered by Nakada et al. (Nakada et al., 2010), who found that OTUB1 suppresses K63 chain formation by the E2 enzyme, UBE2N, and its non-catalytic partner, UEV1a (Nakada et al., 2010; Sato et al., 2012). In response to double stranded DNA breaks, UBE2N/UEV1a and the E3 ligase, RNF168, attaches K63-linked polyubiquitin to the site of damage. These regulatory chains signal for downstream recruitment of two repair protein complexes: RAP80-BRCA1 (Kim et al., 2007; Sobhian and al., 2007; Wang and al., 2007; Wu and al., 2009) and 53BP1 (Doil and al., 2009; Huen and al., 2007; Mailand and al., 2007), which are essential for passing the G/M checkpoint. Independently of its DUB activity, OTUB1 prevents UBE2N/UEV1a from transferring ubiquitin to the E3 (Nakada et al., 2010). Therefore, OTUB1 is a negative regulator of double stranded DNA response repair mechanisms. This result proved to be quite intriguing in that OTUB1 is highly specific for cleaving K48 linked chains and yet is able to inhibit an E2 that produces K63-linked

chains. In addition, OTUB1 is known to inhibit the ubiquitin conjugating activity of the E2, UBE2D both *in vitro* (Clegg et al., 2008) and *in cellulo* (Sun et al., 2012) which affects different biological processes depending on the target **(Table 1.4)**. OTUB1 is able to prohibit UBE2D from ubiquitinating a number of different substrates including: RAS isoforms (Baietti et al., 2016) p53 (Sun et al., 2012), DEPTOR, (Zhao et al., 2018), and SMAD2/3 (Herhaus et al., 2013).

Structural and biochemical studies helped to elucidate the manner by which OTUB1 non-canonically regulates these E2 enzymes by preferentially binding to the charged E2 in a manner that depends on the N-terminus (Juang et al., 2012; Nakada et al., 2010; Wiener et al., 2012). Structural studies show that OTUB1 directly binds to the thioester linkage of the charged E2s, UBE2N (Wiener et al., 2012) and UBE2D2 (Juang et al., 2012; Wiener et al., 2013). Additionally, biochemical studies demonstrate that OTUB1 preferentially interacts with E2~Ub versus the uncharged E2 (Nakada et al., 2010; Wiener et al., 2013; Wiener et al., 2012). By binding to the charged E2, OTUB1 prevents ubiquitin transfer from the E2 to substrates (Juang et al., 2012; Wiener et al., 2013) **(Figure 1.4e)**. By binding to UBE2N~Ub, OTUB1 not only stops ubiquitin transfer but also prevent UBE2N from heterodimerizing with UEV1a, which is necessary for K63 polyubiquitination (Wiener et al., 2012). OTUB1 also prevents the RING domain of both RNF168 (Nakada et al., 2010) and RNF4 (Wiener et al., 2012) E3 ligases from binding to the E2 as OTUB1 and RINGs share the same site. Structural studies also indicate that this mode of E2 inhibition is dependent on an allosteric conformational change initiated by ubiquitin binding to the proximal site on OTUB1, which triggers conformational changes in the proximal ubiquitin-binding site and drives formation of the α-helical N-terminus (Wiener et al., 2012). The N-terminus provides additional contacting surfaces for both the E2 and the proximal ubiquitin binding site, which favors interaction with E2~Ub. Removing the N-terminus completely abolishes OTUB1's ability to non-canonically inhibit UBE2N (Nakada et al., 2010). Binding

preferentially to the charged E2 is correlated with increasing concentrations of free Ub (Wiener et al., 2012).

1.7 Regulation of both canonical and non-canonical activities for OTUB1

Post-translational modifications of OTUB1, ubiquitination, hydroxylation, and phosphorylation, regulate its activity and may have implications for its non-canonical E2 inhibition **(Table 1.4)**. When investigating the role of OTUB1 in inhibited UBE2D ubiquitination of p53, the Dai lab (Li et al., 2014) noted a higher molecular weight form of the DUB that corresponded to ubiquitinated OTUB1. Systematic mutational analysis, in which each lysine on OTUB1 was mutated to an arginine, revealed that OTUB1 can be ubiquitinated at either residue 59 or 109. Substitution of all lysines with arginine (K0) rendered OTUB1 unable to inhibit p53 ubiquitination. It is unclear whether it is the lack of lysines or the lack of ubiquitinated OTUB1 that abolishes the non-canonical inhibition of UBE2D. In addition, OTUB1 can be hydroxylated at N22, which restricts the DUB interactome (Scholz et al., 2016). Although hydroxylation does not change the isopeptidase activity of OTUB1, Scholtz et al. predict that this modification may affect non-canonical inhibition, as the site of hydroxylation is located on the N-terminus which contacts the thioester of the charged E2. Serine 16, also located on the N-terminus of OTUB1, is phosphorylated by casein kinase 2 (CK2) (Herhaus et al., 2013). Although phosphorylation did not affect either the DUB nor the non-catalytic activities of OTUB1, the modification does signal for nuclear localization of the DUB. In response to DNA damage, chromatin is ubiquitinated, so phosphorylating OTUB1 may sequester it in the cytosol. Recent studies have revealed that OTUB1 can be conjugated with the ubiquitin-like modifier, FAT10 (Bialas et al., 2019). Covalently linking FAT10 to OTUB1 targets the DUB for proteasomal degradation; however, when OTUB1 noncovalently interacts with FAT10, it increases the DUB activity in cleaving both

K48 diUbiquitinand Ub-AMC. It is unclear to what extent these post-translational modifications have an effect on either the deubiquitinating and non-catalytic activities of OTUB1.

1.8 The cross-regulatory complex of OTUB1: E2 enzymes

When in complex, OTUB1 and its E2s cross-regulate one another's activity. I previously discussed how OTUB1 non-canonically inhibits UBE2N and UBE2D enzymes from conjugating ubiquitin. In turn, binding of different E2s has implication for the DUB activity of OTUB1. Surprisingly, *in vitro* kinetic studies that assayed the isopeptidase activity of OTUB1 on K48 diUbiquitinshowed that the DUB activity of OTUB1 is broadly stimulated in the presence of UBE2D1, UBE2D2, UBE2D3, UBE2N, and UBE2E1 (Wiener et al., 2013). A detailed kinetic analysis of the effects of UBE2D2 showed that this E2 robustly stimulated the isopeptidase activity of OTUB1 for cleaving K48 linked diUbiquitin (K48 diUb), with a dramatic lowering of K_M from 120 μM to 3.4 μM, and no overall effect on k_{cat} (Wiener et al., 2013). With no change to k_{cat}, the E2 does not affect the turnover rate for OTUB1 to convert diUbiquitininto monoubiquitin. The physiological consequence of lowering the K_M suggests that the DUB activity of OTUB1 is more active at ubiquitin concentrations that it will likely encounter in the cell. Another interesting result from this DUB study showed that UBE2N only weakly stimulated the cleaving ability of OTUB1. Since OTUB1 efficiently inhibits UBE2N from heterodimerizing with its non-cognate UEV1a and sequesters the E2 from making K63 linked chains, it is interesting that UBE2N only modestly affects OTUB1. The *in vitro* kinetic assay also established UBE2W as an interacting partner that can stimulate the catalytic activity of OTUB1 (Wiener et al., 2013). UBE2W is a highly disordered E2 that predominantly monoubiquitinates the N-terminal amine (Scaglione et al., 2013). In contrast with the other E2 enzymes that stimulate OTUB1 DUB activity in vitro,

UBE2W has not been identified as an in vivo OTUB1. The biological significance of stimulated DUB activity in the presence of an E2 is unknown.

Although OTUB1 is specific for cleaving K48 chains, it interacts with E2 enzymes that are from different classes and produce various chain types. One similarity for all seven different E2s is that they all interact with the three different types of E3 ligases: RING, HECT, and RBR (Stewart et al., 2016). From non-catalytic inhibition for some of these E2s, together with the marked stimulated DUB activity in the presence of these same E2s, a model for cross-regulation emerges. The OTUB1:E2 cross-regulation occurs when OTUB1 regulates the ubiquitin conjugating activity of the E2 and in turn, the E2 also affects the deubiquitinating activity of OTUB1.

1.9 Objectives

Mass spectrometry and proteomic studies revealed that OTUB1 interacts with seven different E2s *in cellulo:* UBE2D1, UBE2D2, UBE2D3, UBE2N, UBE2E1, UBE2E2, and UBE2E3 (Nakada et al., 2010; Sowa et al., 2010) **(Table 1.5)**. I sought to study and understand the cross-regulatory complex, OTUB1:E2, through *in vitro* biochemical assays and structural methods. The Wolberger lab found that the isopeptidase activity of OTUB1 is enhanced over a broad range of stimulation. I wondered what molecular mechanisms were governing these differences in stimulation. Since kinetic parameters for DUB activity were already established in the presence and absence of UBE2D2 (3.4 μM to 120 μM respectively) (Wiener et al., 2013), I wanted to fill in the gaps and determine kinetic parameters for the remaining OTUB1-interacting E2s. Some of these OTUB1-interacting E2s are known to be inhibited by OTUB1. As discussed earlier, OTUB1 non-canonically sequesters E2s like UBE2N, UBE2D2, and UBE2D3 from

interacting with their corresponding E3 ligases (Chen et al., 2016; Nakada et al., 2010; Sato et al., 2012; Sun et al., 2012). Non-catalytic inhibition of these E2s was observed using different E3 partners, means of analysis (Western blots vs Coomasie stain), and even different versions of OTUB1 were used. In order to make direct comparisons of inhibition for each E2, those already studied and the additional four remaining OTUB1-interacting E2s, I performed gel-based inhibition assays which brought about a more cohesive manner for analysis. These gel-based assays helped to answer the question, at what concentration is OTUB1 able to successfully sequester the E2? From the stimulation and inhibition parameters I can better understand the mode of regulation that governs the OTUB1:E2 cross-regulatory complex.

The demographics of the ubiquitin system in the cell play a major role in understanding why the OTUB1:E2 complex is so important for regulating both ubiquitylation and deubiquitylation. OTUB1 is one of the most abundant DUBs with an estimated amount of $> 4 \times 10^6$ copies, roughly 2.93 µM, found in human cells (Clague et al., 2015). UBE2N / UEV1 and UBE2D3 rank among the highest abundant E2s in both mice and human cells with relative concentrations of 1.3 µM and 1.7 µM, respectively (Kulak et al., 2014; Schwanhäusser et al., 2011). The fact that in the presence of UBE2D2, the K_M of OTUB1 drops 34-fold, led to the hypothesis that the E2 primarily serves to lower the affinity of OTUB1 for K48 diUbiquitinto concentrations to a more physiological concentration (Wiener et al., 2013). Although the concentrations of K48 diUbiquitinis unknown, it is more likely that OTUB1 will encounter 3.4 µM rather than 120 µM of this substrate in the cell. I are curious to see how the balance between the two different activities: canonical DUB activity and non-canonical E2 inhibition, compare with actual cellular concentration for these different proteins in the cell.

This thesis is divided into studying the two sides of the cross-regulatory complex, OTUB1:E2. Chapter 2 focuses on the DUB stimulation by E2 partners and Chapter 3 In this chapter, I describe the in-depth biochemical studies used to establish binding and FRET-based kinetic parameters to define the molecular mechanisms responsible for E2 facilitated stimulation of OTUB1's DUB activity. The following are determined: binding affinities between the E2 and OTUB1, effective concentrations (EC_{50}s) for E2 facilitated stimulation, and kinetic constants (K_M and k_{cat}) in the absence and presence of the different OTUB1-interacting E2s. Chapter 3 analyzes the role that OTUB1 plays in non-catalytically inhibiting the seven different OTUB1-interacting E2s through gel based biochemical assays. In this thesis, I standardize the analysis for OTUB1 facilitated inhibition for all seven E2s so that all activity is comparable, and I use the same gel based assay, E1 and E3, and concentrations of OTUB1. Chapter 3 summarizes the strategies employed to obtain a structure of OTUB1 with one of its E2 partners, UBE2E1. Currently, the only structures of OTUB1 complexed with an E2 are either with UBE2D2 or with UBE2N, both of which are Class I E2s. UBE2E1 is a Class III E2 and although crystals containing both full length OTUB1 and UBE2E1 were obtained, high resolution crystallography data remained elusive.

OTUB1 is involved in several different biological pathways that are directly linked to the progression and growth of various cancers **(Table 1.3 & 1.4)**. OTUB1 specific inhibitors may be developed to help ail or treat many of these different cancer-promoting pathways. DUBs have frequently been used as drug targets as the active cysteine react readily with most inhibitors in order to reduce catalytic activity (D'Arcy et al., 2015; Farshi et al., 2015; Ndubaku and Tsui, 2015; Wang et al., 2017). Since OTUB1 uniquely possesses both catalytic and non-canonical activities, both serve as potential targets to modulate overall activity of this DUB. Some inhibitors, like N-ethylmaeleimide, have been shown to target active site cysteine and diminish

catalytic activity of OTUB1 (Balakirev et al., 2003). The inhibitor, Ubc.B1.1, attaches to the distal ubiquitin binding and disrupts both deubiquitinating activity of OTUB1 and non-canonical E2 inhibition (Ernst et al., 2013; Gorelik and Sidhu, 2016). Indeed, as more information about the molecular mechanisms that govern the OTUB1:E2 cross-regulatory are more studied, I will begin to elucidate additional routes to target DUB inhibitors.

Table 1. 1 Types of ubiquitin modifications and chain diversities

Ub modification	Quantification	Function
 free Ub	~17 μM, HEK293 (23% of total Ub) ~10 μM, MEF (23% of total Ub) (Kaiser et al. 2011)	• Conjugation to multiple diverse substrates
 monoUb	~50 μM, HEK293 (68% of total Ub) ~28 μM, MEF (63% of total Ub) (Kaiser et al. 2011)	• Protein localization • Transcription regulation • DNA damage response
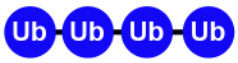 Linear, M1	< 0.05% (Dammer et al. 2011)	• NF-κB signaling
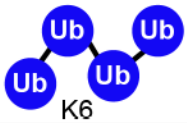 K6	< 1%, HEK293 & MEF (Kaiser et al. 2011)	• UV radiation response • Mitochondiral depolarization
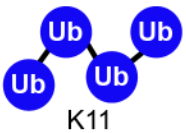 K11	~0.35 μM, HEK293 ~0.6 μM, MEF (Kaiser et al. 2011)	• Cell cycle control
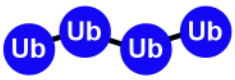 K27	< 0.1% HEK293 & MEF (Dammer et al. 2011)	• DNA damage response • Innate immune response
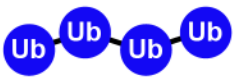 K29	< 0.1% HEK293 & MEF (Kaiser et al. 2011)	• Inhibitor of Wnt signaling • Substrate lysosomal degradation • Kinase modification
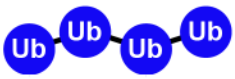 K33	< 1% HEK293 & MEF (Kaiser et al. 2011)	• Anterograde protein trafficking
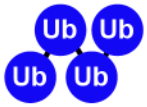 K48	~6 μM, HEK293 ~5 μM, MEF (Kaiser et al. 2011)	• Proteasomal degradation • ER-associated degradation • Transcription regulation • Ubiquitin chaperone activation
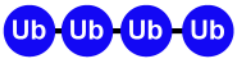 K63	~0.9 μM, HEK293 ~1.1 μM, MEF (Kaiser et al. 2011)	• DNA damage repair • Autophagy
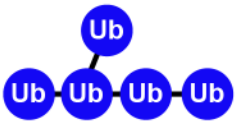 branched	Unavailable	• K11 & K48, substrate proteasomal degradation

Table 1. 2 Known DUBs and their corresponding family that are specific for cleaving the following linkage types

Ub modification	DUB/Family	
Non-specific	Most USPs	
	MYSM1 / JAMM USP3 / USP USP16 / USP	USP22 / USP BAP1 / UCH
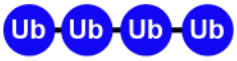 Linear, M1	OTULIN / OTU CYLD / USP	
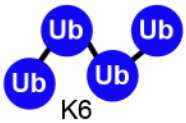 K6	USP30 / USP	
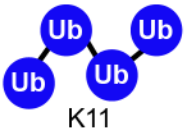 K11	Cezanne / OTU	
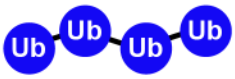 K27		
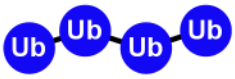 K29	TRABID / OTU	
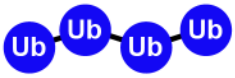 K33	TRABID / OTU	
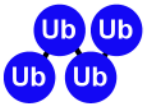 K48	OTUB1 / OTU OTUD4 / OTU A20 / OTU MINDY / MINDY	
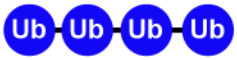 K63	AMSH / JAMM AMSHLP / JAMM BRCC3 / JAMM phospho-OTUD4 / OTU	ZUP1 / ZUP1 CYLD / USP OTUD1 / OTU

Table 1. 3 Deubiquitinating activity of OTUB1 involved in several diverse biological pathways

Pathway	Target	Result
Ovarian Cancer	FOXM1 (Transcription factor)	Stabilizes FOXM1 and mediates epirubicin resistance (Karunarathna et al., 2016)
Breast Cancer	FOXM1 (Transcription factor)	Overexpression of FOXM1 and OTUB1 leads to increased tumour migration and growth (Wang et al., 2016)
Endometrial Cancer	Estrogen receptor, ERα (Transcription factor)	Negatively regulates transcription and stabilizes ERα in chromatin (Stanišić et al., 2009)
Virus-triggered type I interferon induction (INF)	TRAF3 & TRAF6 (E3 Ligases)	Negatively regulates INF (Li et al., 2010)
Apoptosis	c-IAP (E3 Ligase)	Regulates NF-κB and MAPK signalling pathways and cell death by modulating c-IAP1 stability (Goncharov et al., 2013)
T-cell anergy	GRAIL (E3 Ligase)	OTUB1 regulates GRAIL-mediated ubiquitination (Scares et al., 2004)

From left to right: known biological pathways associated with the DUB activity of OTUB1; the substrates that are deubiquitinated; and the role OTUB1 plays in each particular pathway.

Table 1. 4 OTUB facilitated non-canonical inhibition of E2 enzymes is implicated in diverse biological processes

Pathway	E2 / E3	Target	Result
double stranded DNA break response	UBE2N & UEV1a / RNF168	H2A-Ub	OTUB1 inhibits K63 polyubitinating activity of UBE2N & UEV1a heterodimer (Nakada et al. 2010)
DNA damage repair	UBE2D / Mdm2	p53	Overexpression of OTUB1 stabilizes and activates p53, leading to apoptosis and inhibition of cell proliferation (Sun et al. 2012)
Lung Cancer	UBE2D3 / RABEX5	RAS	Overexpression of OTUB1 correlates to tumor growth (Baietti et al. 2016)
mTOR1 signaling	UBE2D	DEPTOR	OTUB1 stabliizes DEPTOR, a regulator of cell growth and metabolism (Zhao et al. 2018)
TGFβ pathway	UBE2D / NEDD4L	SMAD2/3	OTUB1 stabliizes SMAD2/3, regulators of TGFβ-mediated gene transcription and cellular migration (Herhaus et al. 2013)
Endometrial Cancer		Estrogen receptor ERα (Transcription factor)	Negatively regulates transcription and stabilizes ERα in chromatin. Catalytic mutant, OTUB1 C91S inhibits transcription but affected E2 is unknown (Stanišić et al., 2009)

From left to right: known biological pathways associated with OTUB1's non-canonical inhibition of E2 enzymes; the E2 enzymes it inhibits and the known E3 ligases that OTUB1 blocks ubiquitin transfer to; the targets are typically ubiquitinated; and the result of OTUB1 facilitated inhibition.

Table 1. 5 OTUB1-interacting E2s

a

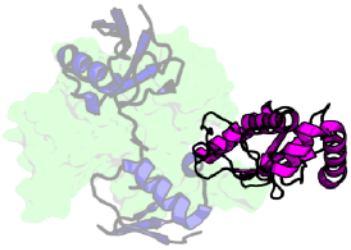

OTUB1-Interacting E2s	Alternate Names	Linkage Type	General Info
UBE2D1 UBE2D2 UBE2D3	UbcH5A UbcH5B UbcH5C	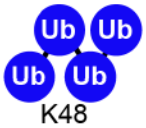 K48	• Class I family of E2s • UBE2D3, highly abundant E2 • Collaborating E3s: RING, HECT, RBR
UBE2N	Ubc13	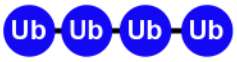 K63	• Class I E2, heterodimerizes with Ube2V family to polyUb • Highly abundant E2 associated with double stranded DNA repair • Collaborating E3s: RING, HECT, RBR
UBE2E1 UBE2E2 UBE2E3	UbcH6 UbcH8 UbcH9/UbcM2	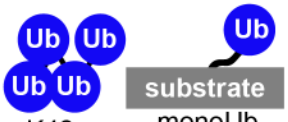 K48 monoUb	• Class III family of E2s polyubiquitination restricted by N-terminal domains • intrinsically disordered N-terminus • Collaborating E3s: RING, HECT, RBR
UBE2W	Ubc16	 monoUb	• Class I E2 • Highly disordered E2 • Collaborating E3s: RING, HECT, RBR

Proteomic and mass spectrometry studies revealed that OTUB1 interacts with seven E2s in cellulo: UBE2D1, UBE2D2, UBE2D3, UBE2N, UBE2E1, UBE2E2, and UBE2E3. Additional in vitro studies revealed that OTUB1 is also capable of interacting with UBE2W. The alternate names that are interchangeably used for these E2s are listed, as well as the chain types that these enzymes are known to create. Additional information (i.e.: E2 Class type, interacting E3 ligases) are listed as well.

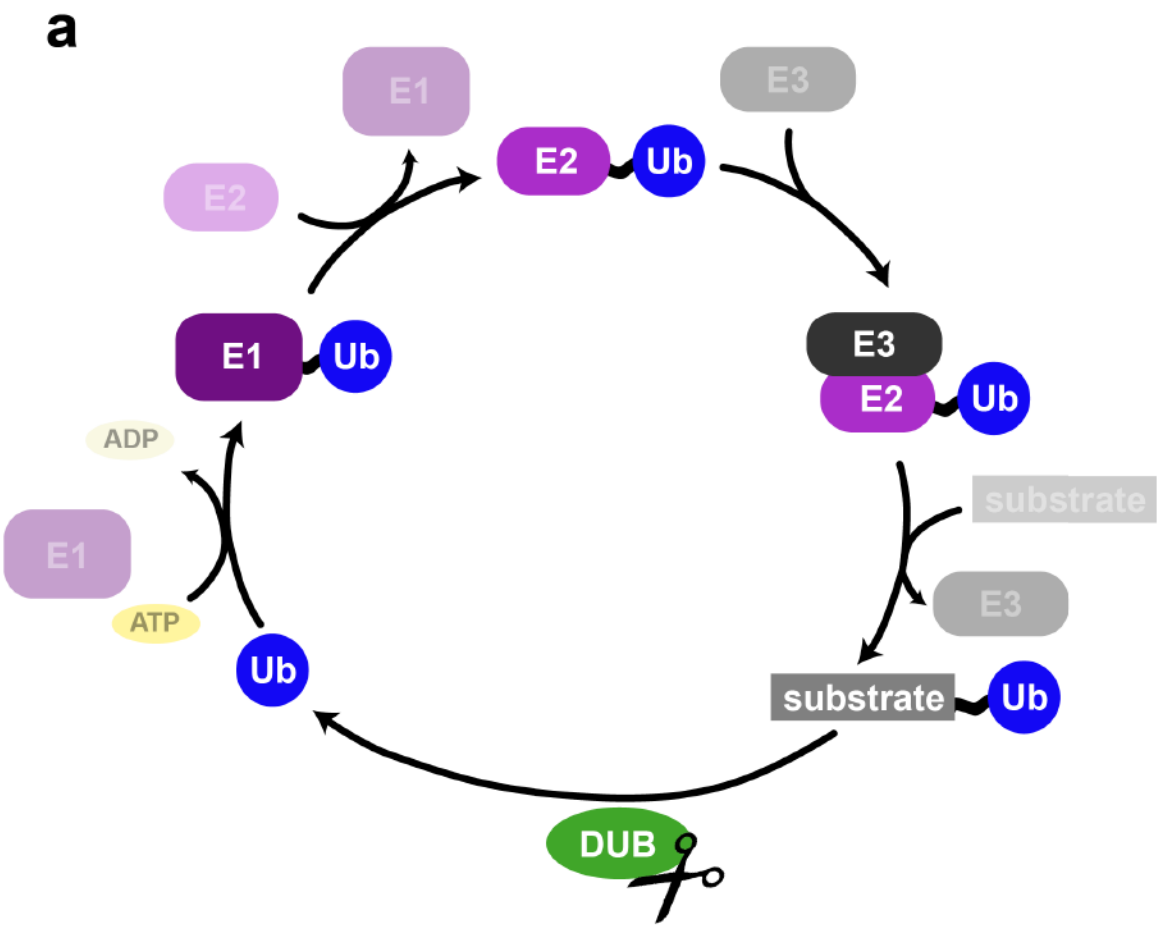

Figure 1. 1 E1-E2-E3 cascade
(a) *Schematic of ubiquitination facilitated by the E1, E2, E3 enzymes. Removal of ubiquitin modification is processed by deubiquitinating enzymes, DUBs.*

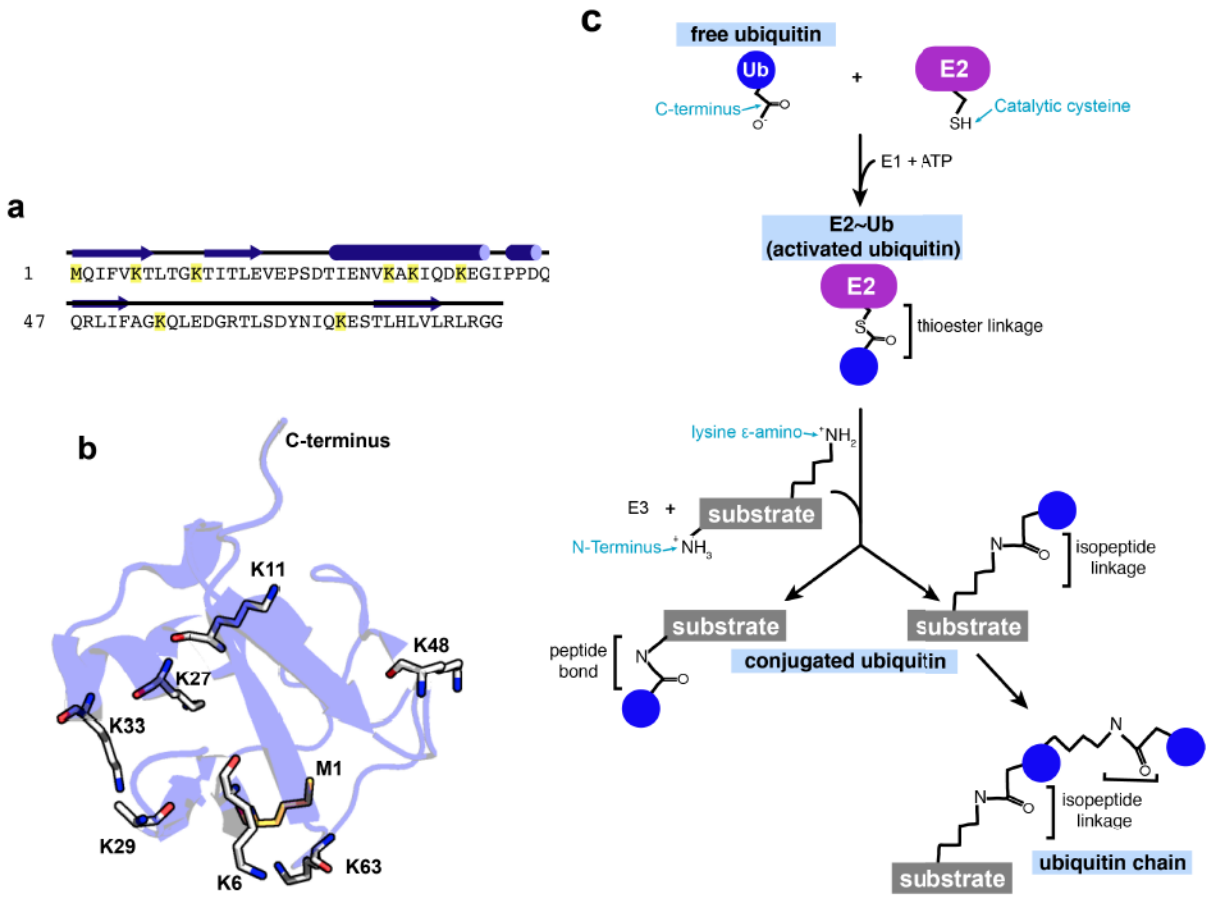

Figure 1. 2 Ubiquitin

(a) *Sequence of Ub wt with the 7 lysines and N-terminal Met highlighted.* ***(b)*** *Structure of Ub with the locations of the lysines along with M1 and the C-terminus.* ***(c)*** *Different states of ubiquitin found in the cell: free ubiquitin; activated via a thioester linkage to an E1, E2, and some E3 enzymes; two types of monoubiquitinated substrates either conjugated to a substrate via the N-terminus (M1) resulting in a peptide bond or conjugated to a substrate lysine forming an isopeptide linkage; and finally, ubiquitin forms chains with the linkage connecting one ubiquitin molecule being an isopeptide bond.*

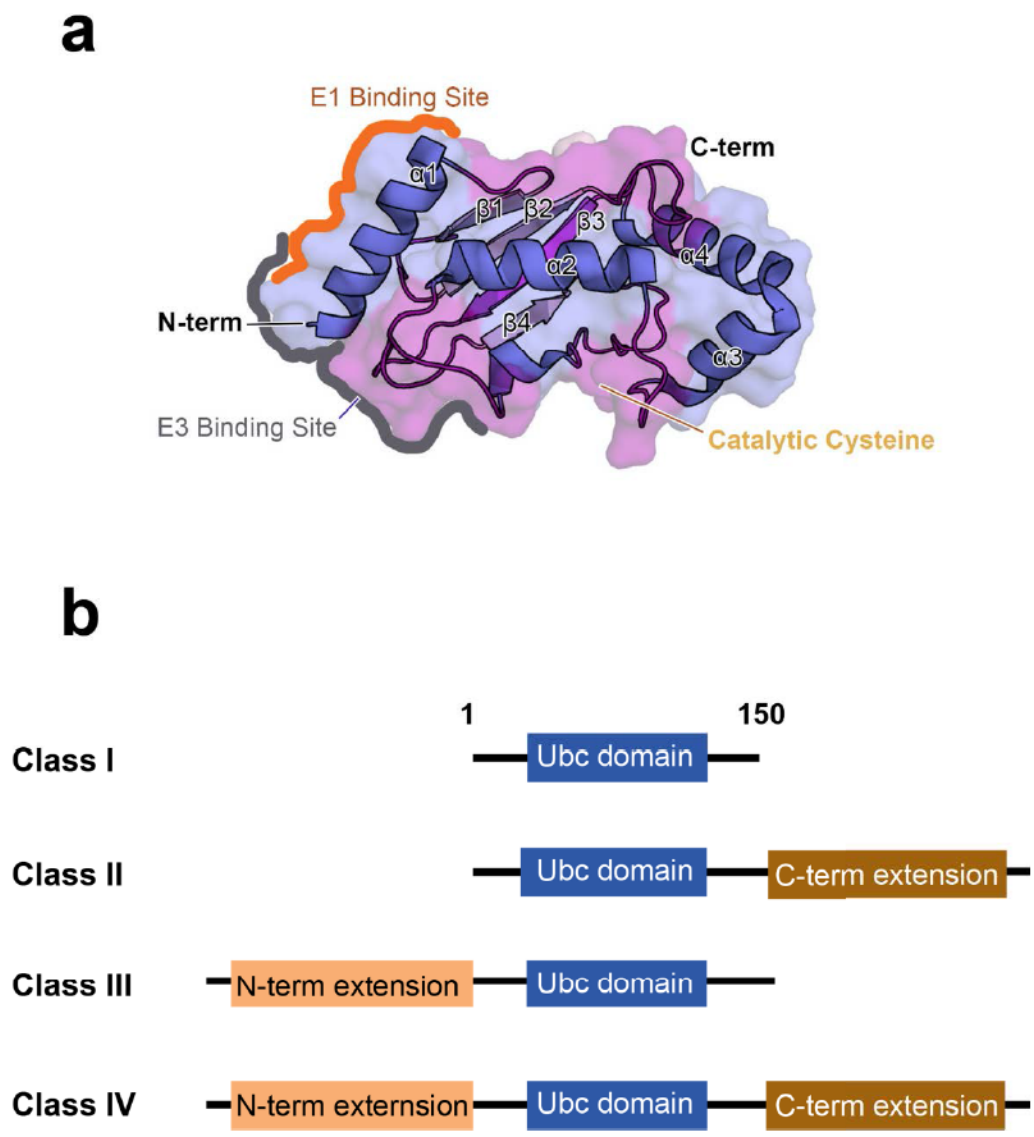

Figure 1. 3 E2 enzymes separated by domain architecture
(a) *Structural schematic from UBE2D3, PDB: 2fUH depicts the conserved catalytic Ubc fold shared by all E2 enzymes. The α -helices and β-sheets that define the Ubc structural elements are indicated. Additionally, known surfaces contacting the E1 and E3 enzymes are designated.* ***(b)*** *Different classifications for E2 enzymes based on domain architecture.*

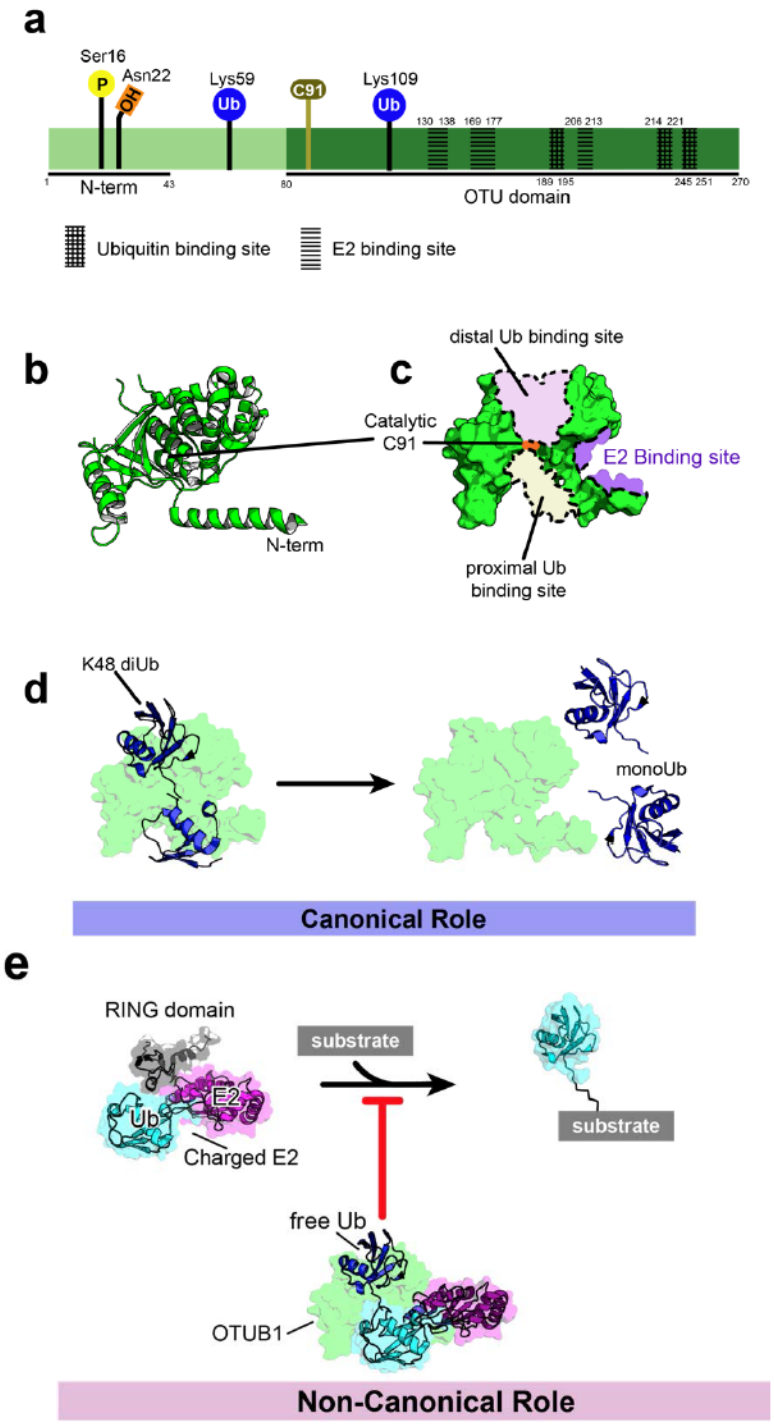

Figure 1. 4 General information about OTUB1

(a) *Schematic of OTUB1. Regions of interest: Ub and E2 binding sites as well as the location of the catalytic cysteine are indicated. In addition, current known locations for post-translational modifications are marked with their corresponding residues on OTUB1.* ***(b)*** *Cartoon depiction of most complete solved structure of OTUB1 from PDB: 4DHZ of hybrid human N-terminus fused to C. elegans OTUB1 body.* ***(c)*** *Surface depiction of apo OTUB1. Locations of the two ubiquitin binding sites, E2 binding site, and catalytic cysteine are depicted.* ***(d)*** *Canonical role of OTUB1, cleaving of K48 ubiquitin chains.* ***(e)*** *Non-canonical role of OTUB1, inhibition of the ubiquitin conjugating activity of select E2 partners.*

Chapter 2 Select E2s stimulate the DUB activity of OTUB1

2.1 Introduction

Although OTUB1 is a well-established deubiquitinase, relatively little is known about the biological role of its DUB activity (Goncharov et al., 2013; Karunarathna et al., 2016; Li et al., 2010; Soares et al., 2004; Stanišić et al., 2009; Wang et al., 2016), as compared to its role in non-canonical inhibition of E2 enzymes (Baietti et al., 2016; Chen et al., 2016; Herhaus et al., 2013; Nakada et al., 2010; Zhao et al., 2018). Several studies have linked the DUB activity of OTUB1 to both the progression and inhibition of cancer **(Table 1.4)** (Goncharov et al., 2013; Karunarathna et al., 2016; Stanišić et al., 2009), making it important to understand how OTUB1 is regulated in vivo. A test of OTUB1 DUB activity in the presence of eleven different E2s unexpectedly showed that a subset could stimulate isopeptidase activity (Wiener et al., 2013). The E2 enzymes that stimulated OTUB1 included UBE2D1, UBE2D2, UBE2D3, UBE2N, and UBE2E1, which had previously been identified as OTUB1-interacting E2s i*n vivo* and whose ubiquitin conjugating activity is non-canonically inhibited by OTUB1 (Nakada et al., 2010; Sowa et al., 2010). Interestingly, UBE2W, which was not known to interact *in vivo* with OTUB1, was also robustly stimulated the DUB activity of OTUB1 (Wiener et al., 2013). In qualitative time course assays, UBE2N only weakly stimulated the DUB activity of OTUB1 as compared with the stimulation by UBE2E2, which was surprising given that OTUB1 strongly inhibits the ubiquitin conjugating activity of UBE2N and UBE2D2 (Nakada et al., 2010). The biological consequence of this E2 facilitated stimulation of DUB activity remains unknown.

The cross-regulatory complex, OTUB1:E2, serves a dual role in regulating ubiquitylation and deubiquitylation. The potential for cross-regulatory networks that govern the conditions under

which OTUB1 binds to its E2 partners and results in either E2 inhibition or OTUB1 stimulation depends on the relative kinetics and thermodynamics of the interactions, which have remained understudied. In the presence of UBE2D2, a robust stimulator, the K_M of OTUB1 for K48 diUbiquitinis greatly reduced from 120 μM to 3.4 μM with no change to k_{cat} (Wiener et al., 2013). This result suggests that interactions between OTUB1 and UBE2D2 change the affinity of the DUB for K48 diUbiquitinwithout affecting the turnover rate. In this chapter, I study the molecular mechanisms responsible for this K_M change by measuring the changes in DUB activity in the presence of the various OTUB1-interacting E2s using a FRET-based assay. I determine the kinetic parameters for the other OTUB1-interacting E2s and show that DUB stimulation occurs over a range of enzyme concentrations that correspond to those measured in cells(Kulak et al., 2014; Schwanhäusser et al., 2011). Understanding the mechanisms that control cross-regulation could give us insights into how DUBs regulate ubiquitination in concert with E2 enzymes.

2.2 Results

2.2.1 OTUB1-interacting E2s partners all stimulate the DUB activity of OTUB1 to varying degrees

Proteomic studies identified UBE2E2 and UBE2E3 as binding partners of OTUB1 in pull-down experiments from whole cell extracts (Nakada et al., 2010), but the consequences of OTUB1 binding to these E2 enzymes has not been explored. I therefore assayed the relative ability of UBE2E2 and UBE2E3 to stimulate the DUB activity of OTUB1 as compared to the remaining E2 partners, UBE2E1, UBE2N, and the three UBE2D enzymes. I also assayed the interaction between UBE2W and OTUB1; although this E2 was not determined to be an *in vivo* partner, *in vitro* methods found that UBE2W can stimulate the DUB activity of OTUB1 (Wiener et al., 2013).

Using a fluorescence resonance energy transfer (FRET) deubiquitylation assay in which fluorescence of an internally quenched fluorophore on TAMRA-labeled K48 diUbiquitin (diUb) increases when OTUB1 cleaves the isopeptide linkage, I found that UBE2E2 and UBE2E3 only modestly enhanced OTUB1 DUB activity **(Figure 2.1)**. Taking the initial rates from this FRET experiment I determined the fold stimulation in the presence of each E2 **(Figure 2.1.b)**. The UBE2D family of enzymes had the elicited the most stimulated response with the robust stimulator, UBE2D2, having a 26-fold enhancement to DUB activity. UBE2N stimulated isopeptidase activity weakly, with an enhancement of less than 10 fold. As compared to the other E2s, the degree of stimulation observed for UBE2E2 and UBE2E3 was the weakest for all the E2s studied, with less than a five-fold enhancement in DUB activity.

2.2.2 E2-dependent stimulation of OTUB1 is not due to differences in binding affinity

Formation of both repressive and active OTUB1-E2 complexes are governed, in part, by the intrinsic affinity of OTUB1 for each of its *in vivo* E2 partners. To assess the contribution of intrinsic affinity of different OTUB1-E2 pairs to E2 repression and OTUB1 activation, I measured equilibrium dissociation constants (K_d) for OTUB1 binding to UBE2D1, UBE2D2, UBE2D3, UBE2N, and UBE2E1 using isothermal titration calorimetry (ITC) **(Figure 2.2).** For these experiments, I used the catalytically inactive mutant, OTUB1 (C91S), which was also used for assays discussed below of OTUB1 binding to its K48 diUbiquitinsubstrate. I determined that the affinity of each E2 for OTUB1 was similar, with K_d values ranging from 3.9 – 9.3 μM **(Figure 2.2.b-c).** The K_d of UBE2N binding to OTUB1 was 8.1 μM, which is consistent with previous studies that obtained a K_d of 7.04 μM using a fluorescence polarization assay (Wiener et al., 2012) and K_d of 8.9 μM using surface plasmon resonance and GST-fused OTUB1 (Sato et al., 2012). To verify that the OTUB1 C91S mutation did not affect binding to E2 enzymes, I assayed

binding of a subset of the E2s, UBE2D1 and UBE2D3, to wild-type OTUB1 and found no significant difference in K_d values **(Figure 2.3)**. I was unable to measure the K_d for the interactions between OTUB1 and UBE2E2 or UBE2E3, as the two proteins precipitated in the ITC cell and yielded unreliable results.

As a control, I also tested binding of OTUB1 to other E2s that have not been recognized as an interacting partner *in vivo.* As expected, I did not detect any binding between OTUB1 and Cdc34, which selectively forms K48 chains **(Figure 2.4)**. I also looked at binding between OTUB1 and Ube2g2, an E2 that predominantly forms K48 linked chains and is implicated in endoplasmic reticulum-associated protein degradation (Kostova et al., 2007). I found no observable binding between these two proteins, which is interesting given that *in vitro* studies have identified Ube2g2 as an interactor for OTUB1, one that was not previously determined through affinity capture mass spectrometry (Scholz et al., 2016). Overall, OTUB1 bound all E2 partners with similar affinities. Differences in DUB stimulation cannot simply be explained by binding between these two sets of factors.

2.2.3 E2 half-maximal stimulation of OTUB1, EC50s, match intracellular concentrations

As shown in **Figure 2.1** and in a previous study (Wiener et al., 2013), the stimulatory effect of different E2 partners varies. Since OTUB1 binds with similar affinity to all its E2 partners, I sought to understand the mechanism that produced a broad range of stimulation on DUB activity. To further characterize the effect of E2 binding to OTUB1 on DUB activity, I assayed OTUB1 activity as a function of E2 concentration to determine a half-maximal stimulatory response dose for 50% enhancement (EC_{50}). Using a FRET-based assay, I measured and tracked the signal over time in order to establish rates of isopeptidase activity for OTUB1 over

increasing log-base 10 concentrations of E2 (0.001 nM – 100 μM) **(Figure 2.5.a).** I found that the E2 concentration to elicit a stimulatory response was between 0.8 – 10.9 μM. Of all seven OTUB1-interacting E2s that I studied, UBE2N had the lowest EC_{50}, (0.8 μM) therefore OTUB1 requires less of UBE2N to exhibit stimulated activity. This result was very surprising given that UBE2N has proven in previous experiments (Wiener et al., 2013) and in my FRET E2 panel (**Figure 2.1)** to be a weak DUB stimulator. The highest half-maximal stimulation occurred in the presence of both UBE2E2 and UBE2E3, with EC_{50} concentrations of 10.9 and 10.7 μM, respectively. The effective concentrations for half-maximal stimulation by the UBE2D family of enzymes was in the range of 1.5 – 3.9 μM. The EC_{50} for UBE2D2 was determined to be 3.8 μM, whereas a previous study determined the EC_{50} to be 0.5 μM using a gel-based assay (Wiener et al., 2013). It is possible that this large discrepancy may be attributed to the method obtaining these EC_{50} values. Interestingly though, the EC50s determined for UBE2N and UBE2D3 matches the intracellular concentrations of those found in human cells (Kulak et al., 2014; Schwanhäusser et al., 2011) which are 1.3 μM for UBE2N and 1.7 μM for UBE2D3. Taken together, our calculated EC_{50}s suggest that these E2 partners can regulate OTUB1 activity over a physiologically relevant range of concentrations.

I next asked whether the binding of the E2 has a cooperative effect on OTUB1 activity on diUb. The Hill slope, or Hill coefficient, is a measure of cooperativity among multiple ligand binding sites (Prinz, 2010; Weiss, 1997). In the context of our biochemical studies, it estimates how binding of the E2 can change the affinity of OTUB1 for K48 diUb. Slopes > 1 signify positive cooperativity, slopes < 1 indicate negative cooperativity, and for slopes = 1, binding of K48 diUbiquitinis independent binding to the E2. I fit the data using the "log-agonist versus response—variable slope" program within GraphPad Prism version 5.0, which calculates both EC_{50}s and Hill Slopes. As shown in **Figure 2.5.b**, the calculated Hill Slopes were 1.2 ± 0.4 for

UBE2D1, 1.8 ± 0.6 for UBE2D2, 2.2 + 0.6 for UBE2D3, 0.7 ± 0.2 for UBE2N, 1.5 ± 0.5 for UBE2E1, 1.1 + 0.5 for UBE2E2, and 0.7 ± 0.3 for UBE2E3. I observe a Hill slope >1 for all E2s except UBE2N and UBE2E3. The Hill slope for UBE2E3 with the error is 0.7 ± 0.3 placing coefficient closer to one. However, even with the error, UBE2N (0.7 ± 0.2), is still less than one. Comparing the slopes for UBE2D3, the largest Hill coefficient to the least, UBE2N, I saw a stark contrast in the curvature. It is possible that binding of the UBE2N can reduce the affinity of OTUB1 for K48 diUb.

2.2.4 Binding an E2 partner raises affinity of OTUB1 for K48 diUb

I next sought to quantify the degree of stimulated DUB activity in the presence of these OTUB1-interacting E2s. A previous study reported a marked stimulation of the isopeptidase activity in the presence of UBE2D2. The K_M, Michaelis Menten constant, of OTUB1 for K48 diUbiquitinwas lowered 34-fold, from 120 μM to 3.4 μM, in the presence of UBE2D2 respectively (Wiener et al., 2013). Although there was a dramatic reduction in K_M, no change in k_{cat} was detected. In terms of this experiment, K_M is the amount of K48 diUbiquitinneeded for OTUB1 to reach a half maximal reaction rate and k_{cat} describes the turnover rate for OTUB1 to convert K48 diUbiquitininto mono-ubiquitin. With the exception of UBE2D2, kinetic constants have not been determined for the remaining E2 partners of OTUB1. To quantify the degree of stimulation by other E2s, I employed the FRET assay and tracked the cleavage of FRET-K48 diUbiquitinover time in the presence and absence of saturating concentrations of E2s, UBE2D1, UBE2D2, UBE2D3, UBE2N, and UBE2E1 **(Figure 2.6).** For these assays, I used saturating concentrations of each E2 (10 μM) since this is 0.5 to 10 fold higher than the half-maximal effective concentrations that I determined **(Figure 2.5)**. In addition, this FRET assay differed from the assay used to measure EC_{50}s in that the substrate concentration was a ratio of FRET-

K48 diUbiquitinto unlabeled K48 diUb. I kept a constant amount 400 nM FRET-K48 diUbiquitinfor each experiment and added the remaining amounts of unlabeled substrate. From this FRET assay I determined kinetic parameters: K_M and k_{cat}.

Our results showed that, in the absence of an E2, the K_M of OTUB1 for K48 diUbiquitinwas 102 µM and the k_{cat} was 0.03 s^{-1} . Within error, these values are comparable to previous measurements, with a K_M of 78 µM (Wang et al., 2009) and a K_M of 120 µM with a k_{cat} of 0.034 s^{-1} (Wiener et al., 2013), both of which were determined using different methods. I found the Km of OTUB1 for K48 diUbiquitinin the presence of members of the UBE2D family of proteins, UBE2D1 (K_M of 11 µM), UBE2D2 (K_M of 6.6 µM), and UBE2D3 (K_M of 13 µM), was lowered to the greatest degree. I note that the decrease in the KM of OTUB1 in the presence of UBE2D2 was just 16 fold, from 102 µM to 6.6 µM, as compared to the 34-fold decrease that was previously determined (Wiener et al., 2013). The K_M in the presence of UBE2N was 24.1 µM. UBE2N has been qualitatively described as a mild stimulator and our results depict exactly that. Stimulation of DUB activity was weakest in the presence of UBE2E1, which lowered the K_M of OTUB1 for substrate to just 64.3 µM. I did not quantify changes in DUB activity in the presence of either UBE2E2 or UBE2E3. From the DUB stimulation panel in **Figure 2.1**, I predicted that the any enchancement by either UBE2E2 or UBE2E3 would be significantly minimal. Additionally, for each experiment I calculated the k_{cat}/K_M , which is a measurement of catalytic efficiency, as it takes into account both substrate binding and product formation (**Figure 2.6.b)**. Since k_{cat} was largely unchanged, differences in catalytic efficiency resulted in K_M differences. In the absence of an E2, the catalytic efficiency of OTUB1 converting K48 diUbiquitininto monoubiqiutin is 292.7 $M^{-1}s^{-1}$. This rate was largely enhanced in the presence of UBE2D2, from 292.7 $M^{-1}s^{-1}$ to 5000 $M^{-1}s^{-1}$, whereas UBE2N showed a mild increase with a corresponding k_{cat}/K_M of 1452.3 $M^{-1}s^{-1}$.

In steady state conditions, where the rate of converting K48 diUbiquitininto monoubqiutiin is significantly smaller than the rate of OTUB1:K48 diUbiquitincomplex formation, the Michaelis Menten constant K_M is directly proportional to the equilibrium dissociation constant, K_d. In the presence of an E2, the K_M changes but the k_{cat} remains largely unchanged, thus the E2 serves to directly affect the binding affinity between OTUB1 and K48 diUb. I utilized ITC to test if the presence of an E2 partner increases the affinity of OTUB1 for its substrate, K48 diUb. Although the isopeptidase activity of OTUB1 for K48 diUbiquitinwas fully characterized to be weak, with a corresponding K_M of ~100 μM (Wang et al., 2009; Wiener et al., 2013), and the overall binding affinity between OTUB1 and K48 diUbiquitinis believed to be low (Edelmann et al., 2008), the interaction has not been quantified. I first measured the binding affinity of OTUB1 for K48 diUbiquitinusing ITC **(Figure 2.7.a)**. I used a catalytic mutant of OTUB1 (C91S) when titrating in K48-diubiquitin to ensure that the K_d I measured was not a function of both binding and simultaneous cleavage of the substrate. I found that OTUB1 (C91S) weakly binds to its substrate, with a K_d of 80 μM. The high K_M of OTUB1 for K48 diUbiquitinis correlated to a weak affinity between these two proteins.

Next, I asked whether the binding affinity of OTUB1 for K48 diUbiquitinchanges in the presence of saturating concentrations of E2 (150 μM) in both the cell and the syringe. This method allowed us to directly measure K48 diUbiquitinbinding to the OTUB1(C91S):E2 complex without dilution of the E2. It is also important to note that at the concentrations used, binding between E2s and K48 diUbiquitinwas not observed **(Figure 2.8).** I determined equilibrium dissociation constants, between OTUB1 (C91S) and K48 diUbiquitinin presence of E2 partners UBE2D1, UBE2D3, and UBE2N (**Figure 2.7.b-c)**. The presence of an E2 increased affinity of OTUB1 (C91S) for K48 diUb, as reflected in an increase in K_d from 84 μM in the absence of an E2 to 12

μM in the presence of UBE2D1, 13.2 μM in the presence of UBE2D3, and 22.3 μM in the presence of UBE2N. These K_ds are very similar to the K_M values for each corresponding E2 that was examined using the FRET assay **(Figure 2.7.c-d)**, indicating that the lowered K_M reflects the increase in OTUB1 affinity for its diubiquitin substrate when this DUB is bound to an E2 partner. Importantly, not only did I show that the OTUB1:E2 complex changes preference of OTUB1 for its substrate, but I also demonstrated that this phenomenon occurs over different methods, FRET assay and ITC.

2.2.5 Characterization of the OTUB1:UBE2W stimulatory complex

The Wolberger lab determined through *in vitro* methods that UBE2W stimulates the DUB activity of OTUB1 (Wiener et al., 2013). In contrast with the other OTUB1-interacting E2 partners, this unique E2 primarily initiates chain formation by preferentially monoubiquitinates N-terminal amines that are intrinsically disordered (Scaglione et al., 2013; Tatham et al., 2013; Vittal et al., 2015). UBE2W itself contains highly disordered regions (Vittal et al., 2015). In cells, UBE2W monoubiquitinates non N-terminal amines on TRIM5α, an E3 ligase responsible for assembling retroviral capsids that inhibits reverse transcription of viral genomes (Fletcher et al., 2015). UBE2N/UEV1a attaches K63 linked polyubiquitin chains to the monoubiquitins on TRIM5α (Fletcher et al., 2015). The biological role of the interaction between OTUB1 and UBE2W, however, is not known.

I first sought to determine the binding affinity between OTUB1 and UBE2W using ITC **(Figure 2.9)**. After titrating increasing amounts of OTUB1 to the E2, it was not possible to determine a reliable binding isotherm from the data. At pH 7.5, which is the pH at which all other OTUB1:E2 binding assays were performed, the heats became endothermic as more and more OTUB1 was

titrated in. I repeated this experiment again and this time removed the contents of the cell after the experiment had concluded **(Figure 2.9.b).** I found that both UBE2W and OTUB1 were precipitating and both proteins were found in the pellet. It is possible that the constant spinning in the cell caused UBE2W to crash out. I attempted to redo this experiment once again but changed the pH from 7.5 to 7. Since the pI of UBE2W is 7.8, I speculated that the pH in the previous experiment was too close to the pI and maybe was causing the protein to precipitate. However, changing the pH did not improve the behavior of the proteins in the calorimeter.

Since UBE2W is able to stimulate the DUB activity of OTUB1 within a range similar to other E2 partners **(Figure 2.1)**, I examined how this E2 affects the kinetics of OTUB1. First, I determined the EC_{50} and found that the concentration of UBE2W at which half-maximal stimulation of OTUB1 occurs is 6.7 µM **(Figure 2.10.a)**. As compared to the EC_{50} values for other E2s that interact with OTUB1, the EC_{50} for UBE2W is closest to that of the UBE2E family of enzymes, 4.6-10.9 µM **(Figure 2.5)**. This result indicates that even though UBE2W strongly stimulates OTUB1 as compared to the other E2s, stimulation requires a higher concentration of UBE2W. I also determined the K_M and k_{cat} for OTUB1 in the presence of UBE2W **(Figure 2.10.b-c)**. The K_M was 22.7 µM and the k_{cat} was 0.0047 s^{-1}. Based on the stimulation panel, I expected the K_M change for UBE2W to be between the K_Ms for UBE2D enzymes and UBE2N, which it was. However, I did not expect to see a difference in k_{cat}, 0.047 s^{-1}, since this change was not observed for the other OTUB1-interacting E2s, which all maintained a k_{cat} around 0.033 s^{-1} **(Figure 2.6)**. The k_{cat} for OTUB1 in the presence of UBE2W is almost twice that in the absence of an E2 **(Figure 2.10.b and c)**. To get a better understanding of how this change in k_{cat} affects the DUB activity of OTUB1, I calculated catalytic efficiency in the presence of UBE2W (k_{cat}/K_M = 2070.5 M^{-1} s^{-1}) and compared this value to ones determined for UBE2D2 (5000 M^{-1} s^{-1}), UBE2N (1452.3 M^{-1} s^{-1}), and no E2 (292.7 M^{-1} s^{-1}) (**Figure 2.10.d)**. Given that the K_M for UBE2W and

UBE2N were very similar, differences in fold stimulation and catalytic efficiency are attributed to differences in k_{cat}. Unlike any of the *in vivo* OTUB1-interacting E2s, UBE2W stimulates the DUB activity of OTUB1 by both affecting the binding affinity of OTUB1 for K48 diUbiquitinand by changing the rate by which OTUB1 cleaves its substrates.

2.3 Conclusion

Previous studies had shown that, in the presence of UBE2D1, UBE2D2, UBE2D3, UBE2N, and UBE2E1, the isopeptidase activity of OTUB1 is broadly stimulated (Wiener et al., 2013). I first sought to characterize and compare the remaining *in vivo* OTUB1-interacting partners: UBE2E2 and UBE2E3, to the other E2 partners and observed a broad range in enhancement. To explain the differences in stimulation, I determined binding affinities between OTUB1 and select E2 partners and found that the K_ds were relatively similar. Unable to explain differences in stimulation, I determined the half-maximal concentrations of E2 needed in order to elicit a stimulate response in DUB activity. I found that the EC_{50}s for UBE2N and UBE2D3 matched the intracellular concentrations of these E2s that were determined through mass spectrometry and proteomic studies (Kulak et al., 2014; Michalski et al., 2011). These E2s stimulate over a physiological concentration. I next sought to explain differences in stimulation through assays where I determined kinetic parameters, K_M and k_{cat}.

Our kinetic FRET data demonstrated that binding of OTUB1 to an E2 lowers the K_M for the substrate while the k_{cat} remained unchanged for all *in vivo* E2 partners studied. These data suggest that forming the OTUB1:E2 complex increases the affinity of OTUB1 for K48 diUb. I confirmed this hypothesis using ITC where I titrated K48 diUbiquitinto OTUB1 with saturating concentrations of E2 in both the cell and the syringe. The K_ds I measured in this experiment

matched the K_Ms I had determined earlier, thus confirming that the binding of the E2 serves to increase affinity of OTUB1 for K48 diUb. Differences in stimulation can be correlated with cooperativity, how much are the binding sites for K48 diUbiquitinchanged when binding certain E2s. I was most surprised by UBE2N, which has been shown to be strongly inhibited by OTUB1 (Nakada et al., 2010; Wiener et al., 2012) and yet act as a weak stimulator for DUB activity (Wiener et al., 2013). The lowest EC_{50} I measured belonged to UBE2N, which was even more puzzling since small amounts of E2 are needed to produce a stimulated effect. However, UBE2N also had a Hill coefficient that was less than one, which suggests negative cooperativity. Unlike the other OTUB1-interating E2s, the binding of UBE2N may yield a conformational change in OTUB1 that only slightly increases preference for K48 diUb. It is unknown whether this change in OTUB1 occurs near the catalytic core or the N-terminus, and mutations to either region would be potential experiment to try and decipher the mechanism of negative cooperativity for OTUB1:UBE2N.

It is important to note that the k_{cat} in the presence of UBE2W slightly increased, which I correlated to an increase in DUB activity and catalytic efficiency. Given that the K_Ms of OTUB1 for K48 diUbiquitinin the presence of UBE2W and UBE2N were very similar, it was the change in k_{cat} that produced a greater enhancement on isopeptidase activity. UBE2N is a chain elongator and requires other E2 enzymes, like UBE2W, to initiate chain formation (Stewart et al., 2016). It is interesting that UBE2W is a better stimulator than UBE2N. It is possible that after monoubiquitinating a substrate, UBE2W binds to OTUB1, leading to stimulated DUB activity and an increase in monoubiquitin, which would serve as a substrate for UBE2N facilitated K63 chains elongation. However, given that UBE2N is functional albeit weak stimulator at *in vivo* concentrations, it is more likely that the formation of OTUB1:UBE2N

complex serves to sequester UBE2N from polyubiquitinating. I will go in further detail about this function in the next chapter.

Using the binding and kinetic that I have determined, I created an interaction scheme or thermodynamic cycle (**Figure 2.11.a)** that illustrates OTUB1 binding to either E2 (**A**) or K48 diUbiquitin(**C**), ultimately forming OTUB1:E2 bound to K48 diUb. Given that OTUB1-interacting E2s bind OTUB1 with a K_d that is tenfold lower (K_d of 3.9—9.3 μM) than that of K48 diUbiquitin(K_d of 84 μM), it is more likely that OTUB1 will bind first to the E2 (**A)** than to K48 diUbiquitin(**C**). Structural studies have revealed that, in the apo state, the N-terminus of OTUB1 is disordered (Edelmann et al., 2008; Sato et al., 2012; Wiener et al., 2012). Binding of ubiquitin to the distal binding site on OTUB1 triggers a conformational change that favors binding to the distal ubiquitin binding site by UBE2N~Ub (Wiener et al., 2012). It is possible that a similar conformational change in OTUB1 might be observed when first binding to an E2 partner also drives formation of the N-terminal helix. Folding of the N-terminal helix therefore favors binding to both the distal and proximal ubiquitin binding site, as evidenced by an increase in binding affinity for K48 diUbiquitinfrom 84 μM that dropped to a range of 6.6—64 μM. Although the affinity of different E2 enzymes was relatively similar for all those measured, it is possible that different E2 enzymes do not induce the identical the conformational change in both the distal and proximal ubiquitin binding sites of OTUB1. Resulting differences in the way in which the OTUB1 N-terminus interacts with the proximal ubiquitin could thus potentially account for the differences in stimulated DUB activity and in affinity for K48 diUb. Given all the data I have collected, I was able to calculate an estimate for change in affinity that OTUB1 (**D)** would have for its E2 partners if the DUB was already bound to K48 diUbiquitin(**Figure 2.11.b-c)**. Binding of K48 diUbiquitinto OTUB1 increases the affinity for the E2. Our binding and kinetic data elucidated the role that the E2 partners play in regulating the deubiquitinating activity of OTUB1.

2.1. Materials and Methods

2.4.1 Cloning and mutagenesis

Ub wt and Ub G77D were cloned into pET3a plasmids as previously described (Wang et al., 2009). For Ub K48/63R, Infusion cloning was used to create both mutations in pET3a plasmid. All E2 enzymes were cloned into a pET-SUMO-2 vector (Addgene) that contained an N-terminal His_6-tag followed by a SENP-2 protease site. The expression vector was assembled through Infusion ligase-free cloning. OTUB1 was cloned into a pProEx HTb (Addgene) that had an N-terminal His_6-TEV protease site. The catalytic mutant, OTUB1 (C91S), was obtained through site-directed mutagenesis, QuikChange mutagenesis kit (Stratagene). All clones were transformed into XL1-Blue cells (Stratagene). **Table 2.1** includes more details about each construct.

2.4.2 Protein expression and purification

All proteins were expressed in *E.coli* Rosetta-2 DE3 cells (EMD Millipore, Merck KGaA, Darmstradt, Germany). Cells were transformed via heat shock (42 °C for 35 secs) and plated on Luria Broth (LB) agar plates with 34 mg/mL Chloramphenicol and 100 mg/mL Carbenicillin. A small starter growth of 50 mLs was initiated by picking 2-5 Rosetta-2 DE3 colonies and placing into LB media with 34 mg/mL Chloramphenicol and 100 mg/mL Carbenicillin. Starter growths were grown at 37 °C (shaking at 250000 rpm) overnight. Large-scale cultures (1L) of M9ZB media (1x M9 salt mix, 0.5% NaCl, 10 g/L casamino acids, 2 mM MgSo4, 5% glycerol, and 0.5x Metal mix) were inoculated with 1% (v/v) overnight saturated starter cultures in addition to Chlor

and Carb antibiotics. Cultures were grown at 37 °C (shaking at 250000 rpm) to an $O.D_{600}$ ~1.5. At this $O.D_{600}$ cells were induced with the addition of 1mM isopropyl βD-1-thiogalactopyranoside (IPTG) and further grown overnight (~16 hrs) at 16 °C. Cells were harvested by pelleting at 4000 x rpm at 4 °C then immediately lysed.

Wild type, G77D, and K48/63R ubiquitin were purified as previously described (Wang et al., 2009). All E2 enzymes (UBE2D1-3, UBE2N, & UBE2E1-3) and OTUB1 proteins (wt and C91S) were purified by resuspending pelleted Rosetta cells in lysis buffer (20 mM HEPES pH 7.3, 300 mM NaCl, 25 mM imidazole, 2 mM β-mercaptoethanol (BME)). 0.1mM phenyl-methyl sulphonyl fluoride (PMSF) was added to cells before being lysed using a Microfluidizer (Microfluidics). The lysate was centrifuged (12,500 rpm at 4 °C for 25 mins) and purified using affinity chromatography, 5mL HisTrap (GE Biosciences). Proteins of interest were eluted using a linear gradient of 250 mM imidazole over 10 column volumes. To cleave the His-tag, 10 mM SENP-2 was added to the eluted fraction, at a concentration ratio of 1:100, and dialyzed overnight at 4 °C in lysis buffer. A second round of HisTrap purification was used to remove cleaved protein from SENP-2. The flow-through was collected and subjected to another round of purification as described below.

After removing the His_6-tag, all E2 enzymes except UBE2E1-3 were purified further using size exclusion chromatography. Fractions were concentrated down to 2 mL and run over a HiLoad 16/60 Superdex 75 ng column with buffer: 50 mM HEPES pH 7.5, 150 mM NaCl, and 0.5 mM TCEP-HCl. Eluted fractions were then concentrated down to 4-10 mg/mL and stored at -80 °C. For UBE2E1-3 proteins, flow through fractions from the second pass through HisTrap were pooled and dialyzed overnight into 25 mM sodium phosphate buffer pH 7.4, 25 mM NaCl, and

7.5 mM β-mercaptoethanol at 4 °C. UbE2E1-3 were further purified using cation exchange chromatography and eluted at 100 mM NaCl. Clean fractions were dialyzed overnight at 4 °C in 25 mM Tris buffer pH 8, 150 mM NaCl and 7.5 mM BME, concentrated to 4-10mg/mL, and stored at -80 °C.

After the His_6-tag was removed, OTUB1 and its catalytic mutant (C91S) were further purified by gel filtration chromatography via a HiLoad 16/60 Superdex 75 ng (GE LifeSciences) column equilibrated in 25 mM HEPES pH 7.6, 150 mM NaCl, and 0.5 mM tris(2-carboxyethyl)phosphine (TCEP). Purified OTUB1 was concentrated to 4-10 mg/mL, flash-frozen in liquid nitrogen and stored at -80°C until use.

2.4.3 ITC experiments

All ITC experiments were performed on a MicroCal ITC_{200} system (Malvern) at 25 °C. The syringe (70 µL) titrated protein into a 300 µL sample cell. Each ITC experiment contained 19 injections, 2 µL each for a duration of 0.8 sec over a 150 sec spacing. All proteins measured were dialyzed in a buffer of 25 mM HEPES pH 7.5, 150 mM NaCl, 0.5 mM TCEP-HCl. For measurements between E2 (cell) and OTUB1 (C91S) (syringe), the sample cell contained 150 µM of E2 and the syringe 1.5 mM OTUB1. For OTUB1 (C91S) interactions with K48 diUb, 1.5 mM K48 diUbiquitinwas titrated into150 µM of OTUB1. For experiments testing the binding of K48 diUbiquitinto OTUB1 (C91S) at saturating concentrations of E2, 3 mM K48 diUbiquitinwas titrated into 150 µM OTUB1 (C91S) with a constant 150 µM of E2 was present in both the syringe and the cell. Heat generated due to dilution of the titrants was subtracted for baseline correction. The baseline-corrected data was then analyzed with MicroCal Origin Ver. 7.0 software.

2.4.4 Generating a Standard Curve for EC_{50}s and Kinetic assays using FRET-K48 diUb

All reactions of 30 µL were performed at 30 °C on a POLARStar Omega plate reader (BMG LABTECH) that measured TAMRA fluorescence (ex. 544 nm; em. 590 nm) every 5 secs over 30 mins. Reactions contained K48 diUbiquitininternally quenched fluorescent (IQF) TAMRA substrate no. 5 (LifeSensors), (FRET-K48 diUb) that ranged in concentrations from 25 - 500 nM to which 50 nM of OTUB1 was added. The experiment incubated in the dark at 30 °C for 1 hr to ensure that the substrate was fully cleaved by OTUB1. Gain was adjusted to 1900 based on the fluorescence from the 500 nM FRET-K48 diUbiquitinreaction. The standard curve was obtained from measuring the fluorescence (AU) and plotting this against the corresponding concentration of FRET-K48 diUb. The data were then fitted to a linear equation to obtain the slope in units of AU $\cdot\mu M^{-1}$. This slope was therefore used for the EC50 and kinetic assays to convert (AU) into a measurement of µM.

2.4.5 Determination of EC_{50}s

All EC_{50} measurements were obtained using a POLARstar omega plate reader (BMG LABTECH) that monitored TAMRA fluorescence (ex. 544 nm; em. 590 nm) at a gain of 1900. EC_{50}s of OTUB1 cleavage of Lys48 diUbiquitinwere measured at 30 °C in buffer containing 20 mM HEPES, pH 7.5, 150 mM NaCl, 1 mM DTT, 0.01% BSA, and 400 nM of FRET-K48 diUb. Reactions (30 µL) contained specified amounts of the various E2 enzymes and were initiated by addition of 50 nM OTUB1. The initial rate of Lys48 diUbiquitincleavage was determined from the slope of the linear region of the fluorescent curves. In GraphPad Prism 5 (GraphPad Software), the smallest and largest values in the data set were normalized to 0 and 1 respectively.

Normalized data were then analyzed through Non-linear Regressions program: “log(agonist) vs response – Variable slope” which utilizes the following equation: Y=Bottom + (Top-Bottom)/(1+10^((LogEC50-X)*Hill Slope)) to fit and calculate the 0.5 stimulation response. Experiments were done in triplicate.

2.4.6 Steady-state kinetic assays

Determination of Michaelis Menten kinetics were determined using a POLARStar Omega plate reader (BMG LABTECH) that monitored a TAMRA fluorescence (ex. 544 nm; em. 590 nm) with a gain of 1900. Steady-state enzyme kinetic assays were determined at 37 °C in a reaction buffer of 20 mM HEPES, pH 7.5, 150 mM NaCl, 1 mM DTT, 0.01% BSA. Reactions (50 µL) in the presence and absence of E2 (10 µM) were initiated with the addition of 50 nM OTUB1. For all experiments, increasing concentrations of non-fluorescent K48 diUbiquitinwere present with a constant 400 nM FRET-K48 diUb. After the time assay was completed, each data point was multiplied by the total K48 diUbiquitinconcentration present in the initial reaction. For example, assays done at 100 µM K48 diUbiquitin(plus 400 nM FRET-K48 diUb), the data set was multiplied by 100.4. To calculate initial rates, fluorescence (AU) was converted to K48 diUbiquitincleavage (µM) using the equation obtained from the standard curve. The transformed data was plotted as a function of time and fit to a line where initial velocity conditions were satisfied, typically within the first three minutes. Initial rates were measured in triplicate, normalized to the enzyme concentration, plotted as a function of substrate concentration, and the resulting curve fit to the Michaelis-Menten equation using non-linear least squares regression implemented in GraphPad Prism 5(GraphPad Software).

Table 2. 1 Plasmid summary for all proteins

Protein	Plasmid	Cleavage Site	MW, g/mol	Extinction coefficient, 1/(M cm)	pI
Ub wt	pET3a	NA	8564.8	1490	6.6
Ub G77D	pET3a	NA	8679.9	1490	5.7
Ub K48/63R	pET3a	NA	8620.8	1490	6.6
UBE2D1	pETSUMO2	SENP2	17300	26930	7.1
UBE2D2	pETSUMO2	SENP2	17460	26930	7.9
UBE2D3	pETSUMO2	SENP2	17400	26930	7.8
UBE2N	pETSUMO2	SENP2	17140	22460	6.1
UBE2E1	pETSUMO2	SENP2	21400	25690	8.8
UBE2E2	pETSUMO2	SENP2	22300	25690	7.6
UBE2E3	pETSUMO2	SENP2	22900	25690	6.7
UBE2W	pETSUMO2	SENP2	18200	24300	7.8
OTUB1 wt	pProEX	TEV	31850	23840	4.9
OTUB1 (C91S)	pProEX	TEV	31834	23840	4.9

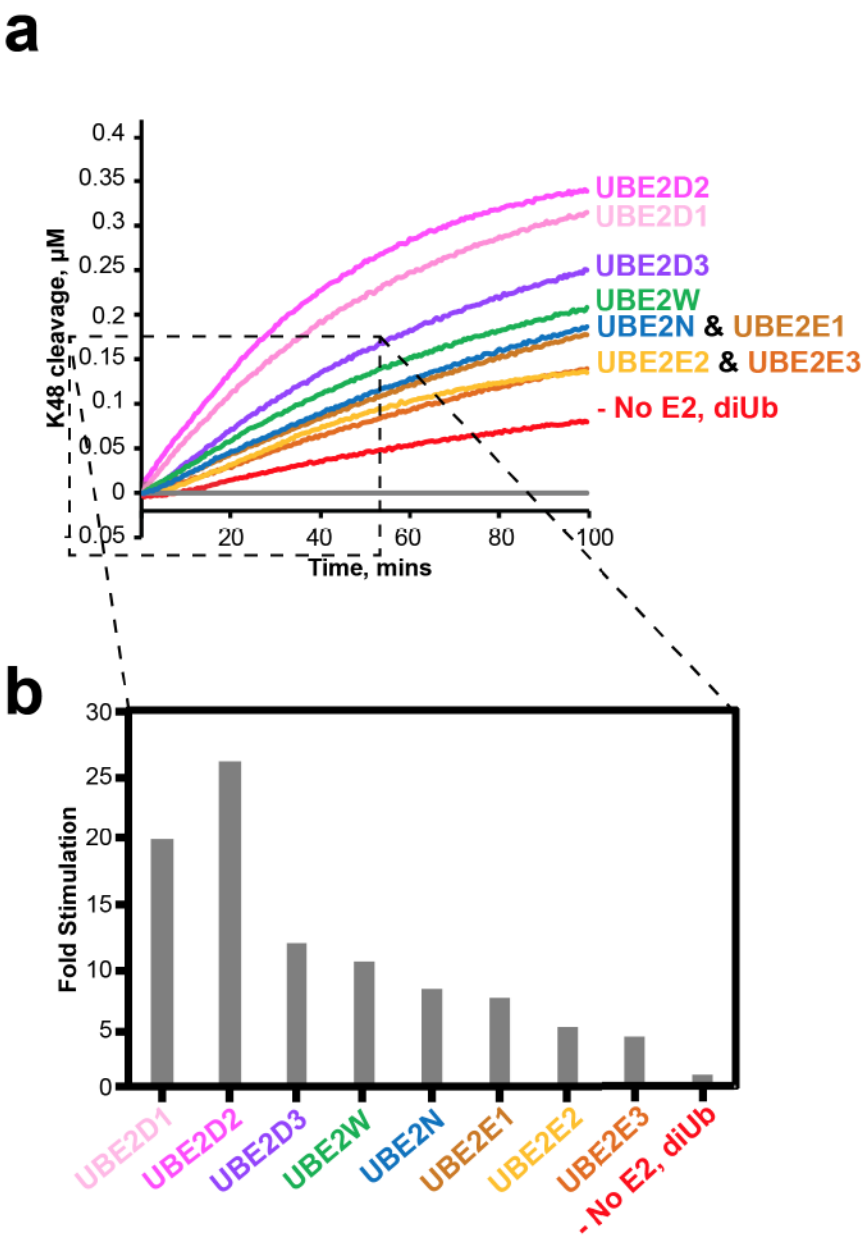

Figure 2. 1 The DUB activity of OTUB1 is broadly stimulated in the presence of E2 partners.

(a) *FRET time course assay which utilizes an internally quenched K48 diUbiquitin(400 nM) to characterize the effects of 50 nM OTUB1's DUB activity in the presence and absence of an E2 (10 µM).* ***(b)*** *The linear initial rates from the FRET-based assay were used to visually represent the fold stimulation that is produced in the presence of the various different E2s. To determine fold stimulation, the rate of each was divided by the rate of stimulation in the absence of an E2, the basal isopeptidase activity of OTUB1.*

a

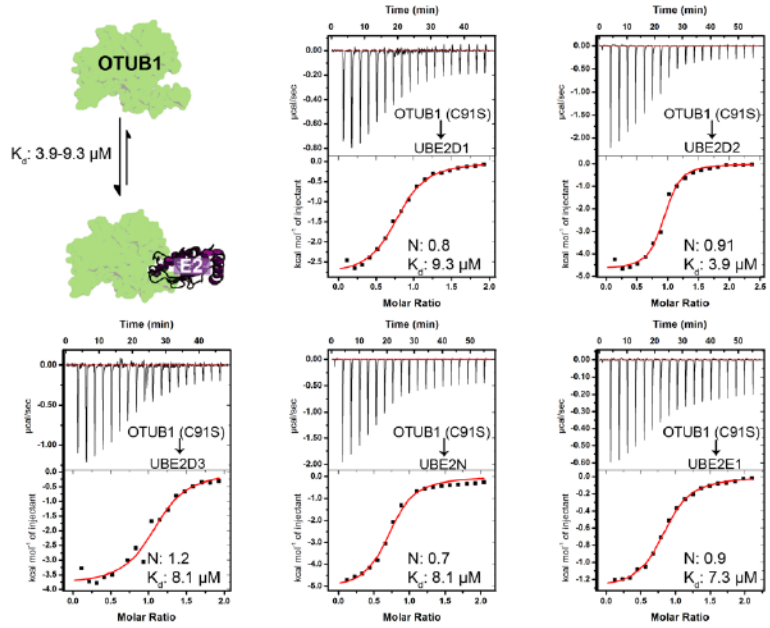

b

proteins interacting with OTUB1	K_D (μM)	Stoichiometry (N)	ΔH (kcal/mol)	ΔS (cal/mol)
UBE2D1	9.3 ± 1.7	0.8 ± 0.01	-3 ± 0.04	12.7
UBE2D2	3.9 ± 1.3	0.9 ± 0.01	-5 ± 0.12	8.5
UBE2D3	8.1 ± 3.6	1.2 ± 0.03	-3.8 ± 0.11	11.5
UBE2N	8.1 ± 2.1	0.7 ± 0.02	-5.2 ± 0.16	6
UBE2E1	7.3 ± 1.4	0.9 ± 0.01	-1.3 ± 0.03	19.3
UBE2E2	unavaliable			
UBE2E3	unavaliable			
K48 diUbiquitin	84 ± 5	0.8 ± 0.02	-12.8 ± 0.4	-24.1

c

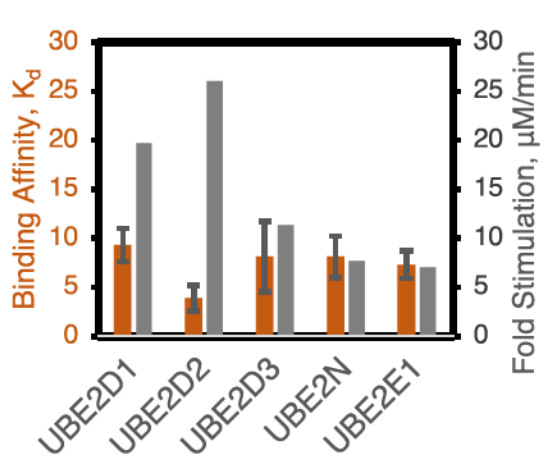

Figure 2. 2 Measuring binding affinity between OTUB1 and E2 interacting partners. ***(a)*** *Binding schematic and ITC experiments for OTUB1 (1.5 mM) and its E2 partners (150 μM). OTUB1 was titrated into the corresponding E2 which was contained within the cell.* ***(b)*** *Summary table of thermodynamic parameters measured using ITC.* ***(c)*** *Visual to comparison of differences in binding affinity for each E2 with corresponding fold stimulation displayed earlier in* ***Figure 2.1****.*

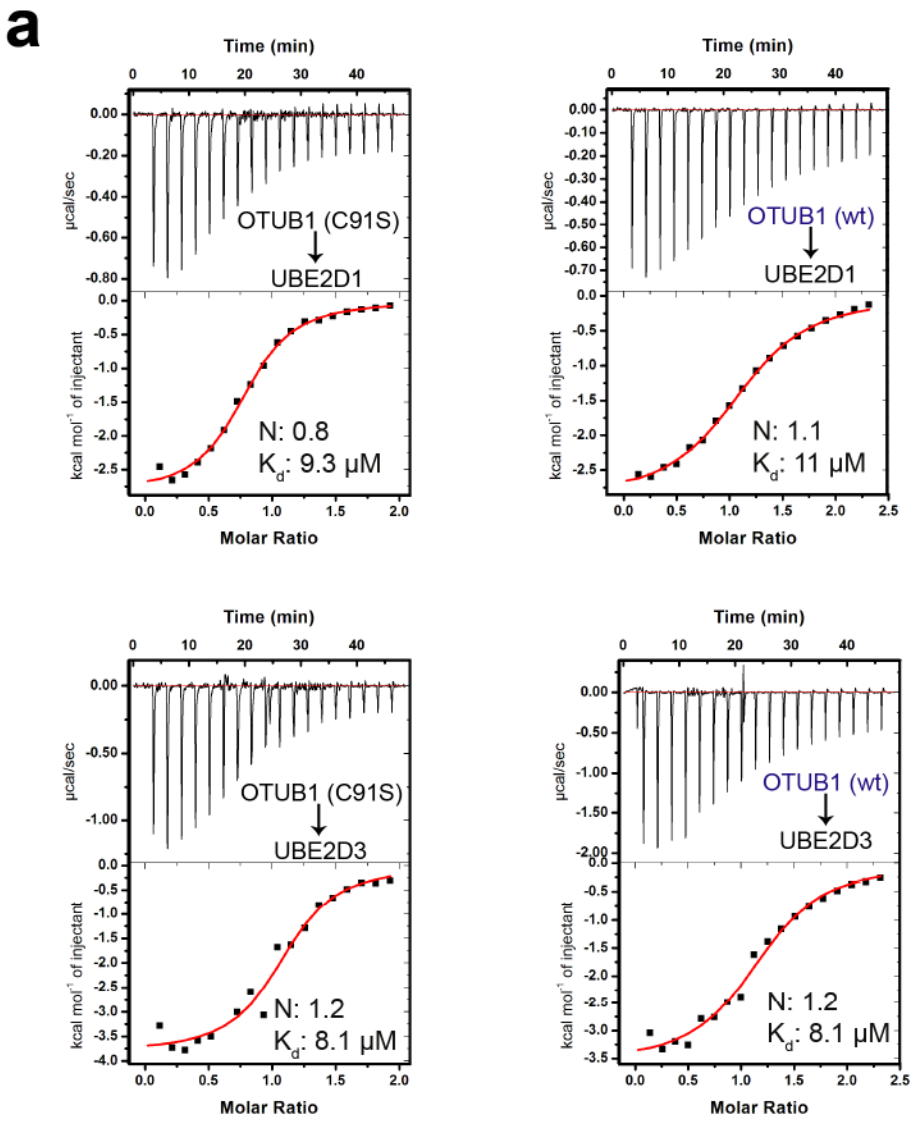

Figure 2. 3 OTUB1 (C91S) binds E2s with equal affinity as OTUB1 wt

(a) *Comparision of data collected for binding of UBE2D1 (150 µM) with either 1.5 mM OTUB1 (C91S) or wt. In addition, binding of UBE2D3 (150 µM) with either 1.5 mM OTUB1 (C91S) or wt.*

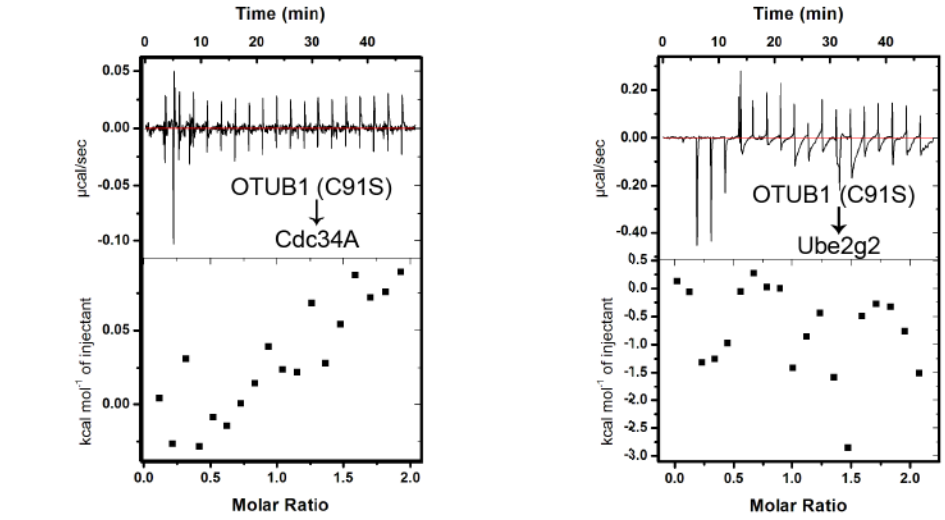

Figure 2. 4 OTUB1 does not bind non-OTUB1 interacting E2s
(a) *OTUB1 (1.5 mM) titrated into the cell containing 150 µM with either Cdc34A or Ube2g2.*

a

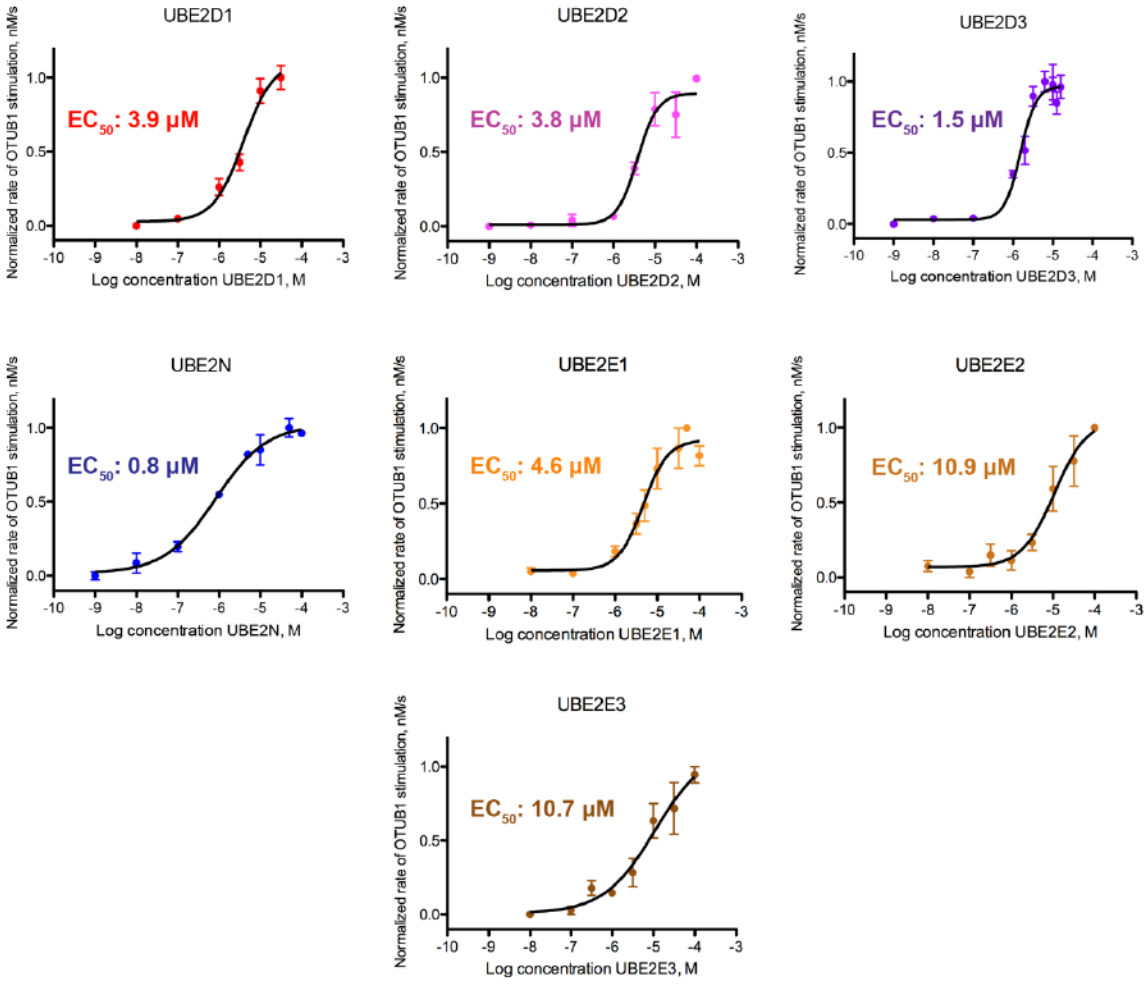

b

OTUB1 interacting E2s	EC_{50} (μM)	Hill Slope
UBE2D1	3.9	1.2 ± 0.4
UBE2D2	3.8	1.8 ± 0.6
UBE2D3	1.2	2.2 ± 0.6
UBE2N	0.8	0.7 ± 0.2
UBE2E1	4.6	1.5 ± 0.5
UBE2E2	10.9	1.1 ± 0.5
UBE2E3	10.7	0.7 ± 0.3

c

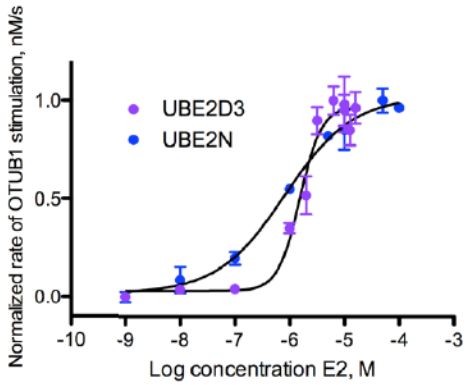

Figure 2. 5 Effective Concentration (EC_{50}) to produce a stimulatory DUB effect for OTUB1. ***(a)*** *FRET-K48 diUbiquitin(400 nM) and 50 nM OTUB1 were assayed with increasing concentrations of E2 enzymes (1pM to ~50 μM). Reactions were assayed in triplicate.* ***(b)*** *Table of EC50s values and corresponding Hill Slopes for each curve. Overlay of EC_{50} curves for UBE2D3 and UBE2N to depict differences in Hill Slopes.*

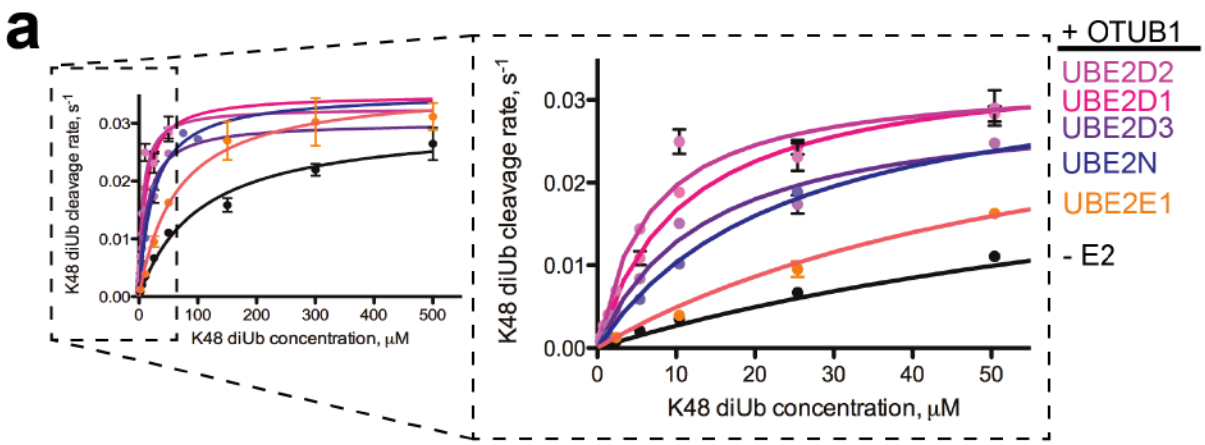

b

proteins interacting with OTUB1	K_M (µM)	k_{cat} (s^{-1})	k_{cat}/K_M ($M^{-1}s^{-1}$)
UBE2D1	11 ± 1.1	0.035 ± 0.001	3181.8
UBE2D2	6.6 ± 1.1	0.033 ± 0.002	5000
UBE2D3	13.5 ± 1.8	0.03 ± 0.002	2222.2
UBE2N	24.1 ± 2	0.035 ± 0.001	1452.3
UBE2E1	64.3 ± 2	0.036 ± 0.001	559.9
K48 diUbiquitin	102.5 ± 18.7	0.03 ± 0.002	292.7

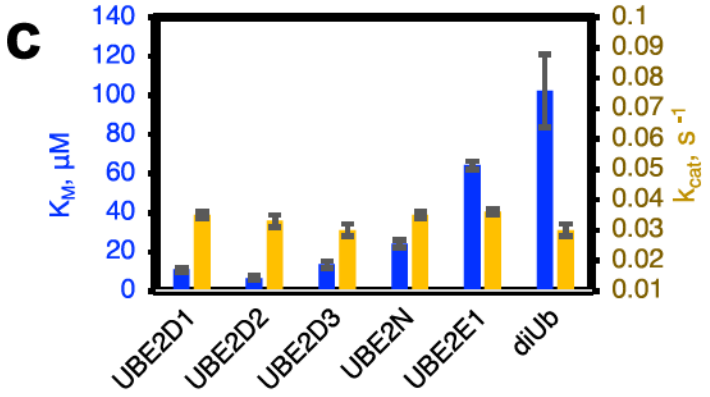

Figure 2. 6 E2 enzymes elicit a K_M effect on OTUB1

(a) *Kinetic FRET assay with the internally quenched fluorescent diUbiquitin(400 nM) to characterize the effects of OTUB1's (50 nM) DUB activity in the presence and absence of an E2 (10 µM). Reactions were performed in triplicate. The full substrate titration (0.4 nM – 500 µM K48 diUb) and excerpt from 0.4 nM to 50 µM K48 diUbiquitinare both shown* ***(b)*** *Summary table of all determined kinetic parameters: K_M, k_{cat}, and the calculated k_{cat}/K_M* ***(c)*** *Visual representation of the kinetic parameters measured for UBE2D1, UBE2D2, UBE2D3, UBE2N, UBE2E1, and in the absence of an E2. The blue bars correspond to KM (left axis) whereas the yellow bars correspond to k_{cat} (right axis).*

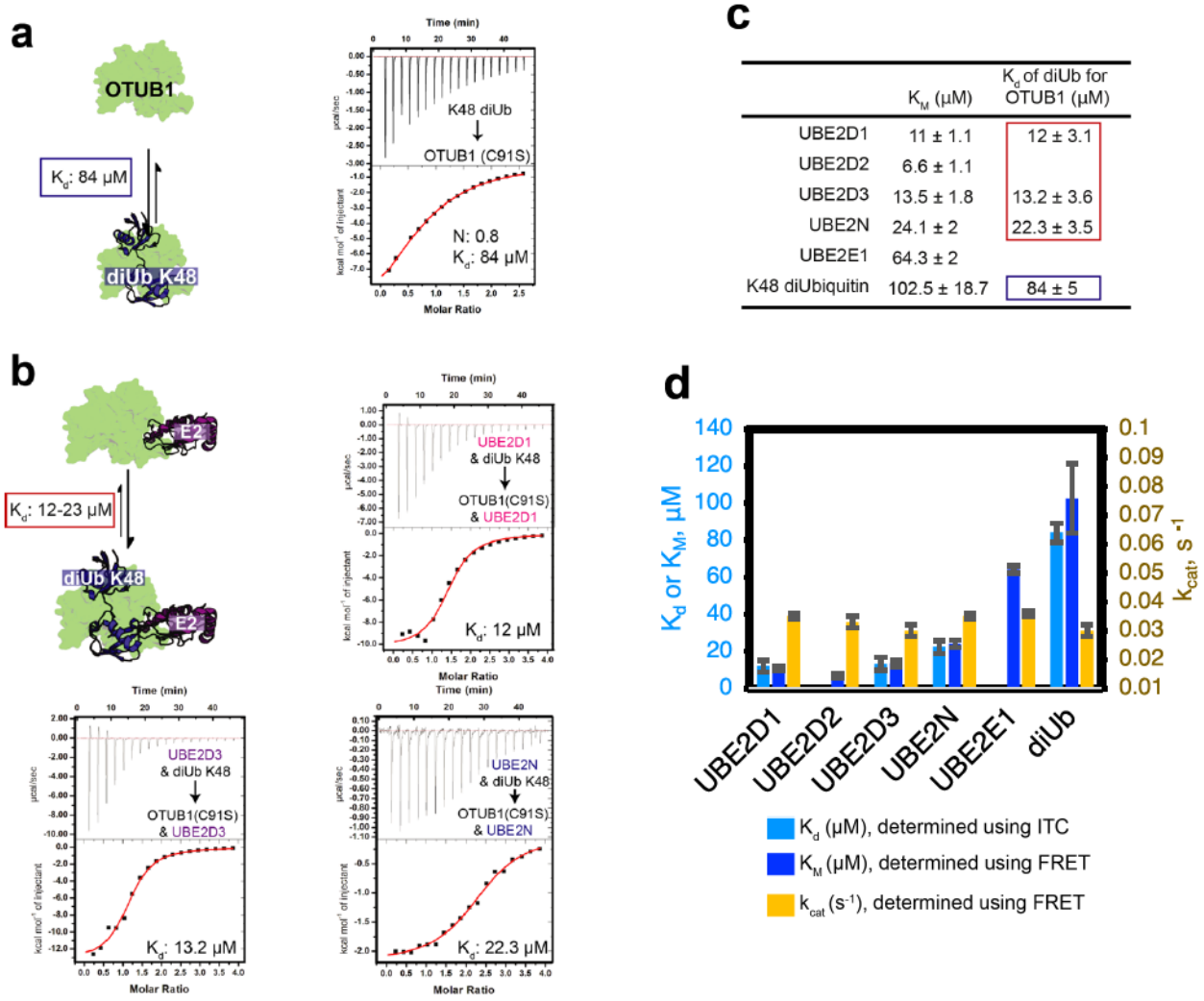

	K_M (µM)	K_d of diUb for OTUB1 (µM)
UBE2D1	11 ± 1.1	12 ± 3.1
UBE2D2	6.6 ± 1.1	
UBE2D3	13.5 ± 1.8	13.2 ± 3.6
UBE2N	24.1 ± 2	22.3 ± 3.5
UBE2E1	64.3 ± 2	
K48 diUbiquitin	102.5 ± 18.7	84 ± 5

Figure 2. 7 Complex, OTUB1:E2 raises the affinity of OTUB1 for K48 diUb
(a) *Schematic and experiment of binding of (3 mM) K48 diUbiquitinto (150 µM) OTUB1 (C91S)* ***(b)*** *Schematic and titration experiment of 3mM K48 diUbiquitinto 150 µM OTUB1 (C91S) with a constant amount of (150 µM) E2 is present in both the cell and syringe* ***(c)*** *Summary table of kinetic and binding constants measured.* ***(d)*** *Visual representation of how well measured K_ds (light blue bars) of diUbiquitinto OTUB1 in the presence of select E2s matches the K_M effect (darker blue bars). Yellow bars represent the k_{cat}, right axis.*

a

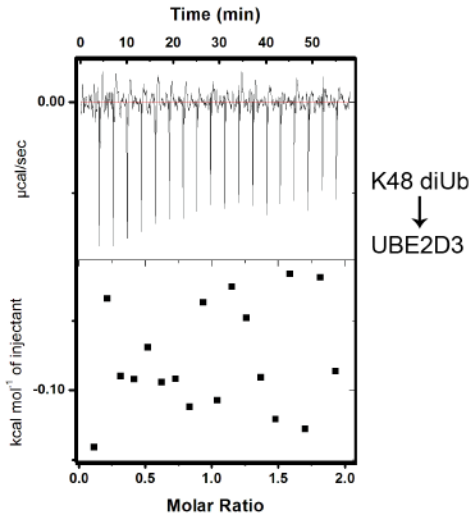

Figure 2. 8 K48 diUbiquitinbinds to UBE2D3 with very low affinity

(a) *ITC experiment where K48 diUbiquitin(3 mM) was titrated into 300 µM UBE2D3 within the cell*

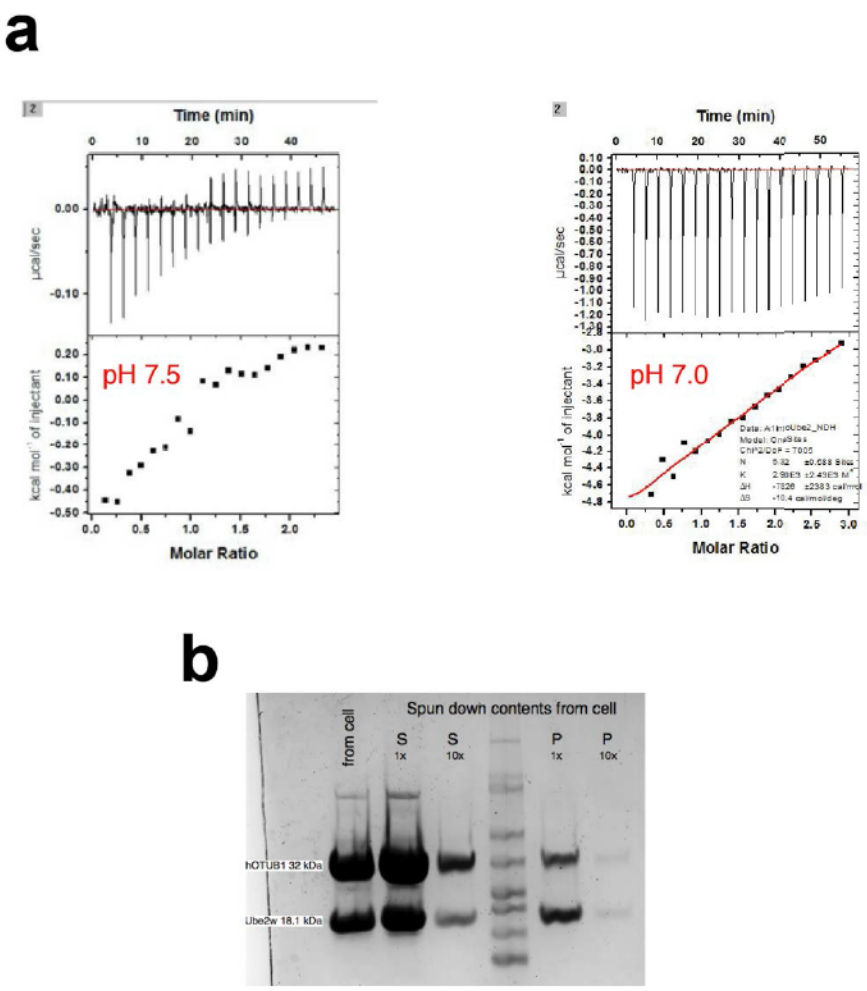

Figure 2. 9 Attempts to utilize ITC to characterize binding between OTUB1 and UBE2W resulted in precipitation of both proteins.

(a) *ITC experiments of OTUB1:UBE2W at different pHs, pH 7.0 and 7.5 did not yield reliable binding data. In the syringe, OTUB1 (1.5mM) was titrated into 100 µM of UBE2W within the cell.* ***(b)*** *After the experiment at a pH of 7.5 finished and OTUB1 was fully titrated into the cell with UBE2W, contents within the cell were removed. A sample was extracted from the cell whereas the rest was spun down, 7000 x rpm for 5 mins at room temperature. A sample from the supernatant was taken to run on a gel as is, 1x, or diluted 10s with the dialysis buffer: 50 mM HEPES pH 7.5, 150 µM NaCl and 0.5 mM TCEP-HCl. Using the same dialysis buffer, the pellet was resuspended and a 1x and 10x sample was analyzed on an SDS-PAGE gel.*

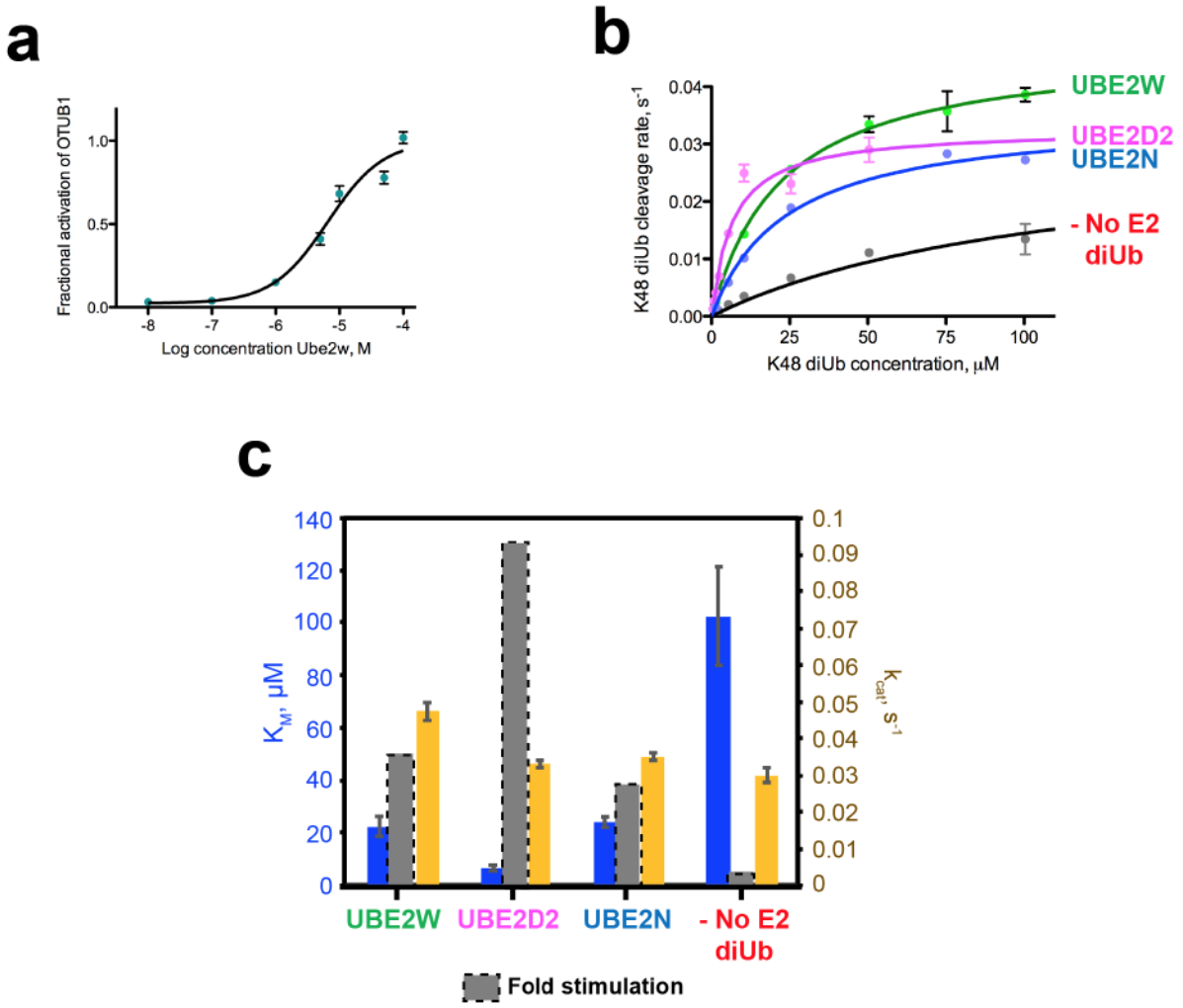

d

	EC_{50} (μM)	Hill Slope	K_M (μM)	k_{cat} (s^{-1})	k_{cat}/K_M ($M^{-1}s^{-1}$)
UBE2W	6.7	0.9 ± 0.2	22.7 ± 3.8	0.047 ± 0.002	2070.5
UBE2D2	3.8	1.8 ± 0.6	6.6 ± 1.1	0.033 ± 0.001	5000
UBE2N	0.8	0.7 ± 0.2	24.1 ± 2	0.035 ± 0.001	1452.3
- No E2, diUb			102.5 ± 18.7	0.03 ± 0.002	292.7

Figure 2. 10 Characterization of OTUB1:UBE2W complex
(a) *The EC_{50} of UBE2W to produce a stimulatory response in DUB activity was determined to be 6.7 μM.* ***(b)*** *Kinetic data was also determined for UBE2W. Parameters for UBE2D2, UBE2N, and in the absence of an E2 were plotted for a comparision.* ***(c)*** *Parameters, K_M and k_{cat}, were plotted to show how the kinetics difffered for UBE2W to the other E2 enzymes. Also shown is how these parameters compare with the fold stimulation determined from* ***Figure 2.1*** *(dark gray dotted boxes).* ***(d)*** *Summary table with all constants determined for UBE2W.*

a

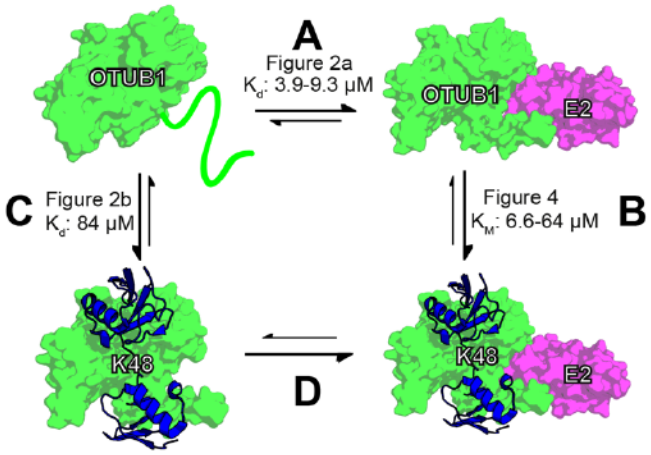

b

$$\frac{K_{dA} \times K_{dB}}{K_{dC} \times K_{dD}} = 1$$

$$\frac{K_{dA} \times K_{dB}}{K_{dC}} = K_{dD}$$

c

OTUB1-Interacting Proteins	**A** K_d, E2 for OTUB1(μM)	**B** K_M, affinity of OTUB1 for K48 diUb in the presence of an E2 (μM)	**C** K_d, K48 diUb for OTUB1(μM)	**D** K_d, affinity of OTUB1 for E2 in the presence of an K48 diUb (μM)
UBE2D1	9.3 ± 1.7	11 ± 1.1		1.2
UBE2D2	3.9 ± 1.3	6.6 ± 1.1		0.3
UBE2D3	8.1 ± 3.6	13.5 ± 1.8		1.3
UBE2N	8.1 ± 2.1	24.1 ± 2		2.3
UBE2E1	7.3 ± 1.4	64.3 ± 2		5.6
K48 diUb			84	

Figure 2. 11 Binding cycle involving OTUB1 interacting with E2 partners and K48 diUb. ***(a)*** *Thermodynamic cycle of OTUB1 binding independently to either an E2 or K48 diUbiquitin which in turns favors binding of the other. Each side of the cycle is designated by a letter along with the binding affinities determined in this paper.* ***(b)*** *When comparing each side of the thermodynamic cycle with equilibrium dissociation constants, A x B must equal C x B. Therefore, the constants can be arranged so that K_d can be calculated.* ***(c)*** *Binding affinities previously determined, A B and C, and those calculated, D.*

Chapter 3 Qualitative analysis of non-canonical inhibition of OTUB1-interacting E2 partners

3.1 Introduction

OTUB1 is a unique DUB in that it binds to E2 enzymes and inhibits ubiquitin transfer in a manner that is independent of deubiquitinating activity (Baietti et al., 2016; Herhaus et al., 2013; Nakada et al., 2010; Sato et al., 2012; Sun et al., 2012; Wiener et al., 2012; Zhao et al., 2018). The non-canonical activity of OTUB1 was first discovered through its role in the double-stranded DNA break response (Nakada et al., 2010). OTUB1 limits accumulation of K63-linked chains on double-stranded DNA breaks, thus attenuating the DNA damage response once the lesion has been repaired (Nakada et al., 2010). OTUB1 non-catalytically inhibits the E2, UBE2N, by binding to the ubiquitin moiety in the E2~Ub thioester intermediate, thus preventing transfer of the ubiquitin to a substrate (Nakada et al., 2010; Sato et al., 2012). OTUB1 also occludes the E3 RING-binding site on the E2, thus providing an additional mechanism for inhibiting ubiquitination (Wiener et al., 2012). It has been shown that OTUB1 non-catalytically inhibits UBE2D proteins from ubiquitinating p53 (Chen et al., 2016; Sun et al., 2012) and SMAD2/3, regulators of TGFβ signaling (Herhaus et al., 2013). OTUB1 also regulates the stability of DEPTOR, a regulator of mTOR signaling, which is thought to occur by inhibiting attachment of K48-linked chains to DEPTOR by either UBE2D enzymes or another E2 (Zhao et al., 2018). In addition, a recent study showed that OTUB1 blocks autoubiquitylation of UBE2E1, thereby rescuing the E2 from proteasomal degradation (Pasupala et al., 2018). The non-catalytic roles of OTUB1 make this DUB an essential regulator for a diverse array of biological processes in the cell.

Structural studies of OTUB1 have provided insights into how this DUB inhibits E2 enzymes. Like other members of the OTU family (Balakirev et al., 2003; Clague et al., 2012; Clague et al., 2019), OTUB1 contains two ubiquitin binding sites, proximal and distal, which bind the two ubiquitin monomers, while the K48 isopeptide linkage is positioned near the catalytic cysteine **(Figure 1.4.c and e)** (Juang et al., 2012; Wiener et al., 2013; Wiener et al., 2012). (Sato et al., 2012; Wiener et al., 2013; Wiener et al., 2012)A flexible N-terminal ubiquitin binding helix that forms part of the proximal site is largely disordered in the apo enzyme (Edelmann et al., 2008; Wiener et al., 2012) but forms an α-helix when ubiquitin is bound (Wiener et al., 2012). When OTUB1 forms an inhibitory complex with the E2~Ub thioester, the E2 is oriented such that the conjugated ubiquitin binds to the proximal site in OTUB1 (Wiener et al., 2012). Binding of the thioester-linked ubiquitin to the proximal site is stimulated when a second ubiquitin binds in the distal site, thus allosterically increasing the affinity of OTUB1 for the ubiquitin in the proximal site (Wang et al., 2009; Wiener et al., 2012)

I sought to characterize the OTUB1-facilitated inhibition of ubiquitin conjugating enzymes with which the DUB interacts. Although non-canonical inhibition has already been observed for UBE2D2, UBE2D3, and UBE2N, these *in vitro* experiments were performed with different E3 ligases and some were done with GST-tagged OTUB1, making it impossible to directly compare results. To make systematic comparisons and conclusions about the non-canonical activity of OTUB1, I looked at inhibition of all seven different OTUB1-interacting E2s under the same conditions. I determine the effective concentration ranges by which OTUB1 is able to inhibit its E2 partners.

3.2 Results

3.2.1 OTUB1 does not disrupt E1 charging of E2 enzymes

Structural studies have shown that OTUB1 sequesters E2~Ub complexes from further interacting with a corresponding E3 ligase. The OTUB1 binding surface on E2 enzymes overlaps with both the E1 and E3 interfaces **(Figure 3.1)**, so I were interested in whether OTUB1 could block E1 charging of the E2 in addition to inhibiting E2 from interacting with the E3. Nakada et al. found that OTUB1 blocked UBE2N from interacting with its non-catalytic UEV1a and with the E3 ligase, RNF168, but did not disrupt the transthiolation reaction that occurs between the E1 and UBE2N(Nakada et al., 2010). I asked whether OTUB1 impacted E1 charging of other OTUB1-interacting E2s, UBE2D2 and UBE2E1. As shown in **Figure 3.2,** OTUB1 did not inhibit E1 charging of UBE2E1 or UBE2D2. For UBE2E1, I see a reduction in autoubiquitylation of the E2 in the presence of increasing concentrations of OTUB1 in both the presence and absence of the reducing agent, β-mercaptoethanol (BME), which disrupts the E2~Ub thioester **(Figure 3.2.b-c)**. I see a substantial amount of high molecular weight species in the presence of BME when OTUB1 is present, which correspond to covalently modified, Ub-UBE2E1. Therefore, OTUB1 does not disrupt E2 charging by the E1 for UBE2D2 and UBE2E1.

3.2.2 OTUB1 inhibits polyubiquitinating and autoubiquitylating activities of UBE2E1

Although UBE2E1 has been shown to stimulate the DUB activity of OTUB1 (Wiener et al., 2013), OTUB1 inhibition of this E2 has not been studied. UBE2E1 is a Class III E2 that contains an N-terminal extension that restricts E2 activity to predominantly monoubiquitinate substrates (Banka et al., 2015; Schumacher et al., 2013). The N-terminal extension serves to regulate and limit the processivity conferred by the Ubc domain, as entirely removing the N-term extension results in a significant increase in polyubiquitinating activity (Schumacher et al., 2013). Fusing

the N-terminal extension of UBE2E1 to a highly processive E2, UBE2D2, which only contains a Ubc domain, severely restricted the chain building activities of UBE2D2 (Schumacher et al., 2013). In addition, the N-terminal extension of UBE2E1 is intramolecularly autoubiquitinated *in vitro* (Banka et al., 2015), which further attenuates the polyubiquitinating activity of this E2 and subsequent transfer of ubiquitin to an E3 ligase (Banka et al., 2015). Mutating all N-terminal extension lysine residues to arginines in UBE2E1, UBE2E2, and UBE2E3 resulted in E2 activity comparable to that of the Ubc domain alone (Banka et al., 2015). A high-throughput assay revealed that, *in vivo*, the N-terminus of UBE2E1 is ubiquitinated at multiple sites (Kim et al., 2007) and UBE2E enzymes are imported into the nucleus when ubiquitinated (Plafker et al., 2004).

I asked whether OTUB1 can inhibit the both polyubiquitinating and autoubiquitylating activities of UBE2E1. I performed a time course assay where I could observe inhibition by OTUB1 in the absence and presence of an E3 ligase **(Figure 3.3)**. In the absence of an E3, there is a persistent high molecular weight band (indicated by the green star between 37 and 25 kDa) that is unaffected by reducing conditions. When blotting for UBE2E1, the higher molecular weight band corresponds to one or two ubiquitin molecules covalently attached to UBE2E1, or the autoubiquitylated UBE2E1 **(Figure 3.3.b)**. Addition of the E3 ligase, RNF4, stimulates synthesis of polyubiquitin chains by UBE2E1. Immunoblotting for either UBE2E1 or K48-linked polyubiquitin shows that both the polyubiquitinating and autoubiquitylating activities of UBE2E1 are stimulated with the presence of RNF4, as shown by the large smears **(Figure 3.3.b)**. In the K48 Ub immunoblot, the large smears correspond to multiple different ubiquitinated species: attachment of multiple polyubiquitin chains to UBE2E1 and/or RNF4, as well as a population of free K48 linked chains formed by UBE2E1 in the presence of RNF4. The addition of saturating amounts of catalytically inactive OTUB1(C91S) significantly reduces the polyubiquitinating

activity of UBE2E1 in the presence and absence of RNF4 **(Figure 3.3b)**. These results show that OTUB1 inhibits the ubiquitin conjugating activity of UBE2E1 in a manner that is similar to that observed for other OTUB1-interacting E2s such as UBE2D2, UBE2D3, and UBE2N (Chen et al., 2016; Nakada et al., 2010). Unlike these E2s, OTUB1 simultaneously disrupts both the polyubiquitinating activity as well as the autoubiquitylating activity of UBE2E1.

The biological significance of OTUB1 inhibition of UBE2E1 was demonstrated by a study from the Wolberger lab, which showed that depleting OTUB1 in both mice and human cells destabilizes of UBE2E1 (Pasupala et al., 2018). Wild type levels of UBE2E1 could be restored in a knockdown by expressing either wild type or catalytically inactive OTUB1, but not by an OTUB1 T135R mutant that is defective in binding to E2 enzymes (Juang et al., 2012; Pasupala et al., 2018). Our in vitro results (**Figure 3.3**) are consistent with a model in which OTUB1 stabilizes UBE2E1 by inhibiting autoubquitylation. This model is supported by a cell-based study showing that OTUB1 rescues UBE2E1 from being degraded by the proteasome. Taken together, these results describe a novel role of regulation for the OTUB1:E2 complex and constitute the first instance where OTUB1 directly modulates the stability of an E2 enzyme.

While doing setting up the experiment for OTUB1-facilitated inhibition of UBE2E1 E2 activity, I ran an experiment using wild-type (wt) OTUB1 as a control (**Figure 3.4).** Since UBE2E1 has been found to form K48 chains (David et al., 2010), I was expecting to see an overall reduction in the ubiquitinated proteins in comparison to the experiment run with the catalytic mutant, OTUB1 C91S. The reduction in ubiquitination should have been attributed to numerous events: cleavage of K48 chains by OTUB1, and inhibition of both polyubiquitinating and autoubiquitylating activities by UBE2E1. However, this was not the case. Wt OTUB1 was less capable of inhibiting the polyubiquitinating activity of UBE2E1, as there was a significant fraction

of ubiquitinated proteins. I repeated this experiment multiple times and received the same result each time.

3.2.3 OTUB1 inhibits polyubiquitinating activities of UBE2E2 and UBE2E3 yet only inhibits autoubiquitylation of UBE2E2

After doing an in-depth analysis of non-canonical inhibition of UBE2E1 by OTUB1, I asked whether OTUB1 inhibits both poly- and auto-ubiquitylation activities for the other E2s within the UBE2E family of E2s that are known to interact with OTUB1. UBE2E1, UBE2E2, and UBE2E3 differ from the other OTUB1-interacting E2s in that they are Class III E2s, which contain an N-terminal extension to the conserved UBC domain (Stewart et al., 2016). UBE2E enzymes have previously been shown to predominantly mono-ubiquitinate E3 ligases (Schumacher et al., 2013) and are intramolecularly autoubiquitinated on an N-terminal extension lysine (Banka et al., 2015) **(Figure 3.5.a)**. The effect of OTUB1 on the poly- and auto- ubiquitylating activities of UBE2E2 and UBE2E3 has not been explored.

I assayed the ability of OTUB1 to inhibit the autoubiquitylation and free chain K48 synthesis by UBE2E2 and UBE2E3 in the presence of the E3 ligase, RNF4. I asked in what concentration range is OTUB1 effective at inhibiting E2 activity. Since the previous study (**Figure 3.3)** of UBE2E1 only looked at inhibition at a single concentration of OTUB1 (10 μM), this E2 was also included in the assays. I used a gel-based assay to monitor the ubiquitylating activity of each E2 over time in the presence and absence of the E3 ligase, RNF4, as well as with increasing concentrations of OTUB1. Immunoblotting using antibodies against either the E2 or K48 were used to track E2 autoubiquitylation and K48 free chain synthesis. In the absence of RNF4, all UBE2E proteins are autoubiquitinated **(Figure 3.5.b-c)**. The ubiquitinated E2 is stable in

reducing conditions, indicating that it is not the E2~Ub thioester, but rather autoubiquitylated UBE2E1, UBE2E2, and UBE2E3 **(Figure 3.5.b).** Moreover, in the absence of RNF4, all UBE2E enzymes form a small amount of K48 chains **(Figure 3.5.c)**. In the presence of RNF4, polyubiquitinating activity for all UBE2E enzymes is significantly increased, which is evident in the diUbiquitin bands and higher molecular weight smears when blotting for K48 chains **(Figure 5c)**.

At increasing concentrations of OTUB1 (0.1 - 50 μM), I tracked the disappearance in both the poly-ubiquitinating activity of K48 free chains and autoubiquitylation of UBE2E enzymes. For UBE2E1, there was a drastic reduction in both autoubiquitination and K48 poly-ubiquitination in the presence of 1-10 μM OTUB1, a range that spans the value for the K_d (7.3 μM) for binding of OTUB1 and UBE2E1 (**Figure 2.2)**. For UBE2E2, both K48 autoubiquitination and poly-ubiquitination were greatly reduced at concentrations of OTUB1 between 0.1–1 μM. There was a significant reduction in band intensity for Ub-UBE2E2, as well as a reduction in K48 smears. Similar to UBE2E1 and UBE2E2, there was a significant decrease in UBE2E3 K48 poly-ubiquitination with addition of OTUB1 at concentrations between 1–10 μM. Unexpectedly, however, it was not possible to fully inhibit autoubiquitination of UBE2E3, even at concentrations of OTUB1 as high as 50 μM. These results suggest that OTUB1 may serve to primarily inhibit poly-ubiquitination of UBE2E3, but not autoubiquitylation. It may be possible to prevent autoubiquitylation of UBE2E3 with larger concentrations of OTUB1 but those quantities would not be in a plausible physiological range found in the cell. I conclude that OTUB1 inhibits autoubiquitination of UBE2E1 at concentrations between 1-10 μM and of UBE2E2 at concentrations between 0.1-1 μM. In the case of UBE2E3 however, I did not observe inhibition of autoubiquitination over physiological concentrations of OTUB1.

3.2.4 OTUB1 facilitated inhibition of UBE2D enzymes in the presence of E3 ligase, RNF4

Although OTUB1-facilitated inhibition of UBE2D2 (Nakada et al., 2010) and UBE2D3 (Baietti et al., 2016; Sun et al., 2012) has already been observed, I wanted to make direct comparisons for all OTUB1-interacting E2s with our gel based assays. Moreover, prior inhibition studies reported for UBE2D2 and UBE2D3 were done using a GST-fused OTUB1(C91S) and in the presence of the RING-E3 ligase, TRAF6 [20]. For a more consistent comparison, I performed the gel-based assays for UBE2D family of proteins using untagged OTUB1(C91S) and the RING-E3 ligase, RNF4 **(Figure 3.6.a)**. I then blotted for Ub, since UBE2D proteins form a variety of chain types **(Figure 3.6.b)** (Brzovic and Klevit, 2006; Brzovic et al., 2006; David et al., 2010; Plechanovov et al., 2012). In the absence of an E3 ligase, all UBE2D proteins exhibited limited ubiquitin conjugating activity, which is consistent with previous findings for most E2s (David et al., 2010; Ernst et al., 2013; Ye and Rape, 2009). There was a significant enhancement of activity, as evidenced by the large smears signifying multiple polyubiquitin species with the addition of the E3. There was a stark reduction in activity with just 1—10 μM of OTUB1. Previous results observed persistent light smears when blotting for Ub in reactions containing UBE2D2/UBE2D3 in the presence of TRAF6 at concentrations 0—4 μM OTUB1 (Nakada et al., 2010). In congruence with previous studies, our results show that OTUB1 inhibits the UBE2D family of enzymes from polyubiquitinating with RNF4 over a concentration range of 1—10 μM.

I attempted a more quantitative approach to measuring inhibition by determining values for each half-maximal inhibitory concentration, IC_{50} **(Figure 3.6.c)**. I measured the rates for E2 activity by quantifying the disappearance of monoubiquitin as the ubiquitin was activated, conjugated, and used to form chains over time. Using a gel-based assay, I tracked the changes in the intensity of the ubiquitin band with increasing concentrations of OTUB1. The initial rates of E2 activity were

normalized and fit to determine the half-concentration by which OTUB1 effectively sequesters ubiquitin conjugation. I found that UBE2D1 was inhibited at a OTUB1 concentration of 5.1 μM, UBE2D2 was inhibited at 0.2 μM, and UBE2D3 was inhibited at 1.1 μM. However, IC_{50}s proved too difficult to quantify non-canonical inhibition. I determined that quantifying the different intensities for monoubiquitin over time were unreliable, so I decided not to continue measuring IC_{50}s but rather report a range of effective inhibitory concentrations for OTUB1.

3.2.5 OTUB1 inhibition of UBE2N

OTUB1 inhibits UBE2N from heterodimerizing with UEV1a in addition to inhibiting the E2 from interacting with the E3 ligases, RNF168, TRAF6, and RNF8 (Nakada et al., 2010; Sato et al., 2012; Wiener et al., 2012). To make direct comparisons for OTUB1-faciliated inhibition of all E2 partners, I assayed OTUB1 inhibition of free chain synthesis by UBE2N in the presence of the E3 ligase, RNF4 **(Figure 3.7)**. The ubiquitin conjugating activity of UBE2N is enhanced in the presence of RNF4 and decreases with increasing concentrations of OTUB1. I observed a reduction in ubiquitination at 0.1—1 μM of OTUB1, similar to previous results which saw inhibition between 0.9-1.8 μM OTUB1 (Nakada et al., 2010).

3.3 Conclusion

OTUB1 non-catalytically inhibits the ubiquitin transfer from E2 to E3. OTUB1 regulates MDM2-mediated p53 ubiquitination (Chen et al., 2016; Sun et al., 2012) and TGFβ signaling (Herhaus et al., 2013) by suppressing ubiquitination by UBE2D proteins. OTUB1 also pays a crucial role in the DNA double-stranded break response by non-catalytically repressing the K63 ubiquitin conjugating activity of UBE2N/UEV1a (Nakada et al., 2010; Sato et al., 2012). Previous studies

examined OTUB1 facilitated inhibition of the K63 ubiquitin conjugating activity of UBE2N in the absence of an E3 (Wiener et al., 2012) and in the presence of the E3 ligases, RNF8, TRAF6, and RNF168 (Nakada et al., 2010; Sato et al., 2012). In addition, inhibition has been observed for UBE2D2, and UBE2D3 in the presence of RNF8, TRAF6, and RNF168 (Nakada et al., 2010; Sato et al., 2012) with increasing concentrations of a GST-fused OTUB1. As a comparison, I looked at inhibition of free chain synthesis for these E2s in the presence of untagged OTUB1 and the E3 ligase, RNF4. I found that OTUB1 inhibits UBE2N at concentrations of 0.1—1 μM which is within the range of the EC_{50}, 0.8 μM **(from Chapter 2)**. Similarly, I observed a stark reduction in E2 activity for the UBE2D family of proteins in the presence of 1—10 μM of OTUB1. The concentration of OTUB1 needed to inhibit also matches the effective concentration of E2 to enhance the DUB activity, 3.9 μM for UBE2D1, 3.8 μM for UBE2D2, and 1.5 μM UBE2D3. I therefore conclude that there is a tradeoff between the two opposing actions of deubiquitinating and ubiquitinating that may be controlled by intracellular concentrations ratios of E2 to E2~Ub.

It was recently shown that OTUB1 not only suppresses the K48 ubiquitin conjugating activity of UBE2E1 but also inhibits autoubiquitination of the E2 (Pasupala et al., 2018). I asked if this was true for the remaining E2s in the UBE2E family, UBE2E2 and UBE2E3. I found that OTUB1 suppresses the K48 free chain synthesis activity for both of these E2s at concentrations of 1—10 μM of the DUB. Once again, this range of concentration of OTUB1 falls within the EC_{50}s that I determined earlier, 4.6 μM for UBE2E1, 10.9 μM for UBE2E2, and 10.7 μM for UBE2E3. Unexpectedly though, OTUB1 inhibits autoubiquitination of UBE2E1 and UBE2E2 but not UBE2E3, even at concentrations of 50 μM of the DUB. The Ubc domain sequence of UBE2E proteins is conserved with 92% identity to other E2s. However unlike the other E2 partners to which OTUB1 binds, UBE2E enzymes possess an N-terminal extension that varies in length for

each protein. It is possible that this additional extension accounts for the varied inhibitory responses with increasing concentrations of OTUB1.

An interesting result from studying the non-canonical E2 inhibition by OTUB1 was that OTUB1 C91S was better at inhibiting UBE2E1 than the wild-type DUB. I checked to make sure that I did not switch the proteins and repeated this experiment several times but received the same results. It is unclear whether wt OTUB1 is less adept at inhibiting the polyubiquitinating or autoubiquitylating activities of UBE2E1. Further analysis is needed to uncover the mechanisms that make OTUB1 C91S a better inhibitor than the native protein.

3.4 Materials and Methods

3.4.1 Protein Expression and Purification

All E2 proteins, OTUB1 enzymes, and ubiquitin proteins were purified as described previously in Chapter 2. Additionally, E1 (Berndsen and Wolberger, 2011) and E3 (DiBello et al., 2016) (**Table 3.1**) enzymes were purified as described.

3.4.2 E1 charging assays

E1 charging of select E2 enzymes were carried out through gel based assays. Reactions contained 0.15 µM of Uba1 (E1), 2 µM of E2, 12.5 µM of Ub wt in a buffer of 50 mM HEPES pH 7.5, 300 mM NaCl, 10mM $MgCl_2$, 0.5 mM DTT, and 0.005 % Tween20. To study whether inhibition of charging occurred with the presence of OTUB1, OTUB1 (C91S) was added at concentrations 1, 5, and 10 µM. Reactions were initiated with the addition of 0.15 µM E1 and 5 mM ATP pH 7.6 and placed in a 37 °C for 10 mins. Assays were quenched with sample buffer

that had 400 mM BME (+BME) added to it or had water added to it (-BME). Samples were immediately analyzed using SDS-PAGE and stained with Coomasie Brilliant Blue.

3.4.3 IC_{50} Determination

Quantitative IC_{50}s, effective concentration of OTUB1 to inhibit ubiquitin conjugating activity of the E2, were determined through gel-based assays. Reactions contained 50 mM HEPES pH 7.5, 300 mM NaCl, 10mM $MgCl_2$, 0.5 mM DTT, and 0.005 % Tween20. In addition, each reaction contained 10 µM 4xSUMO2 substrate, 0.1 µM E1, 2 µM E2, 2 µM RNF4, and 50 µM Ub wt with and without specified concentrations of OTUB1 (C91S), log base -8 to -4) at a constant temperature of 37 °C. Reactions (10 µL) were initiated with 5 mM ATP pH 7.5 and 0.1 µM E1 then at specific time points, quenched with SDS-PAGE loading dye containing BME. Samples were analyzed by gel electrophoresis on 4–12% gradient polyacrylamide Bis-Tris Criterion XT gels (Bio-Rad). For quantitative analysis for IC_{50} determination, gels were then stained overnight with 'longer staining protocol" for SYPRO Ruby Protein Gel Stain (Thermo Fisher Scientific). After staining overnight, gels were further destained in 10% methanol and 5% glacial acetic acid for 30 mins before the gel was imaged on the Typhoon Imager (GE LifeSciences). The concentration of the ubiquitin consumption band for each time point was quantified by densitometry with ImageJ software (Eliceiri et al., 2012). The data was analyzed using GraphPad Prism and fit to determine the 50% inhibition concentrations for each E2. Experiments were done in triplicate.

3.4.4 Qualitative inhibition gel based assays

Gel-based assays inhibition of E2 ubiquitin-conjugating activity were determined at 37 °C in

reaction buffer containing 50 mM HEPES pH 7.5, 300 mM NaCl, 10mM $MgCl_2$, 0.5 mM DTT, and 0.005 % Tween20. In addition, each reaction contained 10 µM 4xSUMO2 substrate, 0.1 µM E1, 2 µM E2, 2 µM RNF4Δ22, and 50 µM Ub wt with and without specified concentrations of OTUB1 (C91S). Reactions (10 µL) were initiated with 5 mM ATP pH 7.5 and 0.1 µM E1 then at specific time points, quenched with SDS-PAGE loading dye containing BME. Samples were analyzed by gel electrophoresis on 4–12% gradient polyacrylamide Bis-Tris Criterion XT gels (Bio-Rad) and were either stained with Coomassie Brilliant Blue (Bio-Rad) or transferred to a PVDF membrane for a Western Blot. For blots, 4 µL samples run by gel electrophoresis on 4–12 % polyacrylamide Bis-Tris Criterion XT gels (Bio-Rad) and immediately transferred to a PVDF membrane via the Bio-Rad Turbo Transfer system. All blots were systematically blocked with 5% BioRad blotting grade blocker in TBST for 1hr at room temperature. Afterwards, they were washed thrice with TBST, rocking at room temperature for 10mins. Blots were then incubated with primary antibody **(Table 3.2)**, diluted in 2% BSA, 0.02% sodium azide in PBS buffer, overnight at 4 °C. The following day, blots were washed again three times with TBST for 10 min intervals before adding secondary antibody, diluted in 5% BioRad blotting grade blocker, and let it shake at room temperature for 1 hr. After another round of washes with TBST, 1:1 BioRad Clarity ECL reagent was used to visualize proteins of interest.

Table 3. 1 Protein characteristic parameters.

	extinction coefficient, 1/M*cm	Molecular weight, g/mol	pI	number of amino acids	Vector	Cleavage site
Uba1	100825	117800	5.6	1058	pProEx	NA
RNF4Δ22	5960	18749	5.2	168	pETSUMO	SENP2

Extinction coefficients, molecular weight, and pI were calculated using Expasy.

Table 3. 2 Primary antibodies for probing UBE2E1 and K48 polyubiquitin.

Target protein	Catalogue Number	Supplier	Species	Dilution with 1x Buffer	Epitope
UBE2E1	A-630 now discontinued	Boston Biochem	rabbit	1 to 800	full-length recombinant human Ube2E1
UBE2E2		Boston Biochem	rabbit	1 to 500	
UBE2E3		Boston Biochem	rabbit	1 to 1000	
K48 polyubiquitin	4289S	Cell Signaling Technology	rabbit	1 to 1000	isopeptide bond between K48 and G76; specific for K48 chains, slight cross-reactivity with linear chains
ubiquitin	clone VU1	Life Sensors	mouse	1 to 1000	recognizes free Ub, monoUb'd proteins, and polyUb'd proteins. Confirmed to pick up K63, K48, K11, and linear chains

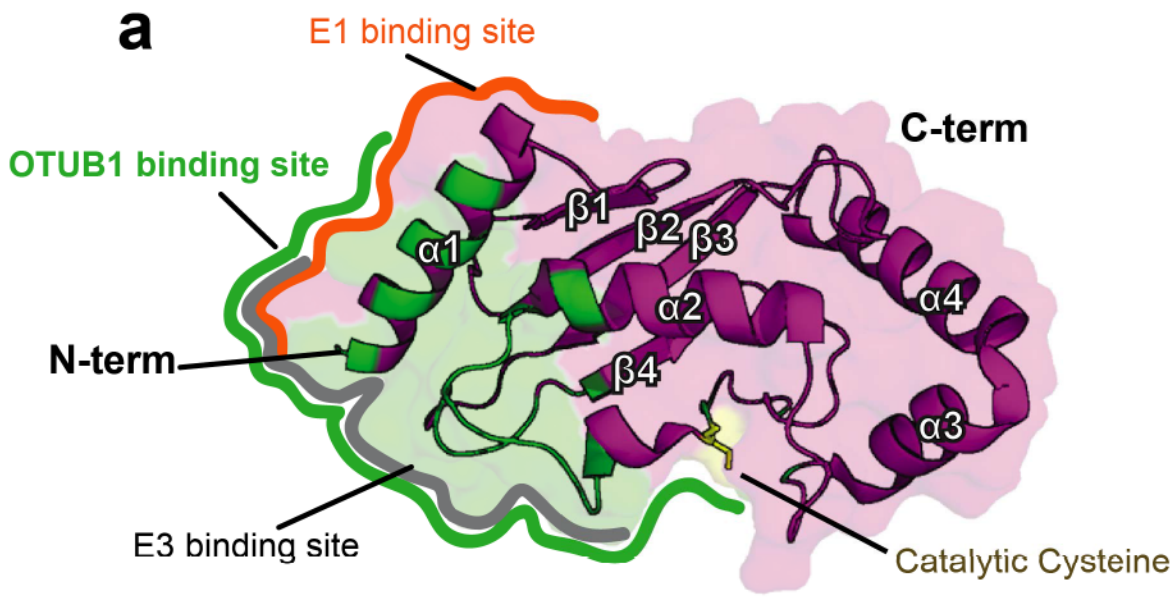

Figure 3. 1 OTUB1 sequesters the E2.
(a) *The structure of UBE2D2 is depicted with labels for the α-helices and β-sheets that compose the Ubc domain. Known structures of each E2 partner were aligned to UBE2D2 in the structure PDB: 4LDT, OTUB1 bound to UBE2D2~Ub. Residues on the E2, calculated using Python, within 5Å of OTUB1 are highlighted in green. The E1 and E3 binding sites were highlighted based on the residues on the E2 that are known to contact.*

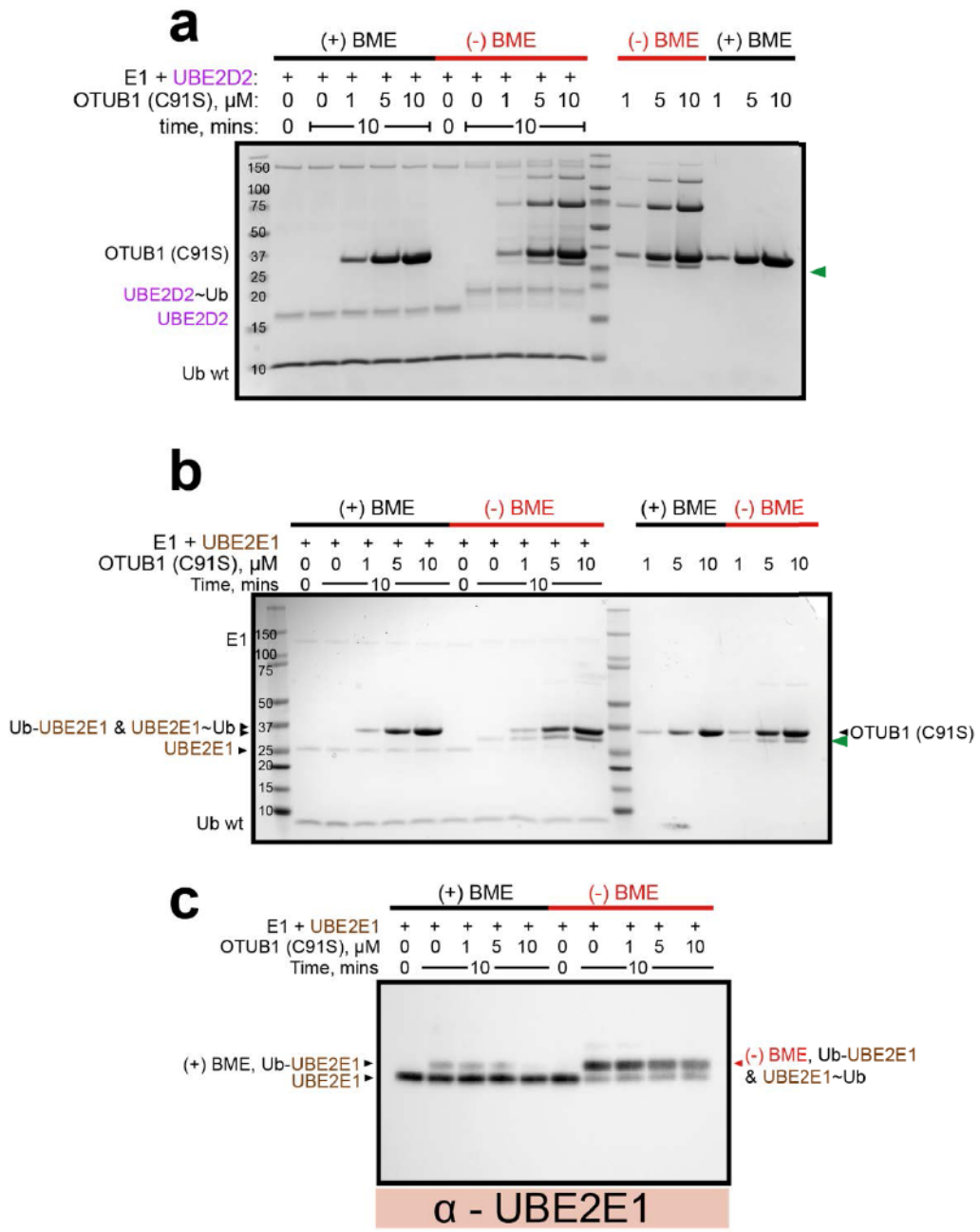

Figure 3. 2 OTUB1 does not interfere with E1 charging of UBE2D2 or UBE2E1
Assay whether OTUB1 disrupts E2 charging by titrating in increasing concentrations of OTUB1 in absence and presence of BME in the quenching buffer. Samples were run immediately on SDS-PAGE then stained with Coomasie. Assays were run at two time points, t=0 and 10 mins. OTUB1 alone samples in the presence and absence of BME were also run to differentiate the appearance of the lower molecular weight band (signified by green triangle) ***(a)*** *charging of UBE2D2 and* ***(b)*** *of UBE2E1. Since Ub-UBE2E1, UBE2E1~Ub, and intramolecularly interacting OTUB1 in the absence of BME all run similarly* ***(c)*** *depicts the Western blot for the UBE2E1 epitope. In (+)BME, the higher molecular weight band corresponds to autoubiquitinated UBE2E1. In (-)BME, the higher band is a mixture of Ub-UBE2E1 and UBE2E1~Ub.*

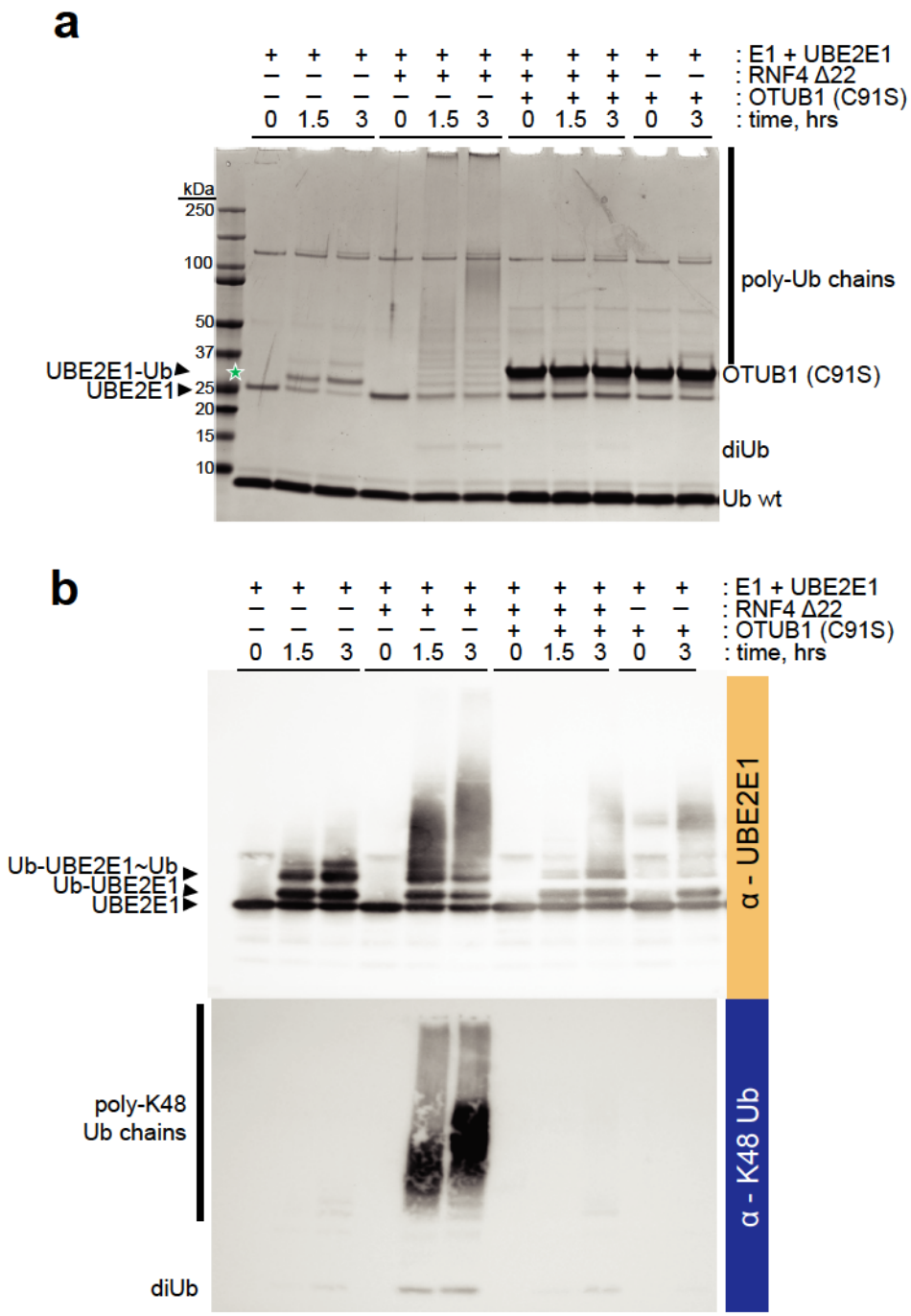

Figure 3. 3 Time course assay for the inhibition of UBE2E1 autoubiquitylation by OTUB1. *In vitro assay of recombinant proteins showing autoubiquitination of UBE2E1 in the presence and absence of the E3 ligase, RNF4, and OTUB1-C91S.* ***(a)*** *Coomassie stained gel of ubiquitination reactions containing 0.1 µM UBA1, 5 µM UBE2E1, 1 µM RNF4, 50 µM Ub wt, and 10 µM OTUB1 C91S. The green star indicates the persistent higher molecular weight band that was present in reducing conditions. Western blot of reactions shown in top panel using antibodies against* ***(b)*** *UBE2E1 (top) and K48-polyubiquitin (bottom).*

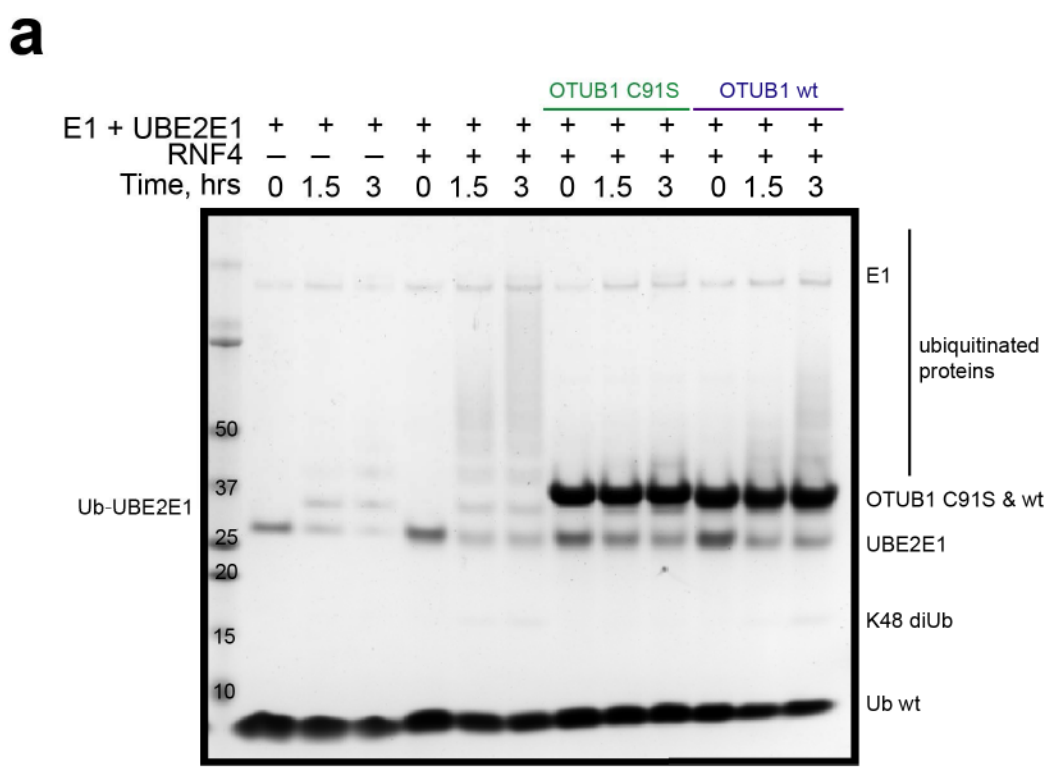

Figure 3. 4 OTUB1 C91S is better at inhibiting UBE2E1 facilitated ubiquitylation than wild-type.

(a) *Time course assay that analyzed OTUB1, C91S vs wt, inhibition of UBE2E1 ubiquitylating activity. Experiments contained 0.1 μM UBA1, 5 μM UBE2E1, 1 μM RNF4, 50 μM Ub wt, and 10 μM OTUB1 C91S or wt. Large smears above 39 kDa correspond with ubiquitinated proteins.*

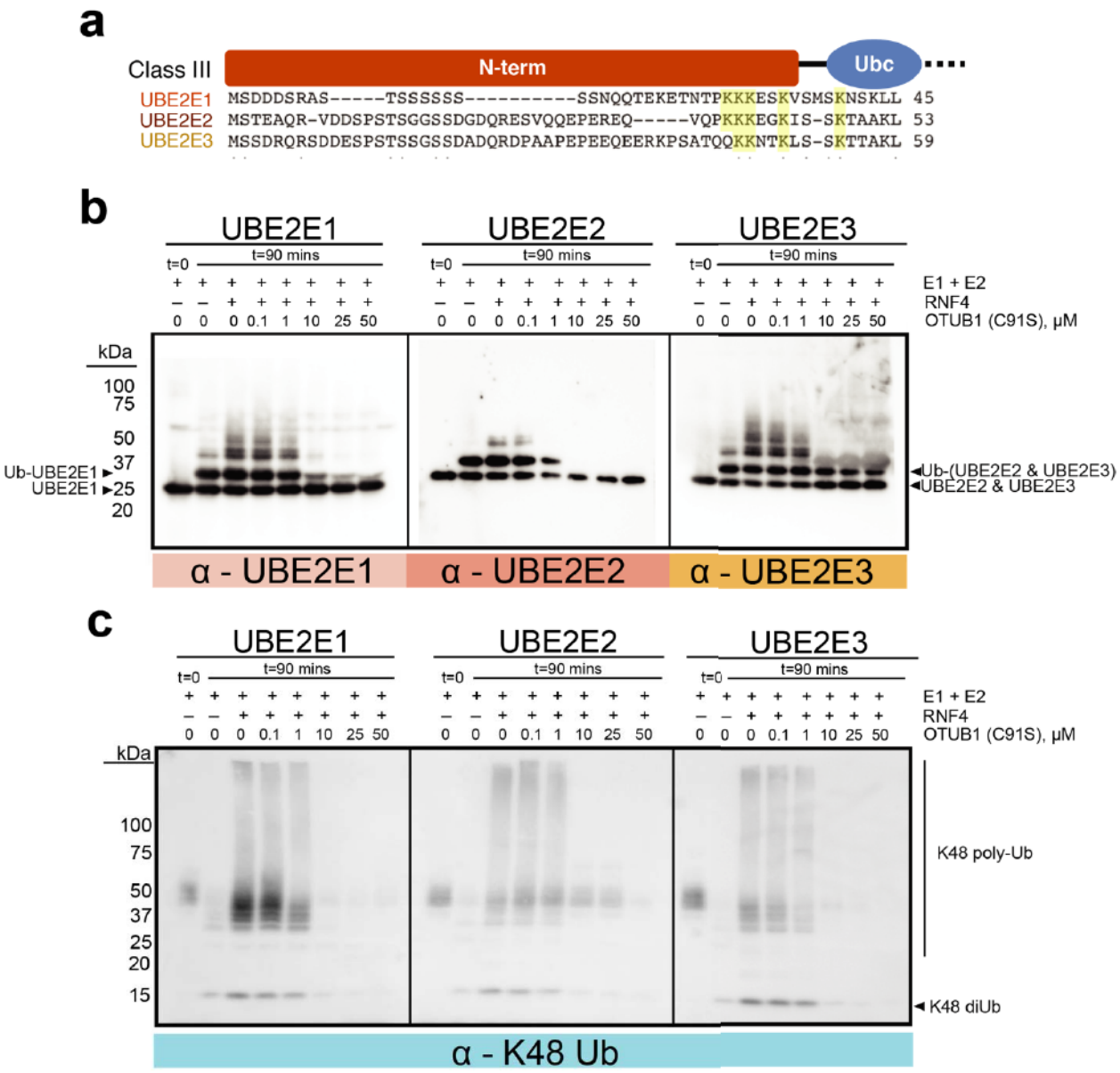

Figure 3. 5 OTUB1 inhibits polyubiquitination by the UBE2E family of enzymes yet only inhibits autoubiquitylation of UBE2E1 and UBE2E2, not UBE2E3

(a) *Sequence alignment of the N-terminal sequences for UBE2E1, UBE2E2 and UBE2E3. Alignment performed with ClustalW. Conserved lysines in the N-terminal extension are highlighted.* ***(b)*** *End point reactions quenched at t= 0 and 30 mins with increasing concentrations of OTUB1 (C91S). Western blot depicting the autoubiquitylation of UBE2E enzymes being inhibited with increasing concentration of OTUB1 (C91S). Probed for individual unique UBE2E epitopes. UBE2E1 runs very similarly to RNF4 therefore the bands overlap.* ***(c)*** *Blot against K48 Ub.*

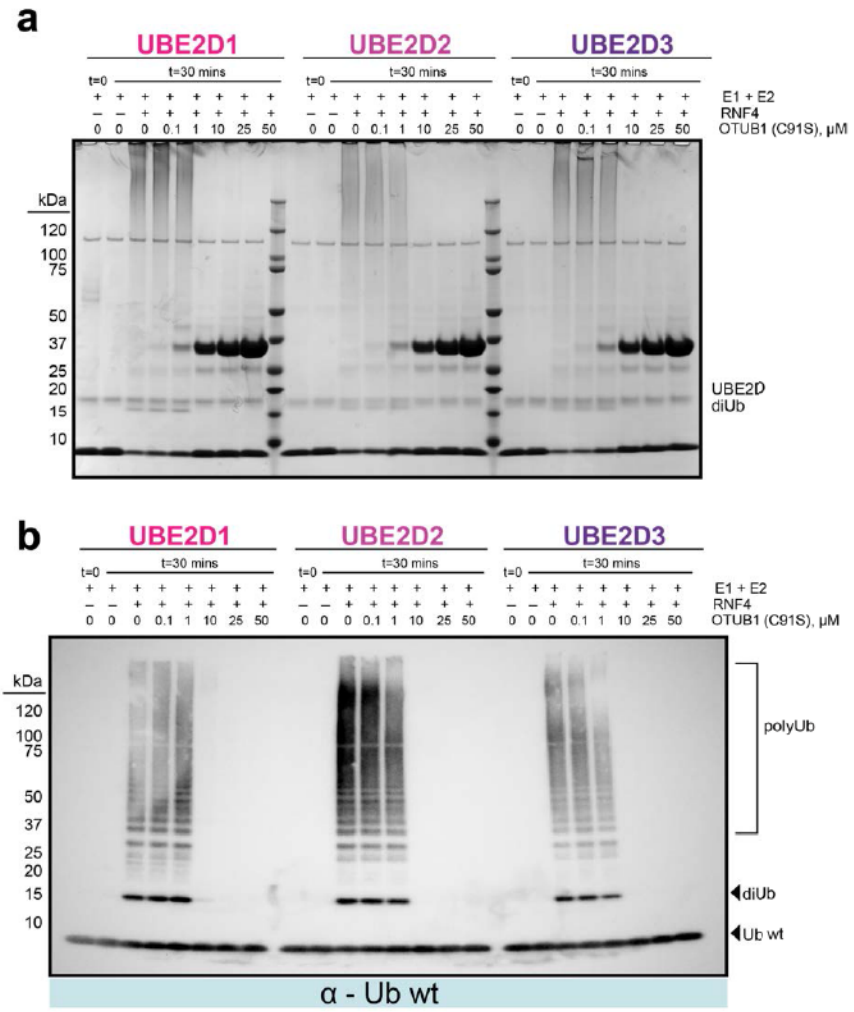

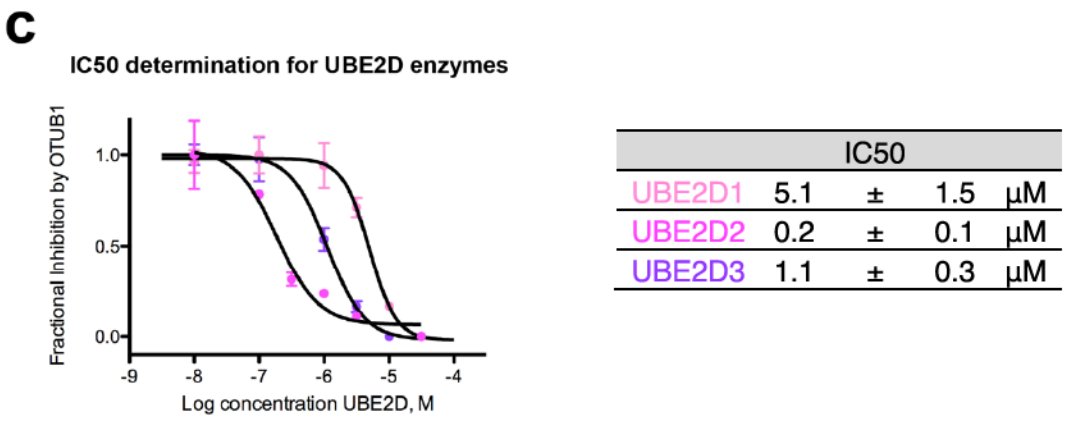

	IC50			
UBE2D1	5.1	±	1.5	μM
UBE2D2	0.2	±	0.1	μM
UBE2D3	1.1	±	0.3	μM

Figure 3. 6 OTUB1 inhibits the polyubiquitinating activity of UBE2D family of enzymes
Qualitative measure of polyubiquitinating activity for UBE2D1, UBE2D2, and UBE2D3 in the absence and presence of RNF4, then in increasing concentrations of OTUB1 (0-0.1 μM). Samples were quenched with SDS sample buffer and either stained in ***(a)*** *Coomasie SDS-PAGE or* ***(b)*** *blotted against ubiquitin wt.* ***(c)*** *IC50s determined by tracking the band of monoubiquitin over time with increasing concentrations of OTUB1. Error bars indicate results for triplicate experiments.*

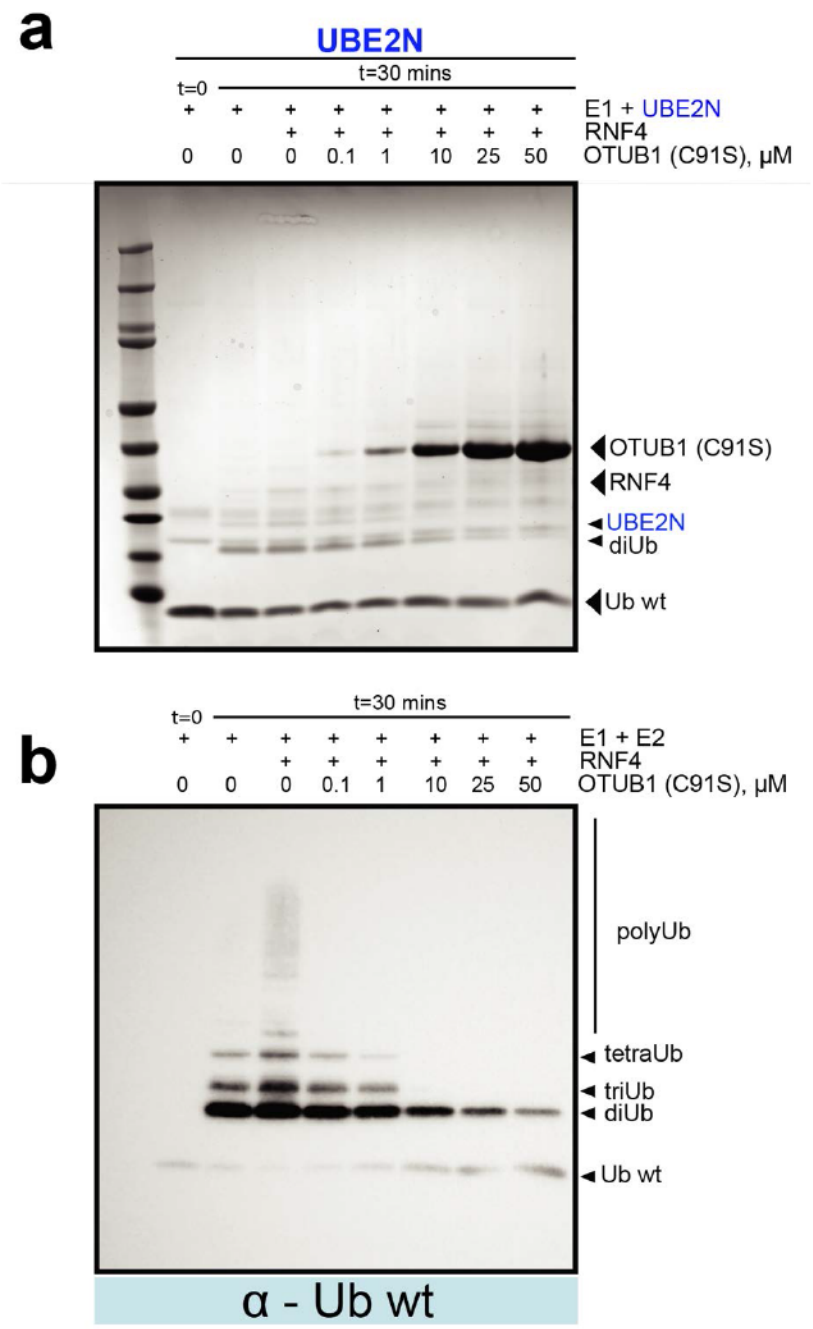

Figure 3. 7 OTUB1 inhibits the polyubiquitinating activity of UBE2N/UEV1a
Qualitative measure of polyubiquitinating activity for Uba1 (0.1 µM) and UBE2N/UEV1a (equimolar concentrations of 2 µM) with 50 µM of Ub wt in the absence and presence of RNF4 (2µM), then in increasing concentrations of OTUB1 (0-0.1 µM). Samples were quenched with SDS sample buffer and either stained in ***(a)*** *Coomasie SDS-PAGE or* ***(b)*** *blotted against ubiquitin wt.*

Chapter 4 Crystallization trials of UBE2E1:OTUB1 (C91S) complex

4.1 Introduction

Structural insights into how OTUB1 interacts with a Class III Ubiquitin Conjugating Enzyme, E2 remain elusive. My results in **Figure 3.4** demonstrate that OTUB1 C91S is better at inhibiting the polyubiquitinating activity of UBE2E1. It is unclear why a mutation to the active site of OTUB1 would affect its non-catalytic role in inhibiting UBE2E1, especially since the catalytic cysteine, C91, is 15 Å from the closest E2 contacting residue on OTUB1. Preliminary data suggest that OTUB1 C91S may actually bind tighter to UBE2E1 than the wild-type DUB. I considered this a fantastic opportunity to obtain a structure of this complex. Although truncated or hybrid versions of OTUB1 (Edelmann et al., 2008; Sato et al., 2012; Wiener et al., 2013; Wiener et al., 2012) and UBE2E1 (Sheng et al., 2012) have been determined, a structure of full length OTUB1 and UBE2E1 is unavailable.

I sought to understand the structural mechanisms behind OTUB1 C91S inhibiting the formation of poly-ubiquitinated species better than OTUB1 wt. Extensive binding studies will be conducted to determine whether the reduced inhibition I observed for wt vs the catalytic mutant is correlated to the differences in affinity between the DUB and the E2. This chapter summarizes the characterization of interactions between full-lengths OTUB1 and UBE2E1 as well as the crystallization attempts for this complex.

4.2 Results

4.2.1 OTUB1 (C91S) binds more tightly to UBE2E1 than OTUB1 wt

OTUB1 (C91S) binds with similar affinity (~ 7 μM) to UBE2D1, UBE2D3 and UBE2E1 **(Figure 4.1).** When testing whether the K_d was also relatively the same for OTUB1 wt (1.5 mM) and these E2s (150 μM), I performed the ITC experiments under the same conditions. I found that the interactions between OTUB1 wt and either UBE2D1 or UBE2D3 were relatively similar and comparable to the measurements of those same E2s with OTUB1 (C91S). However, the binding affinity for UBE2E1 with OTUB1 wt was 4 times higher than that of UBE2E1 and OTUB1 (C91S); OTUB1 (C91S) binds to UBE2E1 with a K_d of 7 μM whereas with OTUB1 wt was 26 μM. It is very surprising that a single point mutation in the OTUB1 active site should produce such a large change in affinity for any E2 partner, as the active site is not near the OTUB1-E2 interface in structures of either UBE2N (REF: Wiener, 2012) or UBCH5B (REFS: Wiener, 2013; Juang 2012) bound to OTUB1. Structural information is needed to address the reason for the observed increase in affinity of OTUB1 (C91S) for UBE2E1.

4.2.2 Summary of Crystallization Trials

Crystallization conditions were screened for the following complexes: (1) UBE2E1: *C. elegans* OTUB1, (2) UBE2E1:wt human OTUB1, (3) UBE2E1:human OTUB1(C91S). Complexes were formed by adding equimolar amounts of both proteins to a final concentration of 5-20 mg/mL **(Table 4.1).** In addition, the complex was diluted in 1x buffer containing, 100 mM NaCl and 0.5mM TCEP-HCl, then screened using JCSG+ (Hampton Research) and HR1422 (Qiagen), Mosquito 96-well plates at a 1:1 ratio (0.5 μL). Needles formed in 100 mM HEPES pH 7.0 and 10% PEG 6000 **(Figure 4.2).** Three-dimensional crystals formed with 100 mM CHES pH 9.5 and 20% PEG 8000. Larger screens (24-well plates) were thus made to reproduce the initial hit but to no avail. Thus, an additive screen (Hampton Research) was used in addition to the CHES/PEG buffer to optimize crystal conditions. It is important to note that crystals grew at

protein concentrations of 7.5, 10, and 20 mg/mL. However, only crystals grown from 7.5 mg/mL protein solution were sufficiently large and well-separated to be handled. This condition was therefore utilized for all further crystal tests.

Using the conditions for the initial hit, an additive screen was performed to optimize crystallization conditions. The additive screen produced several hits that ranged from crystal showers to large single crystals **(Figure 4.3).** Two promising conditions that were taken to the next stage of optimization were those grown in 10 mM strontium chloride and in 100 mM Spermidine **(Figure 4.4).** Crystals with the corresponding additive were grown by mixing 1 µL of complex and 1 µL of well solution in a 1:1 ratio. The resulting crystals ranged in size from 0.1-0.3 µm in length and were always pyramid shaped.

4.2.3 OTUB1 (C91S):UBE2E1 crystals contain both proteins yet yield low resolution data

Before determining the resolution to which these crystals diffracted x-rays, I first sought to determine whether both proteins were present. Two sets of crystals grown 1:1 in 1 µL hanging drops were selected to evaluate protein composition. Crystals were retrieved using a 0.1-0.2 µm loop and washed twice with 2 µL of mother liquor **(Figure 4.5).** After washing the crystal in fresh buffer five times in the mother liquor, the crystal was placed into 2 µL of buffer and vortexed in order to crush it. Samples of each wash and the final homogenized crystal were run on an SDS-PAGE gel and stained with Sypro-Ruby (Thermo Fisher Scientific). From the final sample containing just the crystal I determined that both proteins were indeed present at a 1:1 ratio which was highly encouraging. This procedure was repeated again with a different crystal grown in a different condition **(Figure 4.5, crystal 2)**, which also contained both proteins.

To prepare the crystals for x-ray diffraction data collection, I experimented with cryopreservation conditions. First, I attempted to loop crystals with and without the cryoprotectant, 20% PEG 500, and found that one in every fifteen crystals that I shot actually yielded a diffraction pattern extending to around 10 Å resolution, for crystals grown in 20 °C **(Figure 4.6.b-f).** From these results, I determined that the protein crystals were most likely mosaic, thus producing a low resolution. The next step was to try serial dehydration in an attempt to lower the mosaicity **(Figure 4.6.c-d).** Serial dehydration was attempted using two different dehydrators and yet diffraction only improved to ~ 9 Å**.** Serial dehydration was performed by fishing out single crystals and placing them into solutions of PEG 8000 that was diluted in well solution. Dehydration started from 18% and increasing increments by 2% until a final solution of 28% PEG 8000 coated the crystal. However, this did not improve the diffraction. Another attempt at reducing mosaicity was growing crystals at 4 °C to see if I could slow down crystal formation and thereby improve the resolution **(Figure 4.6.e)**. However, this failed to improve the resolution. In fact, little to no diffraction was observed for all the attempts at optimization. Although crystal growth was highly encouraging, I were unable to achieve a high resolution using the three different methods: cryoprotectant, serial dehydration and changing growth conditions.

4.3 Future Directions

The molecular basis for the higher affinity of OTUB1 (C91S) for UBE2E1 as compared with wt OTUB1 remains unknown. Should it ultimately be possible to obtain well-diffracting crystals, structural studies of this complex will elucidate why the C91S OTUB1 mutant binds more tightly to UBE2E1 than wt. Various structures of both OTUB1 (C91S) (Edelmann et al., 2008; Sato et al., 2012; Wiener et al., 2012) and UBE2E1 (Sheng et al., 2012) have been solved previously,

although not in complex with one another and not as their full length moieties. In addition, since this would be the first structure using full length constructs of both proteins, it will be interesting to see if there is any structure in the predicted unfolded N-terminal tails that has not been observed previously.

Crystals grown with the additive, 100 mM spermidine, produced consistently large crystals that contained both protein in equal ratios. Several methods, such as changing cryoprotectant, serial dehydration and changing growth conditions, were employed to improve the resolution to which the crystals diffractive. Despite these efforts, resolution remained low, at 8-9 Å. It is possible that alternative approaches could lead to well-diffracting crystals. Limited proteolysis can be used to identify regions, like the unfolded N-terminal regions, that can be removed without compromising crystal contacts. Additionally, the mutant OTUB1 (C91A) can also be used to screen; since cysteine to serine mutations yields a reduction in charge and spatial orientation, alanine may prove to be an even tighter binder.

4.4 Methods

4.4.1 Protein expression and purification

Full length UBE2E1 and OTUB1 (C91S) were expressed and purified as described in the Chapter 3.2 Methods Section. Expression and purification of UBE2D1, UBE2D3, and OTUB1 wt are described in the Chapter 2.2 Methods Section.

4.4.2 ITC experiments

All experiments were conducted in buffer conditions of 25 mM HEPES pH 7.5, 150 mM NaCl, 0.5 mM TCEP-HCl at 25°C. Proteins of interest were dialyzed together overnight twice in 4 L at 4 °C. Dialysis occurred over two nights to ensure that both proteins were in equilibrium within the buffer. E2s (150 μM) were placed in the cell while 1.5 mM OTUB1 or OTUB1 (C91S) was titrated in. UBE2D1 and UBE2D3 were also measured as controls. All ITC experiments were performed on a MicroCal iTC_{200} system (Malvern). A total of 20 injections of 40 μl titrant were carried out over 180 s intervals.

Table 4. 1 Example table used to determine concentrations and volumes to use for crystal trays.

Protein	7.5	mg/mL		
Total Volume	30	µL		
[UBE2E1]	21400	g/mol	0.000141	M
[OTUB1 (C91S)]	31850.9	g/mol	0.000141	M
total g/mol	53250.9	g/mol		

	A	dilution	E	[], M	MW, g/mol	Volume	
UBE2E1	2.9	10	25690	0.001129	21400	3.74	µL
OTUB1 (C91S)	1.6	10	23840	0.000671	31850.68	6.3	µL
					1x buffer	19.9	µL

The example here was used to make 30 µL for a 24-well plate, 1:1 7.5 mg/mL 2 µL drops.

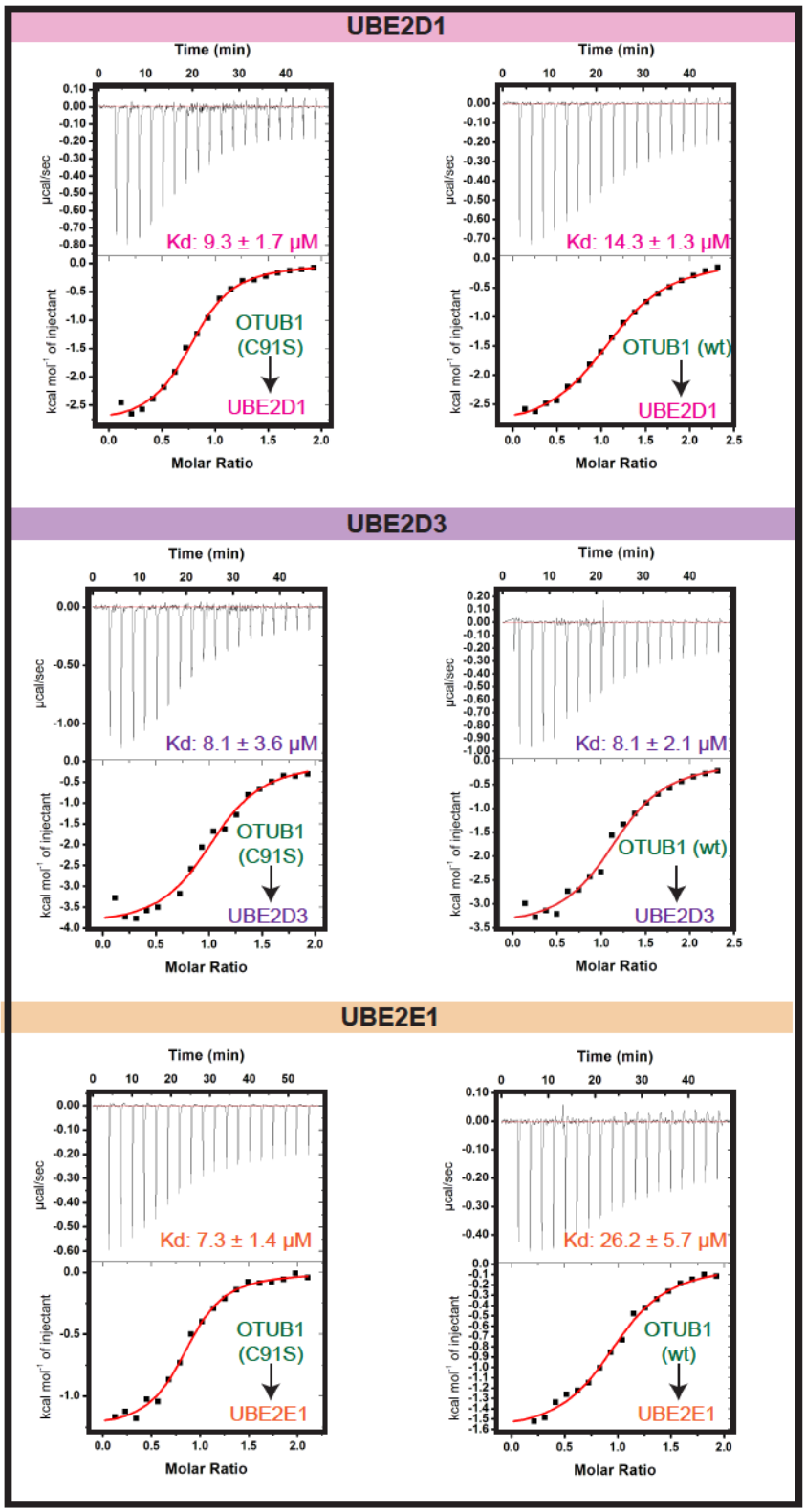

Figure 4. 1 Binding of E2s to OTUB1 (C91S) vs. (wt).

OTUB1 (1.5 mM) titrated into 150 µM E2 within the cell. Proteins were dialyzed in 50 mM HEPES pH7.5, 150 mM NaCl, and 0.5 mM TCEP-HCl buffer twice overnight. Kd values associated with each interaction are displayed with each curve.

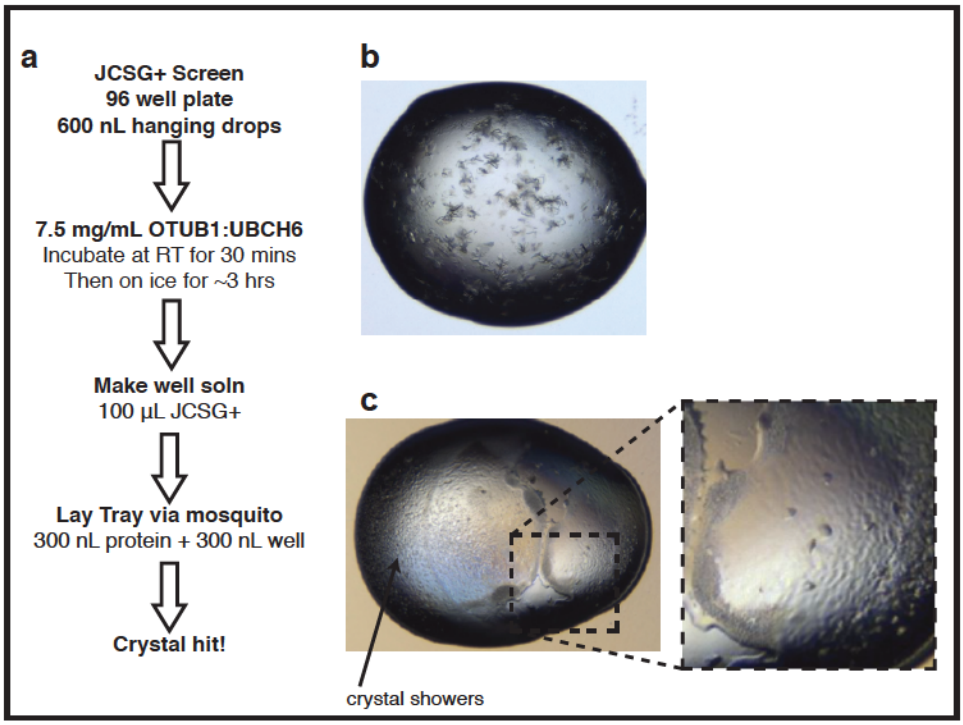

Figure 4. 2 Crystals hits for UBE2E1:OTUB1 (C91S).
(a) *Schematic of setting the 96-well plate with 600 nL hanging drops of JCSG+ condition* ***b)*** *100 mM HEPES pH 7.0 and 10% PEG 6000* ***c)*** *100 mM CHES pH 9.5 and 20% PEG 8000*

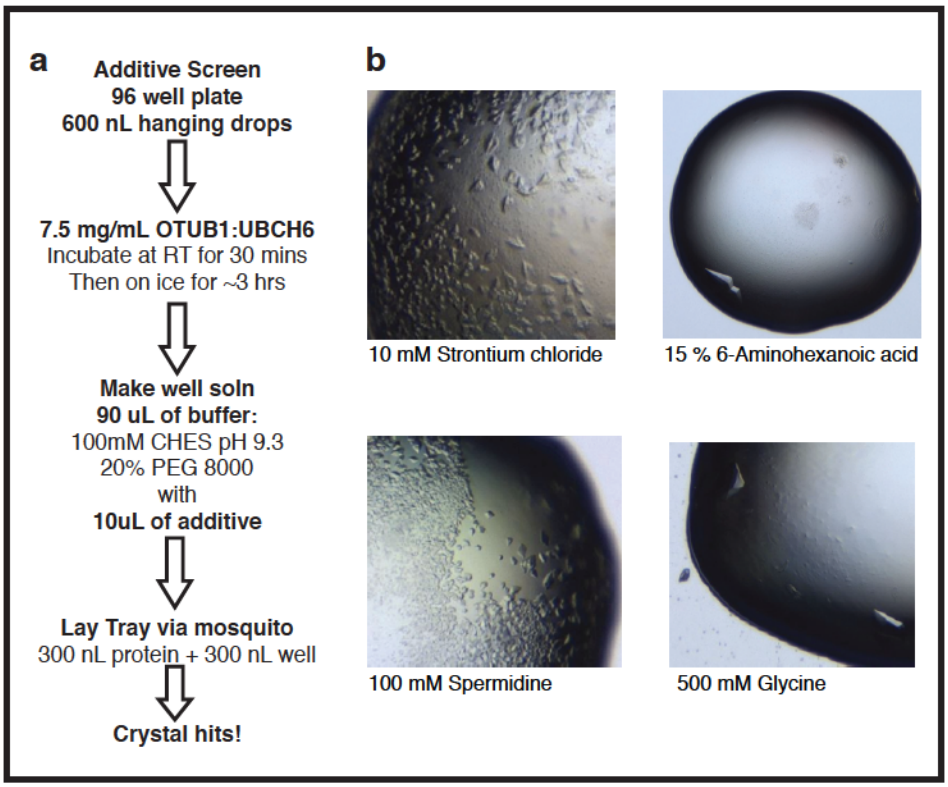

Figure 4. 3 Additive Screen

(a) *Methodology for making 600 nL (300 nL protein with 300 nL buffer) hanging drops using the Mosquito* ***(b)*** *Crystal hits with their additives.*

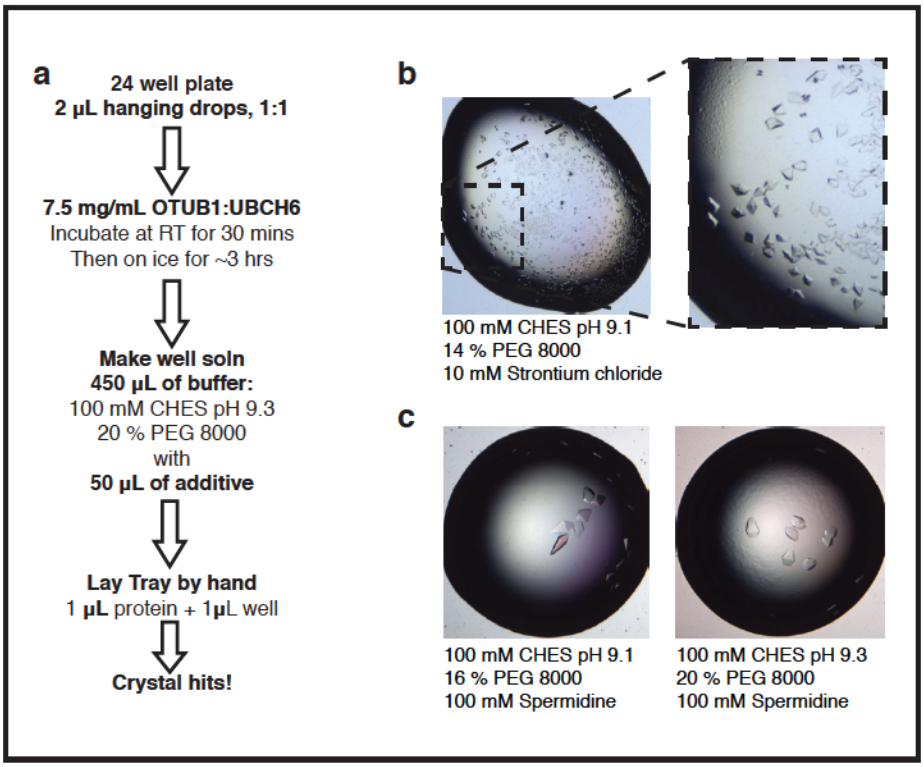

Figure 4. 4 Larger scale optimization crystal trials.
(a) *Schematic of methology for laying the 24 well trays, 1:1, 2 µL drops, 500 µL well solution (450 µL buffer with 50 µL of 100 mM Spermidine.* ***(b)*** *Crystals grown with 10 mM Strontium chloride.* ***c)*** *Example crystals grown with 100 mM Spermidine.*

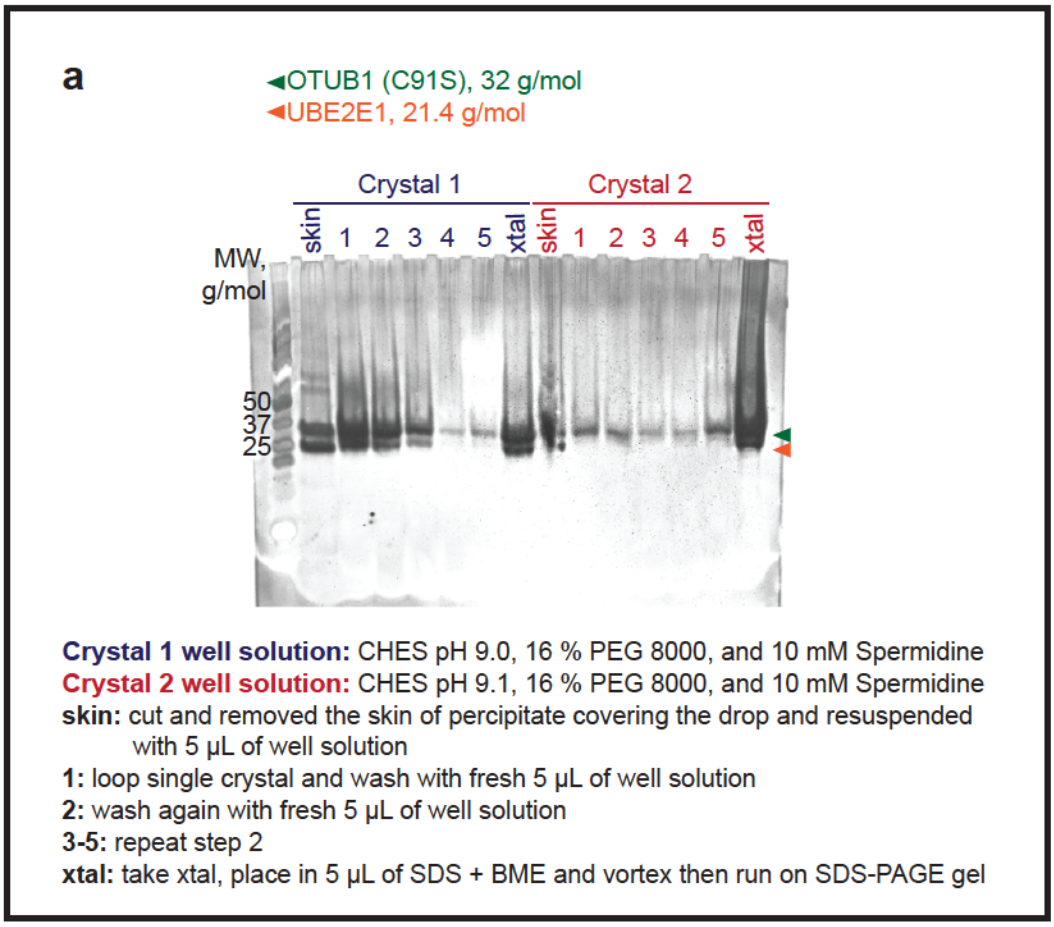

Figure 4. 5 Both UBE2E1 and OTUB1 (C91S) are present in single crystals.
The skin for each drop was removed and a single crystal was subsequently washed multiple times. All wash solutions were run on an SDS-PAGE gel. Gel was stained using Sypro-Ruby stain overnight at room temperature.

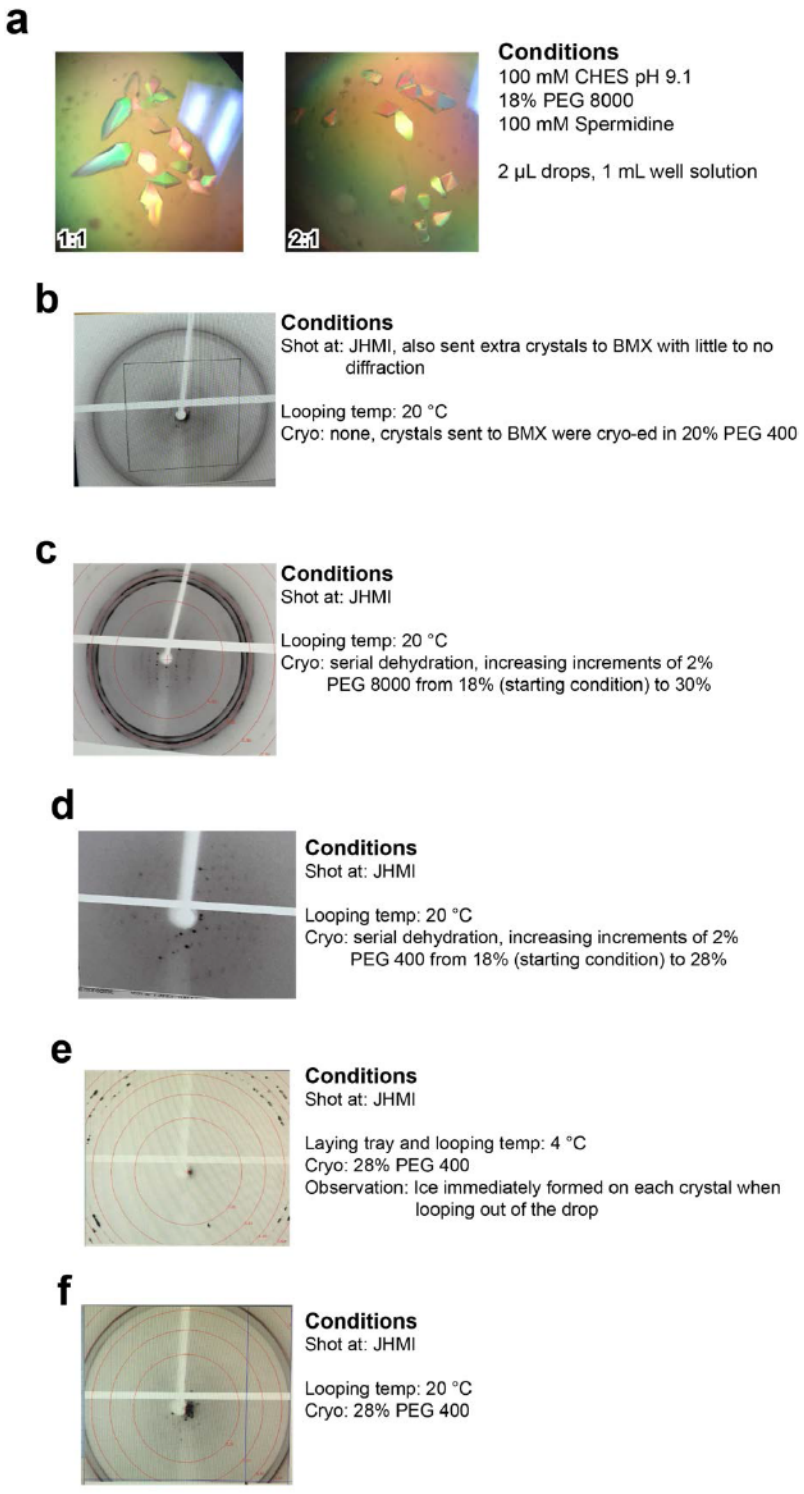

Figure 4. 6 Best diffraction data obtained from several different attempts to optimize resolution

(a) *Example crystals used. Size of crystals varied from 0.1 µM – 0.3 µM in length. Crystals shown are of 1:1 protein complex to buffer and also 2:1. Both sets of crystals were used to see if one condition yielded better results to the other, which is did not.* ***(b-f)*** *Several attempts to increase resolution. Conditions for each attempt are listed for each diffraction set.*

Chapter 5 Conclusion and Future Directions

5.1 Insight into the physiological functions of OTUB1 in complex with E2 enzymes

Deubiquitinating enzymes are modular, frequently found in complex with another protein, which can drive specificity and enhance functionality (Ritorto et al., 2014; Turcu et al., 2009). Several DUBs associate with E3 ligases and to a lesser extent, E2 enzymes, suggesting that DUBs regulate ubiquitylation in addition to the canonical deubiquitylating roles. In the apo form, OTUB1 exhibits low isopeptidase activity which I confirmed in this study (Wang et al., 2009; Wiener et al., 2013). I determined through ITC that the binding affinity of this DUB for K48 diubiquitin was also low, therefore reduced cleaving activity is attributed to low affinity. OTUB1 is a unique DUB that associates with seven E2s in vivo. These interaction partners cross-regulate one another. Additionally, by interacting with these E2s enhances the DUB activity of OTUB1 over a broad range of stimulation. The biological implications for this cross-regulation remained understudied. In this thesis I showed that the cross-regulatory complex, OTUB1:E2 partners, are capable of forming and are functional *in vivo.*

Based on known cellular concentrations in the cell, I predicted that OTUB1 binds to the E2 first before interacting with K48 diUbiquitin. The total ubiquitin concentration in mammalian cells is estimated to be between 20-85 μM depending on the cell type (Clague et al., 2015; Kaiser et al., 2011). These numbers accounts for all forms of ubiquitin: free, mono-, conjugated to enzymes, and in chains. Given that I measured the binding affinity of OTUB1 for K48 diUbiquitin to be 84 μM, it is unlikely that OTUB1 will encounter these high levels of substrate *in cellulo.* In support of OTUB1:E2 complex **(Figure 2. 11, A)** forming before OTUB1:K48 diUbiquitin **(Figure 2. 11,**

B), the combined concentrations of UBE2D3 and UBE2N is about 3.7 μM (Kulak et al., 2014; Schwanhäusser et al., 2011) which I determined to be similar to the binding affinities between OTUB1 and the different E2 partners. As a result of forming OTUB1:E2, the E2 increases the affinity of OTUB1 for K48 diUbiquitin producing an enzyme that is more active at ubiquitin concentrations that it will more likely come across *in cellulo*.

I then determined the effective E2 concentrations needed to produce a stimulated response in deubiquitinating activity, and found that the EC50s for UBE2N and UBE2D3 matched the intracellular concentrations determined through mass spectrometry and proteomic studies in the cell (Schwanhäusser et al., 2011). Therefore enhancement produced in the presence of these E2s is plausible under normal physiological conditions in the cell. In fact, UBE2N and UBE2D3 rank as some of the most abundant E2s to be found in both HeLa and Swiss 3T3 cells (Kulak et al., 2014; Schwanhäusser et al., 2011; Stewart et al., 2016). From our kinetic results I learned that UBE2D3 robustly stimulated OTUB1's DUB activity by lowering the affinity of the enzyme for K48 diUbiquitin. In addition, UBE2D3 possessed the largest Hill Slope when fitting the activity curves for determining EC_{50}s which signifies that binding of the E2 induces a favorable conformational change in OTUB1 that preferentially drives binding of K48 diUbiquitin to both ubiquitin binding sites.

I was puzzled by the data I determined for UBE2N. Of all the E2s that I measured UBE2N had lowest EC_{50} which signifies that small amounts of UBE2N are needed to stimulate OTUB1. UBE2N also had the lowest Hill Slope (0.7) which could indicate that binding of this E2 to OTUB1 induces a conformational change to the DUB that is less productive at binding to K48 diUbiquitin. This negative cooperativity could help to explain why I found that UBE2N only mildly stimulates the DUB activity of OTUB1. In its apo form, OTUB1 possesses an unfolded N-

terminus that spans 45 residues (Edelmann et al., 2008; Wang et al., 2009; Wiener et al., 2012). Based on structural analysis, when OTUB1 solely binds to UBE2N partial folding of the N-terminus (residues 39-45) occurs along with conformational changes in the globular fold of OTUB1 (Wiener et al., 2012). Based on structural analysis, when OTUB1 solely binds to UBE2N partial folding of the N-terminus (residues 39-45) occurs along with conformational changes in the globular fold of OTUB1 (Wiener et al., 2012). I hypothesize that premature folding of the N-terminal helix can lead to unproductive and unfavorable interactions within the proximal ubiquitin binding site.

OTUB1 non-catalytically inhibits the ubiquitin transfer from E2 to E3. OTUB1 regulates MDM2-mediated p53 ubiquitination (Chen et al., 2016; Sun et al., 2012) and TGFβ signaling (Herhaus et al., 2013) by suppressing ubiquitination by UBE2D proteins. I observed a stark reduction in E2 activity for the UBE2D family of proteins from 1—10 μM of OTUB1. I also found that OTUB1 inhibits UBE2N at concentrations of 0.1—1 μM which is within the range of the EC_{50}, 0.8 μM. The concentration of OTUB1 needed to inhibit UBE2D1, UBE2D2, UBE2D3, and UBE2N matches the intracellular concentration of the DUB which has reported to be ~0.5 μM in HeLa and Swiss3T3 cells (Kulak et al., 2014; Schwanhäusser et al., 2011) and 1.1 μM in mouse embryonic fibroblasts (MEFs) (Schwanhäusser et al., 2011). I therefore conclude OTUB1 is capable of inhibiting these E2 enzymes under biological conditions in the cell.

Our studies show that OTUB1 is capable of inhibiting the polyubiquitinating activity of all E2 partners over physiological concentrations of the DUB and I also show that E2s, UBE2D3 and UBE2N, are capable of stimulating isopeptidase activity of OTUB1 over biological concentrations. I prove through biochemical methods that there is a tradeoff between the two opposing actions of deubiquitinating and ubiquitinating that may be swayed by the ratio of

charged to uncharged E2s as well as the local concentration of free ubiquitin. The DUB activity of OTUB1 is enhanced in the presence of both charged and uncharged UBE2D2 however cleavage is significantly reduced for UBE2D2~Ub in increasing concentrations of free Ub. (Wiener et al., 2013). OTUB1:E2. E2 charging states in vivo depend greatly on the type of cell lines used. In HeLa cells UBE2N exists only in a charged form but as a mixture of un/charged states in U2OS cells, the UBE2D family of enzymes on the other hand were primarily uncharged in both cell lines (Wiener et al., 2013). Given that a minimal concentration of 0.1-1 μM OTUB1 was able to significantly reduce the polyubiquitinating activity of UBE2N, OTUB1 primarily inhibits UBE2N in HeLa cells whereas in U2OS cells, OTUB1 can both be inhibited and stimulated by UBE2N. I strongly believe though that OTUB1 serves to primarily inhibit this E2 given how weakly (K_M = 24.1 μM) the DUB activity is stimulated in the presence of UBE2N. I attribute this lower stimulation to negative cooperativity (Hill slope < 1) that occurs when UBE2N interacts with OTUB1. Additionally, high concentrations of free ubiquitin has been shown to drive the balance towards the inhibitory OTUB1:E2 complex (Wiener et al., 2013). In HeLa and U2OS cells where the charged ratio of UBE2D enzymes is similar, regulation of the cross-regulatory complex may also be determined by local cellular concentration of free ubiquitin.

5.2 Future Directions

Based on the work covered in this thesis, I was able to make conclusions about which cross-regulatory OTUB1:E2 complexes function *in vivo*. However, one of the main questions that I was unable to answer was why these particular seven E2s? The Ubc domain of these E2s share sequence similarity of 90%. By taking the known structures of each seven E2 and aligning the structure to UBE2D2 in PDB:4LDT, all E2s contact OTUB1 (within 3 Å) using similar residues. When aligning the structure of CDC34, an E2 that should not interact with OTUB1,

similar residues to the seven OTUB1-interacting E2s are also capable of contacting the DUB. The distinguishing factor that allows the seven E2s to interact with OTUB1 is still unknown based on structural analysis. Another interesting detail is that from studying all the structures of OTUB1, binding of the E2 changes very little to the actual E2 binding site. Conformational changes in the globular fold, distal and proximal ubiquitin binding sites, account for the largest differences in structure (Edelmann et al., 2008; Sakata et al., 2010; Wiener et al., 2013; Wiener et al., 2012). More research is needed to help distinguish why OTUB1 interacts with the select seven E2s *in vivo* over any other ubiquitin conjugating enzyme.

Appendix: Crystallization of tetraubiquitin in complex with a cyclic peptide

A.1 Introduction

This appendix summarizes my crystallography side project that I worked on in addition to my thesis. In this section I discuss my attempts to obtain a structure of wild-type tetraubiquitin (tetraUb) associated with a cyclic peptide, Ub4_a **(Figure A.1.a)**. The process of ubiquitination and deubiquitination are involved in several different biological systems including oncogenic and tumor-suppressor pathways. As a result, the ubiquitin system is an excellent drug target for cancer therapy. Some drugs target DUBs, reacting with the active site cysteine and inhibiting all isopeptidase activity (Farshi et al., 2015; Goldberg, 2012; Harrigan et al., 2018). Another approach for drug development is targeting the ubiquitin molecule itself. A chemical genetic screen found that small molecules 'ubistatins' target ubiquitin by binding to both mono- and poly-ubiquitin chains (Verma et al., 2004). However promising, ubistatins bind with low affinity to their ubiquitin targets and have low chains specificity (Nakasone and al., 2017). The Brik lab at the Technion Institute in collaboration with the Suga lab at the University of Tokyo, synthesized cyclic peptides that bind to various forms of ubiquitin, including chains *(unpublished data)*. These cyclic peptides provide a promising approach towards drug discovery because they are small enough to emulate drug-like characteristics (Nakasone and al., 2017) in addition to binding tightly to their interacting ubiquitin partners. A particular cyclic peptide, Ub4_a, bound with extremely high affinity to K48 tetraUb **(Figure A.1.d)**. K48-linked polyubiquitin chains signal for proteasomal degradation of a protein substrate. And by binding tightly to K48-linked chains it could inhibit recognition by the proteasome and subsequent substrate degradation (Goldberg, 2012; Verma et al., 2004). It is very rare to see such tight affinity for the ubiquitin system, so I

asked how the cyclic peptide was interacting with tetraUb to produce such a low K_d. I sought to understand the molecular interactions between this complex through X-ray crystallography.

A.2 Materials and Methods

A.2.1 Purification of Ub4

TetraUb was made enzymatically by adding 0.1 µM Uba1, 20 µM UBE2K, 500 µM Ub wt, 5 mM ATP pH 7.5, 1 mM $MgCl_2$, 1 mM DTT, and 50 mM Tris pH 7.5 in a total reaction volume of 1000 µL. Reactions incubated for 18 hrs at 37 °C and were diluted with 10x the reaction volume with Ubiquitin Buffer A (50 mM Ammonium acetate, pH 4.5, 10 mM NaCl, 1 mM DTT). Diluted samples were then spun down and filtered to remove any proteins that crashed out in the process. Filtered protein solution was then purified using a SOURCE 15S 20 mL column. Proteins eluted with increasing concentrations of Ubiquitin Buffer B (50 mM Ammonium acetate, pH 4.5, 1 M NaCl, 1 mM DTT). Different ubiquitin species correlated with a particular peak (i.e.: first peak always corresponds to monoUb, second is diUb, and so forth). Samples were run on a SDS-PAGE gel and stained with Coomasie to ensure that the fraction was indeed clean. Fractions corresponding to tetraUb were pooled together, dialyzed into 50 mM Tris pH 7.6, 150 mM NaCl, and 2 mM DTT, then concentrated to 14 mg/mL.

A.2.2 Dissolving Ub4_a

The Brik lab sent us roughly 1 mg of lyophilized Ub4_a. I weighed out ~0.5 mg of this sample and resuspended it to 10 mg/mL with 20 µL of DMSO, this stock was then kept at 4 °C. I kept the rest of the lyophilized sample at -20 °C. I then used the nanodrop to determine the

concentration of Ub4_a in DMSO which was used to calculate the amount needed to form the complex.

A.2.3 Crystal Screen and freezing of Ub4:Ub4_a

To make the Ub4:Ub4_a complex, I made 7 mg/mL of complex since the previous structure of K48 tetraUb solved in the lab grew in 8 mg/mL which was concentrated in 50 mM Tris pH 7.6, 10 mM NaCl, 1 mM EDTA, and 1 mM DTT (Eddins et al., 2006). Conditions for setting up the complex are described in **Table A.1.** The crystal growth conditions for these previous crystals were: 100 mM MES pH 6.5, 2 M Ammonium sulfate, 14% (w/v) PEG 400. Unfortunately, because Ub4_a is so small I could not simply run these crystals on a gel to determine whether both proteins were present in my crystals. Therefore, I needed to shoot each one and solve the structure to see if they contained both tetraUb and the cyclic peptide.

Using the 7 mg/mL complexes, I set up 4 different 96-well crystal screens: JCSG+ (Molecular Dimensions), Protein Complex Suite (Qiagen), Wizard Screen (Molecular Dimensions), and Index Screen HT (Hampton Research) **(Figure A.2)**. The largest crystals were recapitulated in a larger 24-well screen with conditions that were dependent on the initial hit **(Figure A.3)**. Crystals were cryoprotected by soaking in well solution with 35% glycerol, 30% PEG 400, or 2 M ammonium sulfate. Crystals were looped and washed in a cryoprotectant for less than one minute before freezing and storing in liquid nitrogen.

A.2.4 Data Collection and Processing

Some of the largest crystals were shot at the Brookhaven National Laboratory (NSLS II) where I got 1.7 – 3Å resolution data. Data was processed and indexed using the XDSGUI. The best data belonged to crystals grown in 100 mM BisTris pH 5.5, 200 mM ammonium sulfate, 25% and PEG 3350. Structures were solved using molecular replacement with MOLREP from the CCP4 suite using the coordinates of either a single or two copies of human tetraubiquitin (PDB ID 2VO6) as a search model. Refinement via Molecular Replacement using Phenix 7.0 and visualized using COOT for model-building. Three additional rounds of refinement were performed. Maps and models the BisTris crystals are depicted in **Figure A.3.** Based on these data, it does not appear that I collected at least five other datasets from NSLS II that are < 3 Å. A majority of the data was unable to be processed in XDSGUI because the diffraction data showed multiple loons, indicating multiple crystals present in the loop.

Section A Crystallization of tetraubiquitin in complex with a cyclic peptide

Table A. 1 *Reaction setup for Complex of Ub4:Ub4_a*

Protein	7	mg/mL
Total Volume	100	µL

	Molecular weight		Concentration of both Proteins	
[Ub4_a]	1766.5	g/mol	0.00020823	mol/L
[Ub4]	31850.68	g/mol	0.00020823	mol/L
total g/mol	33617.18	g/mol		

	A	dilution	E	[], M	MW, g/mol	Volume, µL	
[Ub4_a] in DMSO	5	10	8605	0.00581058	1766.5	3.58	
[Ub4]	1.6	10	5960	0.00268456	31850.68	7.76	
						88.66	1x Buffer

This table depicts the type of concentrations needed in order to set up the complex for crystal screens. In this example, 100 µL was the final volume and both proteins needed to be at 208 µM in order to make a 7 mg/mL complex. 1x Buffer needed to dilute the concentrated proteins was 50 mM Tris pH 7.6, 150 mM NaCl, and 2 mM DTT.

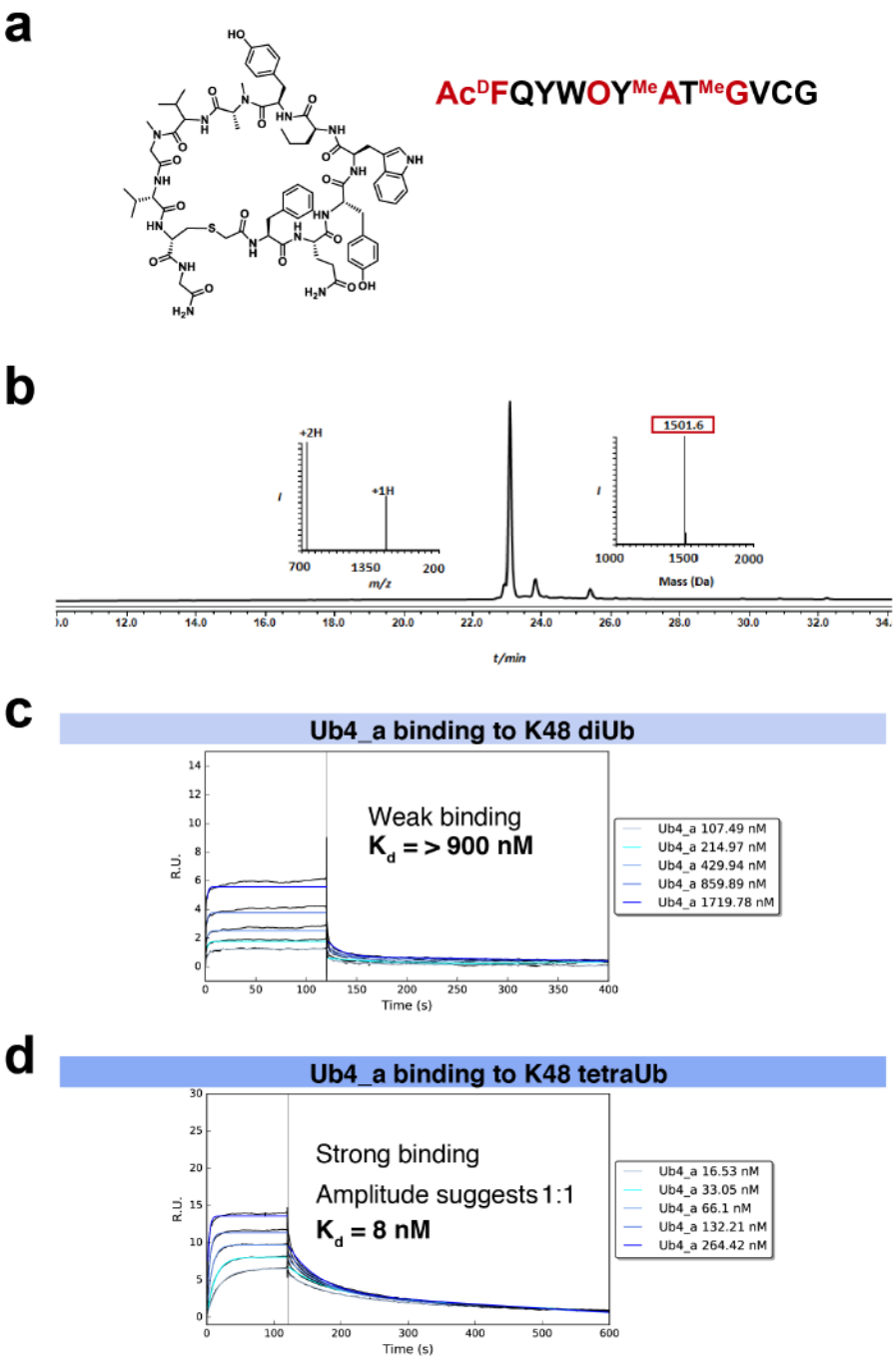

Figure A. 1 Ub4_a

(a) *Cyclic peptide structure and corresponding sequence composition.* ***(b)*** *Analytical HPLC and ESI-MS of the pure cyclic Ub4_a with the observed mass 1501.6 Da* ***(c)*** *SPR binding experiments of titrating increasing amounts of Ub4_a with either a constant concentration of K48 diUbiquitin or tetraUb. The K_d determined for interaction between K48 diUbiquitin and Ub4_a is estimated to be >900 nM.* ***(d)*** *The K_d between tetraUb and Ub4_a is 8 nM, and the complex is predicted to be at a 1:1 ratio given the amplitudes from this experiment.*

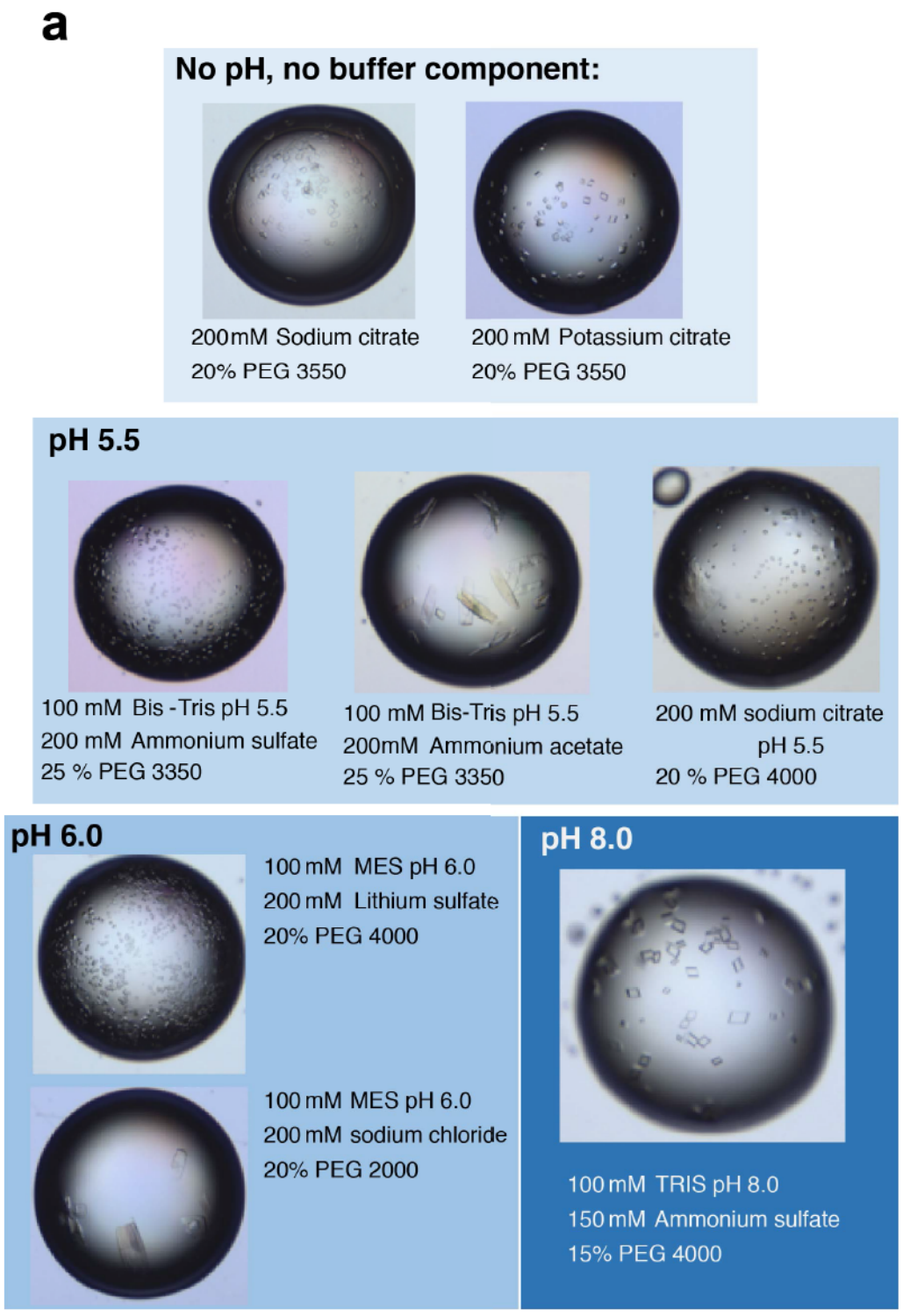

Figure A. 2 Crystal conditions for cyclic peptide bound to tetraUb. Crystals are grouped by pH

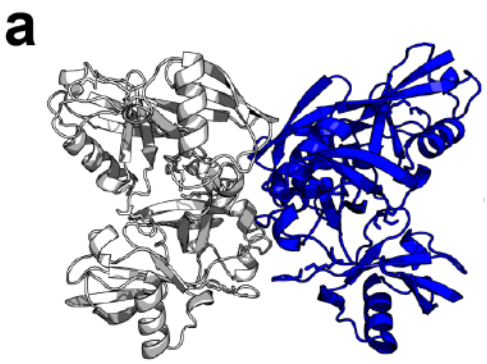

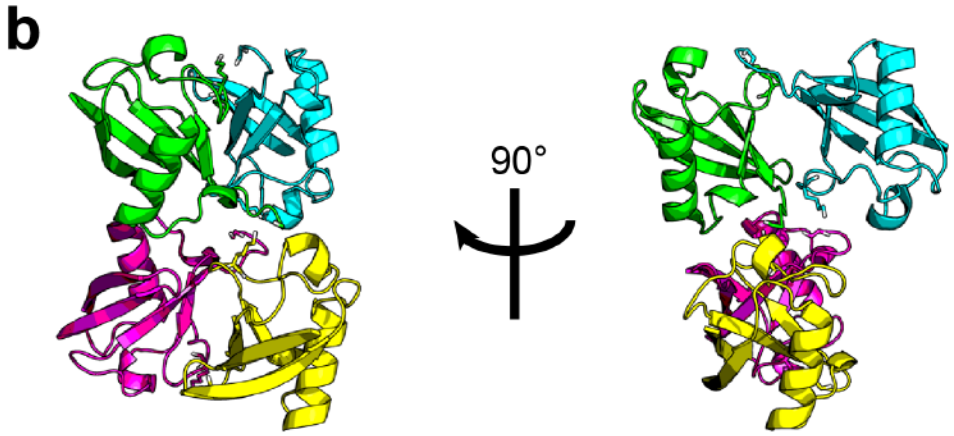

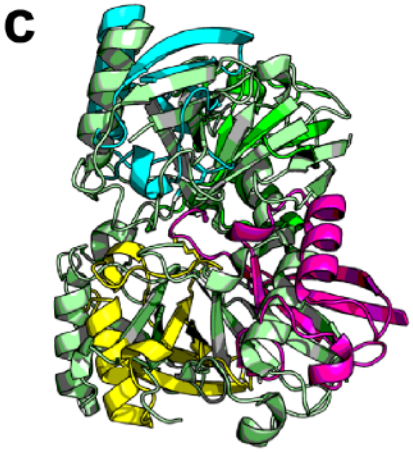

d

	My structure	2O6V
Resolution	1.7 Å	2.1 Å
Space Group	C2	C2
Cell Dimensions	77, 59.2, 136 90°, 90°, 90°	59.1, 77.1, 139.3 90°, 90°, 90.3°
Rfree **Rwork**	0.266 0.219	0.262 0.222

Figure A. 3 Structure determination for crystals grown in 100 mM BisTris pH 5.5, 200 mM ammonium sulfate, 25% and PEG 3350 with Space group, C2

(a) *Using 2O6V.pdb as a search model we found two copies (blue and white) of tetraubiquitin in the asymmetric unit.* ***(b)*** *Showing the 4 ubiquitin molecules that compose one half of the structures in the asymmetric unit cell. Two diUbiquitin molecules stack perpendicular to the other two as shown with the 90° figure.* ***(c)*** *Overlay of the structure that I solved vs the structure from 2O6V.pdb. Given that they had different cell dimensions* ***(d)*** *it is unsurprising that the structures do not perfectly align.*

REFERENCES

Abdul Rehman, S.A., Kristariyanto, Y.A., Choi, S.Y., Nkosi, P.J., Weidlich, S., Labib, K., Hofmann, K., and Kulathu, Y. (2016). MINDY-1 is a member of an evolutionarily conserved and structurally distinct new family of deubiquitinating enzymes. Molecular Cell *63*, 146-155.

Al-Hakim, Abdallah K., Zagorska, A., Chapman, L., Deak, M., Peggie, M., and Alessi, Dario R. (2008). Control of AMPK-related kinases by USP9X and atypical Lys²⁹/Lys³³-linked polyubiquitin chains. Biochemical Journal *411*, 249.

Baietti, M.F., Simicek, M., Abbasi Asbagh, L., Radaelli, E., Lievens, S., Crowther, J., Steklov, M., Aushev, V.N., Martinez Garcia, D., Tavernier, J., *et al.* (2016). OTUB1 triggers lung cancer development by inhibiting RAS monoubiquitination. EMBO Molecular Medicine *8*, 288-303.

Balakirev, M.Y., Tcherniuk, S.O., Jaquinod, M., and Chroboczek, J. (2003). Otubains: a new family of cysteine proteases in the ubiquitin pathway. EMBO reports *4*, 517-522.

Banka, P.A., Behera, A.P., Sarkar, S., and Datta, A.B. (2015). RING E3-Catalyzed E2 Self-Ubiquitination Attenuates the Activity of UBE2E Ubiquitin-Conjugating Enzymes. Journal of Molecular Biology *427*, 2290-2304.

Berndsen, C.E., and Wolberger, C. (2011). A spectrophotometric assay for conjugation of ubiquitin and ubiquitin-like proteins. Analytical Biochemistry *418*, 102-110.

Berndsen, C.E., and Wolberger, C. (2014). New insights into ubiquitin E3 ligase mechanism. Nature Structural &Amp; Molecular Biology *21*, 301.

Bialas, J., Boehm, A., Catone, N., Aichem, A., and Groettrup, M. (2019). The ubiquitin-like modifier FAT10 stimulates the activity of the deubiquitylating enzyme OTUB1. Journal of Biological Chemistry.

Borden, K.L.B. (2000). RING domains: master builders of molecular scaffolds? Journal of Molecular Biology *295*, 1103-1112.

Bremm, A., Freund, S.M., and Komander, D. (2010). Lys11-linked ubiquitin chains adopt compact conformations and are preferentially hydrolyzed by the deubiquitinase Cezanne. Nature Structural & Molecular Biology *17*, 939-947.

Brzovic, P., and Klevit, R. (2006). Ubiquitin transfer from the E2 perspective: why is UbcH5 so promiscuous? Cell Cycle *5*, 2867-2873.

Brzovic, P., Lissounov, A., Christensen, D., Hoyt, D., and Klevit, R. (2006). A UbcH5/ubiquitin noncovalent complex is required for processive BRCA1-directed ubiquitination. Molecular Cell *21*, 873-880.

Buetow, L., and al., e. (2015). Activation of a Primed RING E3-E2-Ubiquitin Complex by Non-Covalent Ubiquitin. Molecular Cell *58*, 297-310.

Burrows, J.F., and Johnston, J.A. (2012). Regulation of cellular responses by deubiquitinating enzymes: an update. Frontiers Bioscience *1*, 1184-1200.

Chandrasekharan, M.B., Huang, F., and Sun, Z.-W. (2009). Ubiquitination of histone H2B regulates chromatin dynamics by enhancing nucleosome stability. Proceedings of the National Academy of Sciences of the United States of America *106*, 16686-16691.

Chen, Y., Wang, Y.-G., Li, Y., Sun, X.-X., and Dai, M.-S. (2016). Otub1 stabilizes MDMX and promotes its proapoptotic function at the mitochondria. Oncotarget *8*.

Chen, Z., and Pickart, C.M. (1990). A 25-kilodalton ubiquitin carrier protein (E2) catalyzes multi-ubiquitin chain synthesis via lysine 48 of ubiquitin. Journal Biological Chemistry *265*, 21835–21842

Chen, Z.J., and Sun, L.J. (2009). Nonproteolytic Functions of Ubiquitin in Cell Signaling. Molecular Cell *33*, 275-286.

Choe, E., Liao, L., Zhou, J.Y., Cheng, D., Duong, D.M., Jin, P., Tsai, L.H., and Peng, J. (2007). Neuronal morphogenesis is regulated by the interplay between cyclin-dependent kinase 5 and the ubiquitin ligase mind bomb 1. Journal of Neuroscience *27*, 9503–9512.

Clague, M.J., Coulson, J.M., and Urbé, S. (2012). Cellular functions of the DUBs. Journal of Cell Science *125*, 277-286.

Clague, M.J., Heride, C., and Urbé, S. (2015). The demographics of the ubiquitin system. Trends in Cell Biology *25*, 417-426.

Clague, M.J., and Urbé, S. (2010). Ubiquitin: Same Molecule, Different Degradation Pathways. Cell *143*, 1-4.

Clague, M.J., Urbé, S., and Komander, D. (2019). Breaking the chains: deubiquitylating enzyme specificity begets function. Nature Reviews Molecular Cell Biology.

Clegg, H.V., Itahana, K., and Zhang, Y. (2008). Unlocking the Mdm2-p53 loop: ubiquitin is the key. Cell Cycle *7*, 287-292.

Cohn, M.A., and D'Andrea, A.D. (2008). Chromatin Recruitment of DNA repair proteins: Lessons from the Fanconi Anemia and Double Strand Break Repair Pathways. Molecular Cell *32*, 306-312.

D'Arcy, P., Wang, X., and Linder, S. (2015). Deubiquitinase inhibition as a cancer therapeutic strategy. Pharmacological Therapy *147*, 32-54.

David, Y., Ziv, T., Admon, A., and Navon, A. (2010). The E2 Ubiquitin-conjugating Enzymes Direct Polyubiquitination to Preferred Lysines. Journal of Biological Chemistry *285*, 8595-8604.

Deshaies, R.J., and Joazeiro, C.A. (2009). RING domain E3 ubiquitin ligases. Annu Rev Biochem *78*, 399-434.

DiBello, A., Datta, A.B., Zhang, X., and Wolberger, C. (2016). Role of E2- RING interactions in governing RNF4-mediated substrate ubiquitination. Journal of Molecular Biology *79*, 211-227.

Doil, C., and al., e. (2009). RNF168 binds and amplifies ubiquitin conjugates on damaged chromosomes to allow accumulation of repair proteins. Cell *136*, 435-446.

Eddins, M.J., Carlile, C.M., Gomez, K.M., Pickart, C.M., and Wolberger, C. (2006). Mms2-Ubc13 covalently bound to ubiquitin reveals the structural basis of linkage-specific polyubiquitin chain formation. Nature Structural Molecular Biology *10*, 915-920.

Edelmann, M.J., Iphoefer, A., Akutsu, M., Altun, M., di Gleria, K., Kramer, H.B., Fiebiger, E., S., D.-P., and Kessler, B.M. (2008). Structural basis and specificity of humain otubain 1 mediated deubiquitylation. Bioscience Reports.

Eletr, Z., Huang, D., Duda, D., Schulman, B., and Kuhlman, B. (2005). E2 conjugating enzymes must disengage from their E1 enzymes before E3-dependent ubiquitin and ubiquitin-like transfer. Nature Structural Molecular Biology *12*, 933-934.

Eliceiri, K., Schneider, C.A., Rasband, W.S., and Eliceiri, K.W. (2012). NIH Image to ImageJ : 25 years of image analysis historical commentary NIH Image to ImageJ : 25 years of image analysis. Nature Methods *9*, 671-675.

Ernst, A., Avvakumov, G., Tong, J., Fan, Y., Zhao, Y., Alberts, P., Persaud, A., Walker, J.R., Neculai, A.-M., Neculai, D.*, et al.* (2013). A strategy for modulation of enzymes in the ubiquitin system. Science (New York, NY) *339*, 590-595.

Evans, P.C., Smith, T.S., Lai, M.-J., Williams, M.G., Burke, D.F., Heyninck, K., Kreike, M.M., Beyaert, R., Blundell, T.L., and Kilshaw, P.J. (2003). A Novel Type of Deubiquitinating Enzyme. Journal of Biological Chemistry *278*, 23180-23186.

Faesen, A.C., Luna-Vargas, M.P., Geurink, P.P., Clerici, M., Merkx, R., van Dijk, W.J., Hameed, D.S., El Oualid, F., Ovaa, H., and Sixma, T.K. (2011). The differential modulation of USP activity by internal regulatory domains, interactors and eight ubiquitin chain types. Chemical Biology *18*, 1550-1561.

Fagerberg, L., Hallström, B., Oksvold, P., Kampf, C., Djureinovic, D., Odeberg, J., Habuka, M., Tahmasebpoor, S., Danielsson, A., Edlund, K.*, et al.* (2014). Analysis of the human tissue-specific expression by genome-wide integration of transcriptomics and antibody-based proteomics. Molecular Cell Proteomics *2*, 397-406.

Farshi, P., Deshmukh, R.R., Nwankwo, J.O., Arkwright, R.T., Cvek, B., Liu, J., and Dou, Q.P. (2015). Deubiquitinases (DUBs) and DUB inhibitors: a patent review. Expert opinion on therapeutic patents *25*, 1191-1208.

Fei, C., Li, Z., Li, C., Chen, Y., Chen, Z., He, X., Mao, L., Wang, X., Zeng, R., and Li, L. (2013). Smurf1-mediated Lys29-linked nonproteolytic polyubiquitination of axin negatively regulates Wnt/β-catenin signaling. Molecular Cell Biology *33*, 4095-4105.

Fletcher, A.J., Christensen, D.E., Nelson, C., Tan, C.P., Schaller, T., Lehner, P.J., Sundquist, W.I., and Towers, G.J. (2015). TRIM5α requires Ube2W to anchor Lys63-linked ubiquitin chains and restrict reverse transcription. The EMBO Journal *34*, 2078-2095.

Freemont, P.S. (2000). RING for destruction? Current Biology *10*, R84-87.

Gerlach, B., Cordier, S.M., Schmukle, A.C., Emmerich, C.H., Rieser, E., Haas, T.L., Webb, A.I., Rickard, J.A., Anderton, H., Wong, W.W.L., *et al.* (2011). Linear ubiquitination prevents inflammation and regulates immune signalling. Nature *471*, 591.

Goldberg, A.L. (2012). Development of proteasome inhibitors as research tools and cancer drugs. Journal of Cell Biology *199*, 583-588.

Goncharov, T., Niessen, K., De Almagro, M.C., Izrael-Tomasevic, A., Fedorova, A.V., Varfolomeev, E., Arnott, D., Deshayes, K., Kirkpatrick, D.S., and Vucic, D. (2013). OTUB1 modulates c-IAP1 stability to regulate signalling pathways. EMBO Journal *32*, 1103-1114.

Gorelik, M., and Sidhu, S.S. (2016). Specific targeting of the deubiquitinase and E3 ligase families with engineered ubiquitin variants. Bioengineering & translational medicine *2*, 31-42.

Haahr, P., Borgermann, N., Guo, X., Typas, D., Achuthankutty, D., Hoffmann, S., Shearer, R., Sixma, T.K., and Mailand, N. (2018). ZUFSP deubiquitylates K63-linked polyubiquitin chains to promote genome stability. Molecular Cell *70*, 165-174.

Haldeman, M.T., Xia, G., Kasperek, E.M., and Pickart, C.M. (1997). Structure and function of ubiquitin conjugating enzyme E2–25K: the tail is a core- dependent activity element. Biochemistry *36*, 10526–10537.

Harrigan, J.A., Jacq, X., Martin, N.M., and Jackson, S.P. (2018). Deubiquitylating enzymes and drug discovery: Emerging opportunities. Nature Review Drug Discovery *17*, 57-77.

Hay, R.T. (2005). SUMO: A History of Modification. Molecular Cell *18*, 1-12.

Herhaus, L., Al-Salihi, M., MacArtney, T., Weidlich, S., and Sapkota, G.P. (2013). OTUB1 enhances TGFβ signalling by inhibiting the ubiquitylation and degradation of active SMAD2/3. Nature Communications *4*, 1-13.

Hofmann, R.M., and Pickart, C.M. (1999a). Enzyme Functions in Assembly of Novel Polyubiquitin Chains for DNA Repair. Cell *96*, 645-653.

Hofmann, R.M., and Pickart, C.M. (1999b). Noncanonical MMS2-encoded ubiquitin-conjugating enzyme functions in assembly of novel polyubiquitin chains for DNA repair. Cell *96*, 5.

Holowaty, M.N., Sheng, Y., Nguyen, T., Arrowsmith, C., and Frappier, L. (2003). Protein interaction domains of the ubiquitin-specific protease, USP7/HAUSP. Journal of Biological Chemistry *278*, 47753– 47761.

Huang, H., Jeon, M.-S., Liao, L., Yang, C., Elly, C., Yates, J.R., III , and Liu, Y.-C. (2010). K33-linked polyubiquitination of T cell receptor-ζ regulates proteolysis-independent T cell signaling. Immunity *33*, 60-70.

Huen, M.S., and al., e. (2007). RNF8 transduces the DNA-damage signal via histone ubiquitylation and checkpoint protein assembly. Cell *131*, 901-914.

Iwai, K., and Tokunaga, F. (2009). Linear polyubiquitination: a new regulator of NF-κB activation. EMBO Reports *10*, 706-713.

Jensen, D., Proctor, M., Marquis, S.T., Gardner, H.P., Ha, S.I., Chodosh, L., Ishov, A., Tommerup, N., Vissing, H., Sekido, Y.*, et al.* (1998). BAP1: a novel ubiquitin hydrolase which binds to the BRCA1 RING finger and enhances BRCA1-mediated cell growth suppression. Oncogene *16*, 1097-1112.

Jin, L., Williamson, A., Banerjee, S., Philipp, I., and Rape, M. (2008). Mechanism of ubiquitin-chain formation by the human anaphase-promoting complex. Cell *133*, 653–665.

Juang, Y.C., Landry, M.C., Sanches, M., Vittal, V., Leung, C.C.Y., Ceccarelli, D.F., Mateo, A.R.F., Pruneda, J.N., Mao, D.Y.L., Szilard, R.K.*, et al.* (2012). OTUB1 Co-opts Lys48-Linked Ubiquitin Recognition to Suppress E2 Enzyme Function. Molecular Cell *45*, 384-397.

Karunarathna, U., Kongsema, M., Zona, S., Gong, C., Cabrera, E., Gomes, A.R., Man, E.P.S., Khongkow, P., Tsang, J.W.H., Khoo, U.S., *et al.* (2016). OTUB1 inhibits the ubiquitination and degradation of FOXM1 in breast cancer and epirubicin resistance. Oncogene *35*, 1433-1444.

Kim, H., Chen, J., and Yu, X. (2007). Ubiquitin-binding protein RAP80 mediates BRCA1-dependent DNA damage response. Science *316*.

Kirkin, V., McEwan, D.G., Novak, I., and Dikic, I. (2009). A Role for Ubiquitin in Selective Autophagy. mOLECULAR cELL *34*, 259-269.

Komander, D., Clague, M.J., and Urbé, S. (2009). Breaking the chains: structure and function of the deubiquitinases. Nature Reviews Molecular Cell Biology *10*, 550.

Komander, D., and Rape, M. (2012). The Ubiquitin Code. Annual Reviews Biochemistry *81*, 203-229.

Kostova, Z., Tsai, Y.C., and Weissman, A.M. (2007). Ubiquitin ligases, critical mediators of endoplasmic reticulum-associated degradation. Seminars in cell & developmental biology *18*, 770-779.

Kulak, N.A., Pichler, G., Paron, I., Nagaraj, N., and Mann, M. (2014). Minimal, encapsulated proteomic-sample processing applied to copy-number estimation in eukaryotic cells. Nature Methods *11*, 319-324.

Lallemand-Breitenbach, V., Jeanne, M., Benhenda, S., Nasr, R., Lei, M., Peres, L., Zhou, J., Zhu, J., Raught, B., and de Thé, H. (2008). Arsenic degrades PML or PML–RARα through a SUMO-triggered RNF4/ubiquitin-mediated pathway. Nature Cell Biology *10*, 547.

Li, M., Brooks, C.L., Kon, N., and Gu, W. (2004). A dynamic role of HAUSP in the p53-Mdm2 pathway. Molecular Cell *13*, 879-886.

Li, S., Zheng, H., Mao, A.P., Zhong, B., Li, Y., Liu, Y., Gao, Y., Ran, Y., Tien, P., and Shu, H.B. (2010). Regulation of virus-triggered signaling by OTUB1- and OTUB2-mediated deubiquitination of TRAF3 and TRAF6. Journal of Biological Chemistry *285*, 4291-4297.

Li, W., and Ye, Y. (2008). Polyubiquitin chains: functions, structures, and mechanisms. Cell Mol Life Sci *65*, 2397-2406.

Li, Y., Sun, X., Elferich, J., Shinde, U., David, L., and Dai, M. (2014). Monoubiquitination is critical for ovarian tumor domain-containing ubiquitin aldehyde binding protein 1 (Otub1) to suppress UbcH5 enzyme and stabilize p53 protein. Journal of Biological Chemistry *289*, 5097-5108.

Li, Z., Na, X., Wang, D., Schoen, S.R., Messing, E.M., and Wu, G. (2002). Ubiquitination of a novel deubiquitinating enzyme requires direct binding to von Hippel-Lindau tumor suppressor protein. Journal Biological Chemistry *277*, 4656–4662.

Li, Z., Wang, D., Messing, E.M., and Wu, G. (2005). VHL protein-interacting deubiquitinating enzyme 2 deubiquitinates and stabilizes HIF-1alpha. EMBO reports *6*, 373-378.

Lovering, R., Hanson, I.M., Borden, K.L., Martin, S., O'Reilly, N.J., Evan, G.I., Rahman, D., Pappin, D.J., Trowsdale, J., and Freemont, P.S. (1993). Identification and preliminary characterization of a protein motif related to the zinc finger. Proceedings of the National Academy of Sciences of the United States of America *90*, 2112-2116.

Mailand, N., and al., e. (2007). RNF8 ubiquitylates histones at DNA double-strand breaks and promotes assembly of repair proteins. Cell, 887-900.

Matsumoto, M.L., Wickliffe, K.E., Dong, K.C., Yu, C., Bosanac, I., Bustos, D., Phu, L., Kirkpatrick, D.S., Hymowitz, S.G., Rape, M.*, et al.* (2010). K11-linked polyubiquitination in cell cycle control revealed by a K11 linkage-specific antibody. Molecular Cell *39*, 477-484.

Metzger, M.B., Pruneda, J.N., Klevit, R.E., and Weissman, A.M. (2014). RING-type E3 ligases: Master manipulators of E2 ubiquitin-conjugating enzymes and ubiquitination. Biochem Biophys Acta *1843*, 47-60.

Meulmeester, E., Pereg, Y., Shiloh, Y., and Jochemsen, A.G. (2005). ATM-mediated phosphorylations inhibit Mdmx/Mdm2 stabilization by HAUSP in favor of p53 activation. Cell Cycle *4*, 1166-1170.

Mevissen, T.E.T., Hospenthal, M.K., Geurink, P.P., Elliott, P.R., Akutsu, M., Arnaudo, N., Ekkebus, R., Kulathu, Y., Wauer, T., Oualid, F.E., *et al.* (2013). OTU Deubiquitinases Reveal Mechanisms of Linkage Specificity and Enable Ubiquitin Chain Restriction Analysis. Cell *154*, 169-184.

Michalski, A., Damoc, E., Hauschild, J.-P., Lange, O., Wieghaus, A., Makarov, A., Nagaraj, N., Cox, J., Mann, M., and Horning, S. (2011). Mass Spectrometry-based Proteomics Using Q Exactive, a High-performance Benchtop Quadrupole Orbitrap Mass Spectrometer. Molecular & Cellular Proteomics *10*.

Middleton, A.J., and Day, C.L. (2015). The molecular basis of lysine 48 ubiquitin chain synthesis by Ube2K. Scientific Reports *5*, 16793.

Moilanen, A.-M., Poukka, H., Karvonen, U., Jänne, O.A., and Palvimo, J.J. (1998). Identification of a Novel RING Finger Protein as a Coregulator in Steroid Receptor-Mediated Gene Transcription. Molecular and Cellular Biology *18*, 5128-5139.

Nakada, S., Tai, I., Panier, S., Al-Hakim, A., Iemura, S.I., Juang, Y.C., O'Donnell, L., Kumakubo, A., Munro, M., Sicheri, F., *et al.* (2010). Non-canonical inhibition of DNA damage-dependent ubiquitination by OTUB1. Nature *466*.

Nakasone, M.A., and al., e. (2017). Structural Basis for the Inhibitory Effects of Ubistatins in the Ubiquitin-Proteasome Pathway. Structure, 1839-1855.

Ndubaku, C., and Tsui, V. (2015). Inhibiting the Deubiquitinating Enzymes (DUBs). Journal of Medicinal Chemistry *58*, 1581-1595.

Nijman, S.M., Luna-Vargas, M.P., Velds, A., Brummelkamp, T.R., Dirac, A.M., and al, e. (2005). A genomic and functional inventory of deubiquitinating enzymes. Cell *123*.

Ozkan, E., Yu, H., and Deisenhofer, J. (2005). Mechanistic insight into the allosteric activation of a ubiquitin-conjugating enzyme by RING-type ubiquitin ligases. Proc Natl Acad Sci *102*, 18890-18895.

Panda, S., Nilsson, J.A., and Gekara, N.O. (2015). Deubiquitinase MYSM1 Regulates Innate Immunity through Inactivation of TRAF3 and TRAF6 Complexes. Immunity *43*, 647-659.

Pasupala, N.M., M. E., Que, L.T., Malynn, B.A., Ma, A., and Wolberger, C. (2018). OTUB1 non-catalytically regulates the stability of the E2 ubiquitin conjugating enzyme UBE2E1. Journal of Molecular Biology.

Petroski, M.D., and al., e. (2007). Substrate modification with lysine 63-linked ubiquitin chains through the UBC13- UEV1A ubiquitin-conjugating enzyme. Journal Biological Chemistry *282*, 29936–29945.

Petroski, M.D., and Deshaies, R.J. (2005). Mechanism of lysine 48-linked ubiquitin-chain synthesis by the cullin-RING ubiquitin-ligase complex SCF-Cdc34. Cell *123*, 1107-1120.

Pickart, C.M. (2001). Mechanisms underlying ubiquitination. Annual Reviews Biochemistry *70*, 503-533.

Plafker, S.M., Plafker, K.S., Weissman, A.M., and Macara, I.G. (2004). Ubiquitin charging of human class III ubiquitin- conjugating enzymes triggers their nuclear import. Journal of Cell Biology *167*, 649-659.

Plechanovov, A., Jaffray, E.G., Tatham, M.H., Naismith, J.H., and Hay, R.T. (2012). Structure of a RING E3 ligase and ubiquitin-loaded E2 primed for catalysis. Nature *489*, 115-120.

Popov, N., Wanzel, M., Madiredjo, M., Zhang, D., Beijersbergen, R., Bernards, R., Moll, R., Elledge, S.J., and Eilers, M. (2007). The ubiquitin-specific protease USP28 is required for MYC stability. Nature Cell Biology *9*, 765-774.

Prinz, H. (2010). Hill coefficients, dose-response curves and allosteric mechanisms. Journal of Chemical Biology *3*, 37-44.

Priolo, C., Tang, D., Brahamandan, M., Benassi, B., Sicinska, E., and Ogino, S. (2006). The Isopeptidase USP2a Protects Human Prostate Cancer from Apoptosis. Cancer Res *66*.

Rape, M., Reddy, S.K., and Kirschner, M.W. (2006). The processivity of multiubiquitination by the APC determines the order of substrate degradation. Cell *124*, 89-103.

Ritorto, M.S., Ewan, R., Perez-Oliva, A.B., Knebel, A., Buhrlage, S.J., Wightman, M., Kelly, S.M., Wood, N.T., Virdee, S., Gray, N.S., *et al.* (2014). Screening of DUB activity and specificity by MALDI-TOF mass spectrometry. Nature Communications *5*, 4763.

Sahtoe, D.D., van Dijk, W.J., Ekkebus, R., Ovaa, H., and Sixma, T.K. (2016). BAP1/ASXL1 recruitment and activation for H2A deubiquitination. Nature Communications, 10292.

Sakata, E., Satoh, T., Yamamoto, S., Yamaguchi, Y., Yagi-Utsumi, M., Kurimoto, E., Tanaka, K., Wakatsuki, S., and Kato, K. (2010). Crystal structure of UbcH5b~ubiquitin intermediate: insight into the formation of the self-assembled E2~Ub conjugates. Structure *18*, 138-147.

Sancho, E., Vilá, M.R., Sánchez-Pulido, L., Lozano, J.J., Paciucci, R., Nadal, M., Fox, M., Harvey, C., Bercovich, B., Loukili, N., *et al.* (1998). Role of UEV-1, an inactive variant of the E2 ubiquitin-conjugating enzymes, in in vitro differentiation and cell cycle behavior of HT-29-M6 intestinal mucosecretory cells. Molecular and cellular biology *18*, 576-589.

Sato, Y., Yamagata, A., Goto-Ito, S., Kubota, K., Miyamoto, R., Nakada, S., and Fukai, S. (2012). Molecular basis of Lys-63-linked polyubiquitination inhibition by the interaction between human deubiquitinating enzyme OTUB1 and ubiquitin- conjugating enzyme UBC13. Journal of Biological Chemistry *287*, 25860-25868.

Scaglione, K., Basrur, V., Ashraf, N., Konen, J., Elenitoba-Johnson, K., Todi, S., and Paulson, H. (2013). The ubiquitin-conjugating enzyme (E2) Ube2w ubiquitinates the N terminus of substrates. Journal of Biological Chemistry *288*, 18784-18788.

Schnell, J.D., and Hicke, L. (2003). Non-traditional Functions of Ubiquitin and Ubiquitin-binding Proteins. Journal Biological Chemistry *278*, 35857-35860.

Scholz, C., Rodriguez, J., Pickel, C., Burr, S., Fabrizio, J., and al., e. (2016). FIH Regulates Cellular Metabolism through Hydroxylation of the Deubiquitinase OTUB1. PLOS Biology *14*.

Schumacher, F.R., Wilson, G., and Day, C.L. (2013). The N-terminal extension of UBE2E ubiquitin-conjugating enzymes limits Chain assembly. Journal of Molecular Biology *425*, 4099-4111.

Schwanhäusser, B., Busse, D., Li, N., Dittmar, G., Schuchhardt, J., Wolf, J., Chen, W., and Selbach, M. (2011). Global quantification of mammalian gene expression control. Nature *473*, 337.

Sheng, Y., Hong, J.H., Doherty, R., Srikumar, T., Shloush, J., Avvakumov, G.V., Walker, J.R., Xue, S., Neculai, D., Wan, J.W.*, et al.* (2012). A human ubiquitin conjugating enzyme (E2)-HECT E3 ligase structure-function screen. Molecular & Cellular Proteomics *11*, 329-341.

Shrestha, R.K., Ronau, J.A., Davies, C.W., Guenette, R.G., Strieter, E.R., Paul, L.N., and Das, C. (2014). Insights into the mechanism of deubiquitination by JAMM deubiquitinases from cocrystal structures of the enzyme with the substrate and product. Biochemistry *53*, 3199-3217.

Soares, L., Seroogy, C., Skrenta, H., Anandasabapathy, N., Lovelace, P., Chung, C.D., Engleman, E., and Fathman, C.G. (2004). Two isoforms of otubain 1 regulate T cell anergy via GRAIL. Nature Immunology *5*, 45-54.

Sobhian, B., and al., e. (2007). RAP80 targets BRCA1 to specific ubiquitin structures at DNA
damage sites. Science *316*, 1198–1202.

Sowa, M.E., Bennett, E.J., Gygi, S.P., and Harper, J.W. (2010). Defining the Human Deubiquitinating Enzyme Interaction Landscape. Cell *138*, 389-403.

Spratt, D.E., Walden, H., and Shaw, G.S. (2014). RBR E3 ubiquitin ligases: new structures, new insights, new questions. Biochemical Journal *458*, 421-437.

Stanišić, V., Malovannaya, A., Qin, J., Lonard, D.M., and O'Malley, B.W. (2009). OTU domain-containing ubiquitin aldehyde-binding protein 1 (OTUB1) deubiquitinates Estrogen receptor (ER)α and affects ERα transcriptional activity. Journal of Biological Chemistry *284*, 16135-16145.

Stewart, M., Ritterhoff, T., Klevit, R., and Brzovic, P. (2016). E2 enzymes: more than just the middle men. Cell Research *26*, 423-440.

Sun, H., Leverson, J.D., and Hunter, T. (2007). Conserved function of RNF4 family proteins in eukaryotes: targeting a ubiquitin ligase to SUMOylated proteins. The EMBO journal *26*, 4102-4112.

Sun, X.-X., Challagundla, K.B., and Dai, M.-S. (2012). Positive regulation of p53 stability and activity by the deubiquitinating enzyme Otubain 1. EMBO Journal *31*, 576-592.

Swatek, K., and Komander, D. (2016). Ubiquitin modifications. Cell Research *26*, 399-422.

Tatham, M.H., Geoffroy, M.-C., Shen, L., Plechanovova, A., Hattersley, N., Jaffray, E.G., Palvimo, J.J., and Hay, R.T. (2008). RNF4 is a poly-SUMO-specific E3 ubiquitin ligase required for arsenic-induced PML degradation. Nature Cell Biology *10*, 538.

Tatham, M.H., Plechanovová, A., Jaffray, E.G., Salmen, H., and Hay, R.T. (2013). Ube2W conjugates ubiquitin to α-amino groups of protein N-termini. The Biochemical Journal *453*, 137-145.

Tran, H., Hamada, F., Schwarz-Romond, T., and Bienz, M. (2008). Trabid, a new positive regulator of Wnt-induced transcription with preference for binding and cleaving K63-linked ubiquitin chains. Genes & development *22*, 528-542.

Turcu, F.E.R., Ventii, K.H., and Wilkinson1, K.D. (2009). Regulation and Cellular Roles of Ubiquitin-specific Deubiquitinating Enzymes. Annual Review Biochemistry *78*, 363-397.

Uzunova, K., Göttsche, K., Miteva, M., Weisshaar, S.R., Glanemann, C., Schnellhardt, M., Niessen, M., Scheel, H., Hofmann, K., Johnson, E.S.*, et al.* (2007). Ubiquitin-dependent Proteolytic Control of SUMO Conjugates. Journal of Biological Chemistry *282*, 34167-34175.

VanDemark, A.P., Hofmann, R.M., Tsui, C., Pickart, C.M., and Wolberger, C. (2001). Molecular insights into polyubiquitin chain assembly: crystal structure of the Mms2/Ubc13 heterodimer. Cell *105*, 711-720.

Ventii, K., and Wilkinson, K.D. (2008). Protein Partners of Deubiquitinating Enzymes. Biochemical Journal *45*, 788-802.

Verma, R., Feldman, R.M., and Deshaies, R.J. (1997). SIC1 is ubiquitinated in vitro by a pathway that requires CDC4, CDC34, and cyclin/CDK activities. Molecular Biology and Cell *8*, 1427–1437.

Verma, R., Peters, N.R., D'Onofrio, M., Tochtrop, G.P., Sakamoto, K.M., Varadan, R., Zhang, M., Coffino, P., Fushman, D., Deshaies, R.*, et al.* (2004). Ubistatins inhibit proteasome-dependent degradation by binding the ubiquitin chain. Science *306*, 117-120.

Vittal, V., Shi, L., Wenzel, D.M., Scaglione, K.M., Duncan, E.D., Basrur, V., Elenitoba-Johnson, K.S.J., Baker, D., Paulson, H.L., Brzovic, P.S.*, et al.* (2015). Intrinsic disorder drives N-terminal ubiquitination by Ube2w. Nature chemical biology *11*, 83-89.

Wada, K., and Kamitani, T. (2006). UnpEL/Usp4 is ubiquitinated by Ro52 and deubiquitinated by itself. Biochem Biophys Res Commun *342*, 253-258.

Wang, B., and al., e. (2007). Abraxas and RAP80 form a BRCA1 protein complex required for
the DNA damage response. Science *316*, 1194–1198.

Wang, F., Wang, L., Wu, J., Sokirniy, I., Nguyen, P., Bregnard, T., Weinstock, J., Mattern, M., Bezsonova, I., Hancock, W.W.*, et al.* (2017). Active site-targeted covalent irreversible inhibitors of USP7 impair the functions of Foxp3+ T-regulatory cells by promoting ubiquitination of Tip60. PLOS ONE *12*, e0189744.

Wang, M., and Pickart, C.M. (2005). Different HECT domain ubiquitin ligases employ distinct mechanisms of polyubiquitin chain synthesis. The EMBO journal *24*, 4324-4333.

Wang, T., Luming, Y., Cooper, E.M., Lai, M.-Y., Dickey, S., Pickart, C.M., Fushman, D., Wilkinson, K.D., Cohen, R.E., and Wolberger, C. (2009). Evidence for bidentate substrate binding as the basis for the K48
linkage specificity of otubain 1 Journal of Molecular Biology *386*, 1011–1023.

Wang, Y., Zhou, X., Xu, M., Weng, W., Zhang, Q., Yang, Y., Wei, P., and Du, X. (2016). OTUB1-catalyzed deubiquitination of FOXM1 facilitates tumor progression and predicts a poor prognosis in ovarian cancer. Oncotarget *7*, 36681-36697.

Weiss, J.N. (1997). The Hill equation revisited: uses and misuses. FASEB Journal, 835-841.

Wiener, R., DiBello, A.T., Lombardi, P.M., Guzzo, C.M., Zhang, X., Matunis, M.J., and Wolberger, C. (2013). E2 ubiquitin-conjugating enzymes regulate the deubiquitinating activity of OTUB1. Nature Structural & Molecular Biology *20*, 1033-1039.

Wiener, R., Zhang, X., Wang, T., and Wolberger, C. (2012). The mechanism of OTUB1-mediated inhibition of ubiquitination. Nature *483*, 618-622.

Williamson, A., and al., e. (2009). Identification of a physiological E2 module for the human anaphase promoting complex. Proc Natl Acad Sci *12*.

Windheim, M., Peggie, M., and Cohen, P. (2008). Two different classes of E2 ubiquitin-conjugating enzymes are required for the mono-ubiquitination of proteins and elongation by polyubiquitin chains with a specific topology. Biochemical Journal *409*, 723–729

Wu, J., and al., e. (2009). Histone ubiquitination associates with BRCA1-dependent DNA
damage response. Molecular Cell Biology *29*, 849-860.

Wu, X., Yen, L., Irwin, L., Sweeney, C., and Carraway, K.L. (2004). Stabilization of the E3 ubiquitin ligase Nrdp1 by the deubiquitinating enzyme USP8. Molecular and Cellular Biology *24*, 7748–7757.

Ye, Y., and Rape, M. (2009). Building ubiquitin chains : E2 enzymes at work. Nature Reviews Molecular Cell Biology *10*, 755-7644.

Yin, Q., Lin, S.-C., Lamothe, B., Lu, M., Lo, Y.-C., Hura, G., Zheng, L., Rich, R.L., Campos, A.D., Myszka, D.G.*, et al.* (2009). E2 interaction and dimerization in the crystal structure of TRAF6. Nature structural & molecular biology *16*, 658-666.

Zhao, L., Wang, X., Yu, Y., Deng, L., Chen, L., Peng, X., Jiao, C., Gao, G., Tan, X., Pan, W.*, et al.* (2018). OTUB1 protein suppresses mTOR complex 1 (mTORC1) activity by deubiquitinating the mTORC1 inhibitor DEPTOR. Journal of Biological Chemistry *293*.

Zheng, N., and Shabeck, N. (2017). Ubiquitin Ligases: Structure, Function, and Regulation. Annual Review Biochemistry *86*, 129-157.

Zhou, W., Zhu, P., Wang, J., Pascual, G., Ohgi, K.A., Lozach, J., Glass, C.K., and Rosenfeld, M.G. (2008). Histone H2A monoubiquitination represses transcription by inhibiting RNA polymerase II transcriptional elongation. Molecular Cell *29*, 69-80.

REFEREES:

Cynthia Wolberger, Ph.D.
Dissertation Advisory
Primary Dissertation Reader
Professor, Department of Biophysics and Biophysical Chemistry Johns Hopkins University School of Medicine cwolberg@jhmi.edu

James Berger, Ph.D.
Secondary Dissertation Reader
Thesis Committee Member
Professor, Department of Biophysics and Biophysical Chemistry Johns Hopkins University School of Medicine jmberger@jhmi.edu

Rachel Green, Ph.D.
Thesis Committee Member
Professor, Department of Molecular Biology and Genetics Johns Hopkins University School of Medicine ragreen@jhmi.edu

Taekjip Ha, Ph.D.
Thesis Committee Member
Professor, Department of Biophysics and Biophysical Chemistry Johns Hopkins University School of Medicine tjha@jhmi.edu

Jennifer Kavran, Ph.D.
Thesis Committee Member
Assistant Professor, Department of Biochemistry and Molecular Biology Johns Hopkins School of Public Health jkavran@jhu.edu

Mario Amzel, Ph.D.
Thesis Committee Member
Director & Professor, Department of Biophysics and Biophysical Chemistry Johns Hopkins University School of Medicine mamzel@jhmi.edu

Lauren Que ***Curriculum Vitae***

Place of Birth:

Van Nuys, CA

Education:

2013—Present
Ph.D. Candidate in Biophysics
Johns Hopkins School of Medicine, Baltimore, MD.
Anticipated graduation on June 2019

2009—2013
B.S. Biochemistry minor in Computer Programming
Mount St. Mary's University, Los Angeles, CA
summa cum laude; Dean's list (2009-2013)

Research Experience:

2014—Present
Ph.D Candidate, Supervisor: Cynthia Wolberger, Ph.D.
Johns Hopkins School of Medicine, Baltimore, MD
Thesis: Characterizing the Cross-Regulatory Complex, OTUB1:E2

March—May 2013
Rotation Student, Supervisor: Juliette Lecomte, Ph.D.
Johns Hopkins University, Baltimore, MD
Investigating the functional role of helix capping histidines

2010—2013
NIH Minorities Access to Research Careers (MARC) Scholar
Supervisor: Deniz Cizmeciyan, Ph.D.
Mount St. Mary's University, Los Angeles, CA
Enantiomeric Interactions of D, L, DL Methionine in Zeolites NaY

June—Aug 2012
NSF Research Experience for Undergraduates Fellow
Supervisor: Alice Barkan, Ph.D.
University of Oregon, Eugene, OR
Elucidating the role of plant pentatricopeptide repeat (PPR) proteins in chloroplast development

June—Aug 2011
Summer Applied Biotechnology Research Experience Research Intern
Supervisor: Galen Stucky, Ph.D.
University of California, Santa Barbara, CA
Synthesis of Functionalized Silica Nanoparticles that Aid in Coagulation

Teaching Experience:

2017
Lecturer, Topics in Molecular Structure and Function
Johns Hopkins School of Medicine
'Structural analysis of *H. pylori's vacuolating toxin, VacA'*

2014
Lecturer, in Molecular Structure and Function

	Johns Hopkins School of Medicine 'Translocation of *H. pylori's cytotoxin, CagA'*
2012—2013	Teaching Assistant, General Chemistry Mount St. Mary's University
2011—2012	Supplemental Instructor, General Biology Mount St. Mary's University

Additional Experience:

2016-2017	Extern, Society for Women's Health Research *Biological Sex Differences in the Bladder Review Paper*
2015-2017	Event Coordinator, Biophysics Student Evening Series Johns Hopkins School of Medicine
Aug 2017	Chair, Institute for Biophysical Research Johns Hopkins University
2011-2012	President, Women in Science and Health Organization Mount St. Mary's University

Peer Reviewed Publications:

Pasupala N.*, Morrow M.*, **Que L.**, Ma A., and Wolberger, C. (2018). OTUB1 non-catalytically regulates the stability of the E2 ubiquitin conjugating enzyme UBE2E1. Journal of Biological Chemistry. 293(47) 18285–95.

Abelson B.*, Sun D.*, **Que L**., Nebel R.A., Baker D., Popiel P., Amundsen C.L., Chai T., Close C., DiSanto M.,Fraser M.O., Kielb S.J., Kuchel G., Mueller E., Palmer M.H., Parker-Autry C., Wolfe A.J., and Damaser M. (2018). Sex Differences in Lower Urinary Tract Biology and Physiology. Biology of Sex Differences. 9:45.

Preimesberger M., Majumdar A., Rice S., **Que L.,** and Lecomte J., (2015). Helix-capping histidines: Diversity of N-H(...)N hydrogen bond strength revealed by (2h)JNN scalar couplings. Biochemistry. 54:46.

Awards and Recognitions:

2015	The Johns Hopkins Fred and Ruth Young Scholar Fund.
2013	MSMU Award for Excellence in Computer Science and the Physical Sciences
2012-2013	MSMU Award for Outstanding Tutor in the Biological & Physical Sciences
2012	Best Oral Presentation, Annual Biomedical Research Conference for Minority Students
2011-2013	National Institute Health, Minorities Access to Research Careers (MARC) Scholar
Dec. 2011	Public Leadership Education Network (PLEN) Awardee, Washington D.C.